Západočeská univerzita v Plzni
Fakulta aplikovaných věd

INTERVALOVÉ METODY ŘÍZENÍ ENERGETICKÝCH SÍTÍ

Ing. et Ing. Přemysl Voráč

disertační práce
k získání akademického titulu doktor
v oboru Kybernetika

Školitelé: Doc. Ing. Eduard Janeček, CSc.,
Doc. M.Sc. et M.Sc. Daniel Georgiev, Ph.D.
Katedra: Katedra Kybernetiky

Plzeň, 2018

University of West Bohemia
Faculty of Applied Sciences

INTERVAL BASED POWER NETWORK OPERATION

Ing. et Ing. Přemysl Voráč

A dissertation work
submitted in conformity with the requirements for
the degree of Doctor of Philosophy

Supervisors: Doc. Ing. Eduard Janeček, CSc.,
Doc. M.Sc. et M.Sc. Daniel Georgiev, Ph.D.

Department: Department of Cybernetics

Pilsen, 2018

Prohlášení

Prohlašuji, že jsem předloženou disertační práci vypracoval samostatně s použitím odborné literatury a pramenů, jejichž úplný seznam je její součástí.

V Plzni, dne 10.6.2018 .....

Přemysl Voráč

ANOTACE
Tato práce se zaměřuje na vývoj intervalových metod v oblasti optimalizace energetických sítí s ohledem na měnící se technologické, tržní a enviromentální podmínky. Teoretická část představuje základní metody výpočtů ene rgetické sítě včetně jejich historického vývoje. Zmíněny jsou klasické metody Optimal Power Flow (OPF) a Load Flow (LF) a také jejich rozšíření o pravděpodobnostní modelování (POPF) či bezpečnostní kritéria (SCOPF). Rešerše literatury ukazuje, že v současné době neexistuje konvexní optimalizační nástroj, který maximalizuje intervaly uzlových výkonů vzhledem ke zadaným limitům na uzlová napětí a toky na vedeních. Na základě tohoto zjištění byla vyvinuta metoda Intervals of Secure Power Injection (ISI) a její rozšíření, která představují ústřední téma této práce. Tato metoda je rigorózně definována a výsledky jejího testování na akademických i reálných sítích jsou představeny v příslušných kapitolách. Základní metoda a její možná rozšíření byla publikována na několika světových konferencích. Důležitým přínosem práce představuje reálná aplikace metody ISI, která byla vyvinuta v rámci výzkumného projektu AnSVaL, do oblasti aktivace a rezervace podpůrných služeb.

SUMMARY

This work focuses on development of innovative interval based methods in the area of power system optimization with respect to changing environmental, technological, and market conditions. In the review part, a thorough introduction into the history of power network computation was given. An emphasis was placed on the optimal power flow (OPF), load flow (LF) problems, and their probabilistic (POPF) and security extensions (SCOPF). The literature review has shown that there are no interval based optimization tools focused on the maximization of nodal power injection intervals w.r.t. nodal voltage limits and line current constraints. Supported by this finding a new method called Intervals of Secure Injections (ISI) was formulated. This method was rigorously defined and verified on academic and real power systems. It represents an original interval based optimization tool potentially applicable in short term network operation and in electricity markets. Several conference papers with basic formulation and extensions of this method were published. The main contribution of this work represents a real application of the ISI method in the area of energy markets developed during the realization of project AnSVaL.

ZUSAMMENFASSUNG

Die vorliegende Arbeit beschäftigt sich mit der Entwicklung der innovativen intervallbasierten Methoden im Bereich der Optimierung von Stromnetzen im Hinblick auf sich verändernde Umwelt-, Technologie- und Marktbedingungen. In der Übersicht wurde eine ausführliche Einführung in die Geschichte der Stromnetzberechnung gegeben. Sowohl die klassischen Methoden wie beispielsweise Optimal Power Flow (OPF) und Load Flow (LF) wurden erwähnt als auch deren Erweiterungen um die Wahrscheinlichkeitsmodellierung (POPF) oder die Sicherheitskriterien (SCOPF). Die Literaturrecherche hat bestätigt, dass es zurzeit keine intervallbasierten Optimierungswerkzeuge gibt, die sich explizit auf die Maximierung der Knotenenergie-Injektionsintervalle konzentrieren, in Bezug auf Knotenspannungsgrenzen und Leitungsstrombeschränkungen. Basierend auf diesem Befund wurde eine neue Methode mit dem Namen Intervals of Secure Injections (ISI) und ihre Erweiterung, die das Hauptthema dieser Arbeit darstellt, entwickelt. Diese Methode wurde genau definiert und die Ergebnisse der Tests, die in den akademischen und realen Energiesystemen durchgeführt wurden, wurden in den entsprechenden Kapiteln dieser Arbeit präsentiert. Die neue Methode stellt ein inovatives intervallbasiertes Optimierungswerkzeug dar, das potentiell für den kurzfristigen Netzbetrieb und für Strommärkte geeignet ist. Mehrere Konferenzbeiträge mit grundlegenden Formulierungen und Erweiterungen dieser Methode wurden veröffentlicht. Die Anwendung der ISI-Methode in den Energiemärkten wurde in verschiedenen Netzwerk-Szenarien gezeigt, die während der Realisierung des Projekts AnSVaL durchgeführt wurden. Eine mögliche Anwendung in einem Prozess der europäischen Kapazitätsmarktintegration wurde vorgeschlagen.

CONTENTS

1

INTRODUCTION

Power networks play an essential role in modern economics providing secure distribution of electrical energy. The electrification process, which has begun in 20th century, and stable energy supply allowed a rapid economic growth. With the development of power transmission systems, the operators begin to consider where to generate energy, what fuel type should be used, how will the injected powers affect branch currents, how to satisfy the power demand with respect to a given criteria, or is the power network able to manage possible network congestion.

At the beginning of this work, a brief history of power networks since the beginning of the 20th century is presented. The most cited problems, i.e., power flow (later denoted by load flow), economic dispatch, and optimal power flow (OPF) are introduced in Chapter 2. Methods used to solve these problems are presented providing relevant citations. To document the historical development, a brief review of computation times is given. At the end of the chapter, the phenomena of renewable energy sources (RES) and other active network elements are introduced.

An incorporation of RES brings up important issues in the area of energy market balancing. The energy markets are introduced in Chapter 3. The main determinants of energy supply, demand and market equilibrium compared with classic economic theory are presented. This chapter describes situations in which the market may fail to reach an equilibrium, therefore, reserve capacities called ancillary services have to be contracted in advance to mitigate risk of power system imbalance. Basic taxonomy of ancillary services is given in this chapter.

After reviewing the historical development of power network computation and presentation of ancillary mechanisms in energy markets, Chapter 4 focuses solely on relevant point optimization methods. The analytic representation of the OPF problem is presented and possible extensions are defined. To document the complexity of the problem, an example of a solution by Newton method with comments on the critical parts of the problem is given. After the definition of the classic OPF problem, the work focuses on advanced optimization methods, i.e., Security-Constrained OPF, probabilistic load flow, and probabilistic optimal power flow and provides relevant citations.

Point optimization methods represent a main stream of power network optimization tools but the interval optimization methods, e.g., Available transfer capacity (ATR), power capability, and power supply capacity (PSC) are also reviewed in Chapter 5 providing relevant citations.

The review in Chapter 6 concludes with the finding that there are no interval based methods focused on the maximization of nodal power injection sets with respect to a defined set of network physical constraints. Based on this finding, a new interval optimization problem denoted by Intervals of Secure Injections (ISI) is formulated and an approximate solution is presented.

The Intervals of Secure Power Injection (ISI) method defined in Chapter 7 solves an optimization problem that maximizes admissible sets of power injections under network voltage and current constraints. Voltage and current constraints together form an admissible set of nodal voltages called the Network security domain. It can be shown that any point from the interval of secure power injections yields a secure nodal voltage, i.e., the voltage corresponding to a chosen power injection lies within the Network security domain. Moreover, power injections at each node can be set independently without violation of physical constraints of the system as long as the injections stay within ISI. The method was tested on academic and real networks with success and the results are provided in the work.

Chapter 8 presents relevant adjustments of the ISI method that extend principles defined in Chapter 7, e.g., incorporation of PQ diagrams of generators or an extension to satisfy the N-1 security criteria which can be used as a complementary tool to contingency analysis.

Chapter 9 introduces a modular extension of the ISI method suitable for fast and robust network operation considering marginal changes in the network topology. It comprises problem formulation, the solution proposal, and a heuristic method that solves the proposed optimization problem. Additional extensions of the modular ISI method is the subject of further research.

The ISI method can be reformulated to a form suitable for electricity markets. The optimization problem called BID-ISI is defined Chapter 10. Potential applications of this method within Czech control area supported by various testing scenarios are presented in this chapter. It is shown that the BID-ISI method can be used to compute security margins when acquiring or activating ancillary services or as a decision support tool when computing cross-border capacities. Moreover, relevant applications for European market integration are proposed.

2

History of Power Network Computations

2.1. Power network foundations

Fundamentals of electric power transfer were founded in 1880s starting the industrial revolution that influenced the world economy. Together with industry development, the corresponding infrastructure and energy supply had to be installed. During 50 years between 1880 to 1930 the first world transmission and distribution networks as we know it today were built. A detailed history of the electrification process and the state of electrification in the first half of 20th century is given in [1].

Since the early 1930s, the mankind was trying to utilize the newly constructed power networks efficiently. The methods of energy usage optimization can be divided into three main classes:

- Economic dispatch,
- Load Flow,
- Optimal power flow.

In this work, a brief history of economic dispatch and load flow is given providing reviews and books for further studies. Optimal power flow and its security constrained and probabilistic extensions are studied in more detail.

The first systematic efforts in efficient use of power networks are dating back to 1930s and were put into a problem called minimization of fuel costs (MFC) [2]. The power network was represented as a lossless medium transmitting power from a central supplier (power plant) to the consumers (industry and households). The computation of MFC was done using the graph theory or by a dedicated slide-rule. Adding the real part of transmission losses in the MFC problem in the late 1940s and early 1950s has led to the formulation of economic dispatch (ED) [3] further developed into various forms known today [4].

As the computation techniques developed, the load flow (LF) (originally denoted by power flow) problem was derived from economic dispatch. The LF problem finds nodal voltages to meet desired power injections. First publications on load flow appear in late 1940s [5]. With the discovery of transistor in 1947 and then the digital computers, the load flow solution techniques begin to develop rapidly. In 1957 LF calculations for planning purposes have been carried out on the entire 138kV and 345kV interconnected system of the American Electric Power Company using the IBM 704 [6]. In 1964 a 1000 bus test system has proven to be computationally tractable [7] using IBM 7094. Advanced algorithms based on Gauss-Seidel techniques were published in 1960s [8], [9], replaced by Newton and then by the Newton-Raphson algorithms [10],[11] in 1970s. Load flow problem has also been studied intensively and the developed methods are well described in load flow review papers [12], [13], and [14]. Currently available Matlab LF solvers are available in [15]. To increase computation speed, Krylov subspaces were recently used to solve the load flow problem [16]. All methods solving the load flow problem mentioned before are based on numerical methods, a deterministic method called holomorphic embedding load flow (HELM) has been developed and patented [17].

The problem of solving optimal power flow (OPF), i.e., an optimization problem with a defined criteria function under a set constraints imposed on a transmission network, was first introduced by J. Carpentier in [18] in early 1960s using Karush-Kuhn-Tucker conditions [18]. Although the OPF problem was formulated in early 1960s, its computation on larger systems remained computaitionaly intractable due to low hardware capabilities. The first efficient solution of the OPF was accomplished solving KKT conditions with the adjusted gradient method presented by Dommel and Tinney in 1968 [19]. Further development of optimization algorithms in late 1970s has led to a quadratic group of problems presented in [10]. These methods have solved the KKT conditions using the Newton-Raphson non-linear solver and later Lagrange-Newton methods. These algorithms have became the mainstream of OPF solutions in 1970s and 1980s [20]. With a rise of computer speed in 1980s, the optimization methods have began to develop rapidly (e.g., the interior point method) increasing the computation limits of the classical OPF problem. A compact review of the OPF literature up to 1993 has been published in [21] and [22].

The cost and efficiency of computing time caused difficulties for scientists to code and perform studies on digital computers. As can be seen in Figure 2.1, the cost of memory used to be a big burden for researchers and algorithm developers complicating thorough testing and analysis on digital computers. The cost of memory becomes bearable in 1980s and allows fast development of power network commercial packages MINOS, or software package ESCA developed by General Electric [23]. MatPower [15] is another example of a currently developed power system software package with GNU General Public License implemented in Matlab .

2.1.1. TIME DEMANDS OF COMPUTATION TOOLS

The computation of the problems mentioned in Section 2.1 comes hand to hand with the computer revolution starting in 1930s continuing to the present. The first algorithmic computations of LF and ED in 1947 using the punched-card tabulator took about 10 hours for a 14 bus system [5]. In 1955 the similar sized problem could be solved in 39

minutes [24]. In 1959 IBM 704 was able to compute 142 bus system with 243 lines in 7.2 minutes [6].

The computation of OPF was approximately equal to two to five load flow computations [25], e.g., solving 600 bus system in 1982 was estimated to 12 minutes using IBM 370/168 and 60 minutes using DEC-VAX 11/780 with almost linear scaling [26]. The computation of 39 bus test system on DEC-VAX 11/780 in 1989 took about 4 minutes [27]. In 1993, the 118 bus test system was solved using Silicon Graphics Iris 4D/240S computer with four processors rated at 20 MIPS and 4 DP MFLOPS in 54 seconds [28]. In 1997, the 1047 bus test system with all line constraints was computed on the SUN-SPARC station 10 (100 MIPS) using the interior point method in approximately 12 seconds [29]. Recently the system containing 15000 buses, 4500 generators and 11265 contingencies was computed on a PC 2.4 GHz Intel Core Duo P8600 with 1.9GB RAM in 663 seconds [30]. Nowadays, the OPF problem represent a standard optimization problem which can be solved in matter of seconds even for very large systems [15].

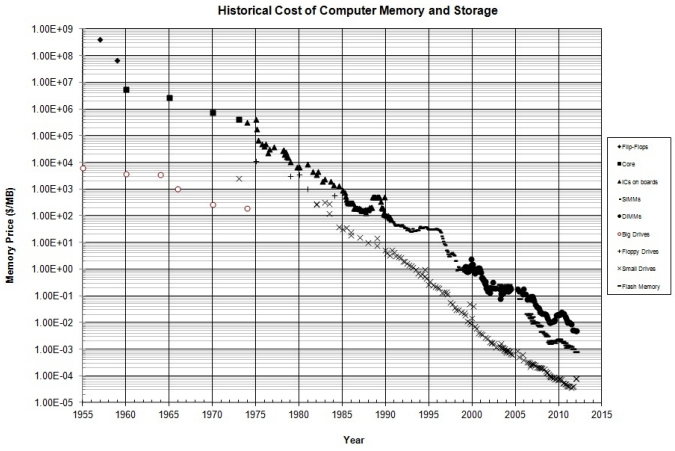

Figure 2.1: Dollar cost of MB of memory between years 1950 and 2010. The cost of memory has decreased from 1E+09 in 1950 to 1E-04 dollar per MB in 2010. The cost of memory becomes bearable in 1980s with memory cost between 1E+04 and 1E-01 dollar per MB. Source: http://www.jcmit.com/

2.2. RISE OF RENEWABLE ENERGY SOURCES

Between 1930s and 1980s the structure of power networks remained unaffected. The orientation of power flowing through the network also remained unchanged. Massive power plants are producing energy and transmitting it through the transmission and then distribution network to many areas of consumption. The situation begins to change in 1990s with the development of commercially usable Renewable energy sources (RES) [31]. The demand side management (DSM) begin to be widely used [32] and incorporated in Energy management systems (EMS). Smart grids [33] and Active distribution networks [34] represent new challenges in the area of power network computations at the beginning of 21st century.

2.2.1. THE IMPACT OF RENEWABLE ENERGY

The impact of RES on the structure of rigid energy networks caused a breaking of the centralized energy supply model. The distributed generation supplying power on an intermittent base has opened a new set of challenges needed to be solved because the distributed generation

- injects intermittent power to the system on the level of customers (i.e., to the distribution network),
- represents a new stochastic part entering into the system, i.e., in the power system, there is no longer only a stochastic power demand but also a stochastic power supply,
- has to be connected to the power network in a place with minimal chance of network failure due to RES intermittent nature,
- can cause serious damage to the power system elements and infrastructure in case of an unpredicted supply peak resulting in the load shedding or blackouts.

On the other hand RES

- are the source of a clean energy generated without any greenhouse gas emissions or any other environmental threats caused by coal or nuclear power plants,
- do not require any fuel to operate, the energy is produced from sun, wind, tidal waves, geothermal energy or biomass and generate little if any waste or pollutants,
- production cost are becoming lower [35] allowing economic feasible installations even in distribution system, so the energy can be supplied and balanced directly in the distribution network.

Figure 2.2 shows the Shell company international scenario showing the expected contribution of energy sources on the total energy consumption. The consumption classic fossil energy sources like gas, coal, and oil is decreasing while the utilization of solar, biomass, and wind energy sources is increasing. Rising penetrations of RES require a lot of work hidden behind their safe connection to power networks. Without proper tools, utilization of high amounts of RES would be impossible due to their intermittent nature which would make the system uncontrollable [36].

To incorporate uncertainty of demand and supply, extensions of classical methods have to be studied and defined. Pioneer work in area of uncertainty in power system was published in 1974 by Borkovska [37] defining the fundamentals of Probabilistic Load Flow (PLF) algorithm. Uncertainties in power demand were further studied in 1980s, published in [38] and used in demand side management tools as reviewed in [39] and remains to be widely used in present day. Uncertainties in power supply have led to development of new range of optimization problems. PLF methods were reintroduced to incorporate the influence of RES and other uncertainties in the classical load flow problem. A review was done by Chen in [40], some papers about PLF were also published at the University of West Bohemia [41]. Probabilistic OPF formulations treating increasing

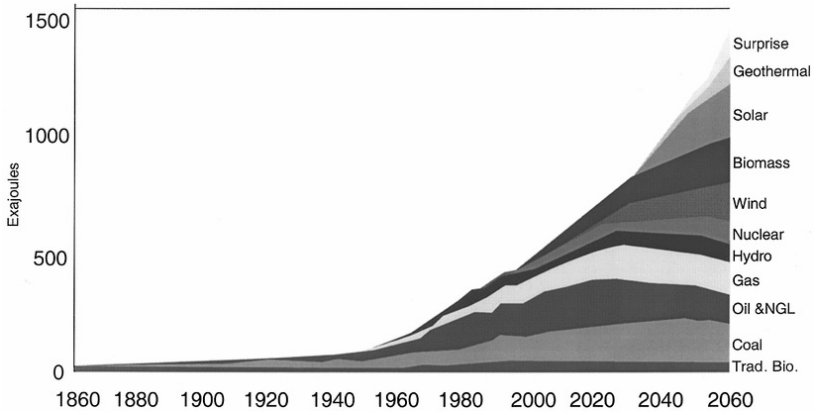

Figure 2.2: Royal Dutch Shell company international scenario forecast the contribution of different energy sources on total energy consumption. According to these scenarios, the increases in world energy demand will be supplied by renewable energy technologies, which will provide 30% to 50% of world energy by 2050. Source: [35]

penetrations of RES has been formulated in last decade in [42], [43], and [44]. More information about these advanced power system optimization tools will be given in Section 4.1.

With the increasing penetration of RES, the Security constrained OPF (SCOPF) problem gained interest in the academic area. SCOPF begin to emerge in 1980s [45] as reviewed by Scott. The importance of safe power system operation with the integration of RES once again put the pressure on computational tractability (since the SCOPF requires OPF to run n-times, where n is the number of possible contingencies). The full AC SCOPF problem remains computationally intractable for real-time applications, however, there has been a lot of effort to reduce the computation time of SCOPF close to the real-time even for large systems [46]. Complete review of SCOPF literature was published by Capitanescu [47].

3

ENERGY MARKETS

Chapter 2 presented theoretical background of developed optimization methods. The goal of system operators is to keep the system secure with the lowest cost possible, therefore, power system optimization tools have to satisfy both physical and economical criteria. This chapter describes general behavior of electricity markets and their incorporation into power system optimization. Section 3.1 introduces electricity markets together with its supply and demand curves. The specific nature of electricity markets supported by the fact of incorporation of new RES mentioned in Section 2.2, can result in situations in which the equilibrium cannot be reached. These situations are described in Section 3.1.2.

3.1. GENERAL PRINCIPLES

European electricity markets have progressively developed and integrated since the liberalization introduced by the First Energy Package in 1996[1]. Integration is well advanced, especially in the day ahead period, where a number of national markets are coupled at the regional level (see Appendix E). Initiatives have been undertaken in Central-Western Europe (France, Germany, Benelux); the Nordic region (Denmark, Sweden, Norway, Finland, Estonia); the Iberian Peninsula; Czech Republic, Slovakia and Hungary; Italy and Slovenia). At the level of intraday markets, with the exception of the Nordic regional market, integration is less advanced, with cross-border trading platforms mainly developed bilaterally between member states. The Network Code Capacity Allocation and Congestion Management (CACM)[2], which has already entered into force, shall further increase the integration of national electricity markets.

For the purposes of this work, the energy market is defined as a global market comprising all electricity products with supply and demand that are not limited by physical constraints of the network. The equilibrium corresponds to an amount of power that is to be transmitted through the transmission network.

[1] http://www.europarl.europa.eu/atyourservice/en/displayFtu.html?ftuId=FTU_2.1.9.html
[2] https://electricity.network-codes.eu/network_codes/cacm/

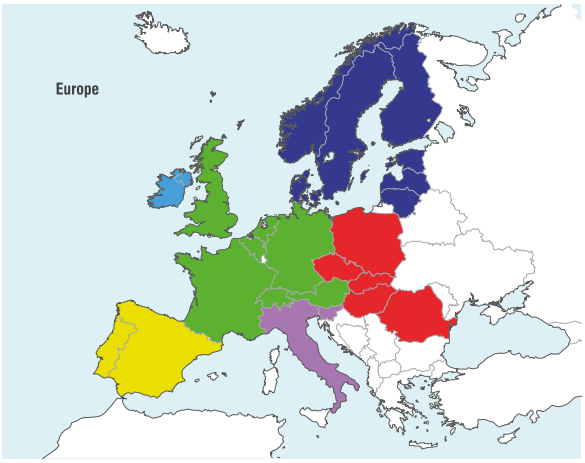

Figure 3.1: Day ahead electricity markets in Europe. Green color shows EPEX (EEX https://www.eex.com/en/), yellow color shows OMIE (http://www.omie.es/en/), red color shows PXE (https://www.pxe.cz/) (OTE), dark blue color shows Nord Pool (http://www.nordpoolspot.com/) and light blue color show SEM (https://www.semcommittee.com/) or I-SEM.

3.1.1. MARKET SUPPLY AND DEMAND

Each market has its own specifications of market demand and supply and its sensitivities to changes in the price of the underlying product [48]. This section describes these discrepancies in comparison with the classic market supply and demand curves.

The classic demand curve (D) captures relationship between price and demanded quantity of a given commodity. In this work, the price of the commodity (P) is an affine function of its demanded quantity (Q), i.e, $P = aQ + b$, where $a \in \mathbb{R}^-, b \in \mathbb{R}^+$. The supply curve (S) captures relationship between price and supplied quantity of a given commodity. In this work, the price of the commodity (P) is an affine function of its supplied quantity (Q), i.e, $P = cQ + d$, where $c \in \mathbb{R}^+, d \in \mathbb{R}$. Detailed supply and demand analysis with, description of markets marticipants and market modes are given in Appendix A. For derivations of demand and supply curves for individual or for the whole market, see [49], [50], or [48].

Energy consumers ability to reduce power demand is often very limited. This yields a very inelastic market demand curve, i.e., consumed amount of energy is not sensitive on differences in electricity price. The illustration of comparison between classic and electricity demand curves is shown in Figure 3.2.

The market supply curve comprises individual supply curves of each producer. In the presence of a limited number of producers each willing to produce a specified amount of energy for a given price. The market supply curve, therefore, represented by a piecewise constant function. The comparison between the power supply curve and the classic market supply curve is given in Figure 3.3.

The reasons for differences between the supply curves are the following. First, there is a limited number of producers. Second, each producer represent an important frac-

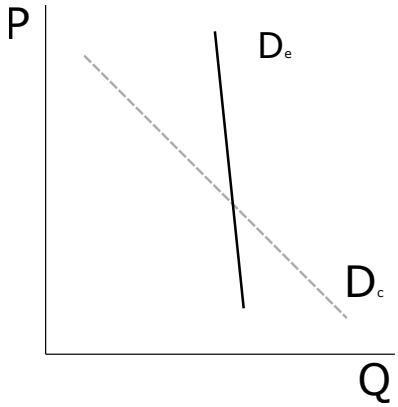

Figure 3.2: Comparison between classic and electricity demand curves: D_c corresponds to a classic demand curve. The demand is price sensitive. D_e represents the electricity demand curve. The sensitivity of demanded electricity to a change in price is lower.

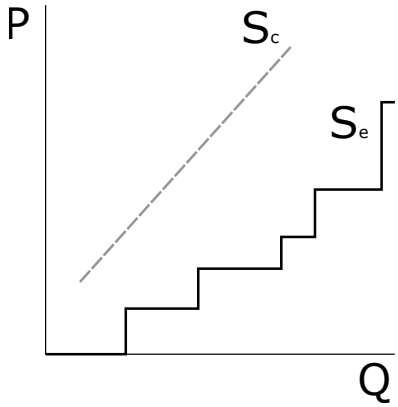

Figure 3.3: Comparison between classic and electricity supply curves: S_c corresponds to a classic demand curve. Due to high number of suppliers the market supply can be modeled as a linear function. S_e represents the electricity demand curve. The number of suppliers is lower, the market model is closer to a model of an oligopoly. The supply function is piecewise constant.

tion of the market and are often able to influence the market price. Third, the entry and exit barriers are high especially in terms of initial capital investment and technology requirements.

3.1.2. MARKET FAILURES

Electricity markets represent a model of an imperfect market competition in a form of a monopolistic competition or an oligopoly (see Apendix A). Using the market supply and demand curves from the previous section, the theoretical equilibrium of an electricity market is shown in Figure 3.4.

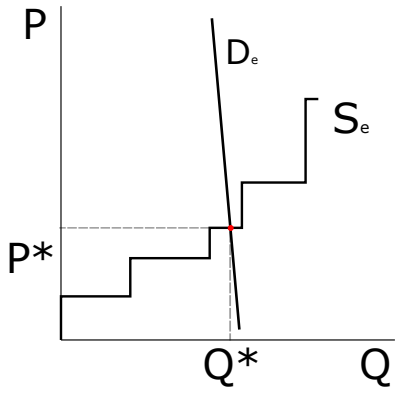

Figure 3.4: Equlibrium in the electricity market.

In this market, bids are arranged in ascending order, according to the marginal costs of generating units (the so-called 'merit order', see Chapter 10), and the price is set at the level of the marginal cost [48] of the most expensive unit dispatched in order to meet demand. However, this model, often described as the 'energy only' market suffers from a notable failure: demand and supply do not necessarily meet at times of extreme scarcity, i.e., there is no guarantee of the market clearing.

The market mechanism appear efficient for most situations, however, in times with increased electricity demand, the producers may not be able to satisfy the demand and the market equilibrium will not be reached. This problem, thoroughly described in [51], is denoted as the Missing money problem because of the failure to provide high enough returns to maintain the level of capacity adequate to meet demand. This situation is illustrated in Figure 3.5.

Nowadays, the massive installations of RES represent an important part of the electricity market supply. The marginal costs for producing electricity from RES are very close to zero. Therefore, large penetrations of RES cause a shift in market supply. The market situation before and after the incorporation of the RES is shown in Figure 3.6.

The incorporation of RES appear to hava a positive impact, but as a consequence of a massive penetration of RES, the firm sources with marginal cost higher than the the equilibrium price have to shut the production down because they are not economically effective and may exit the market. The distortions caused by the RES is partly caused by

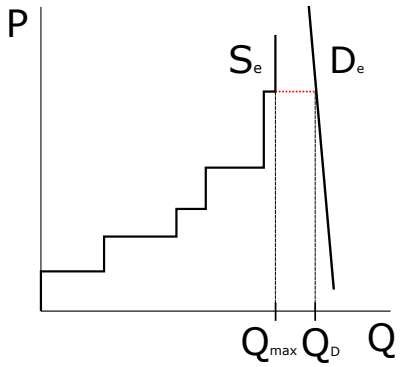

Figure 3.5: Missing money problem. Situation, in which the electricity market fails to find an equilibrium.

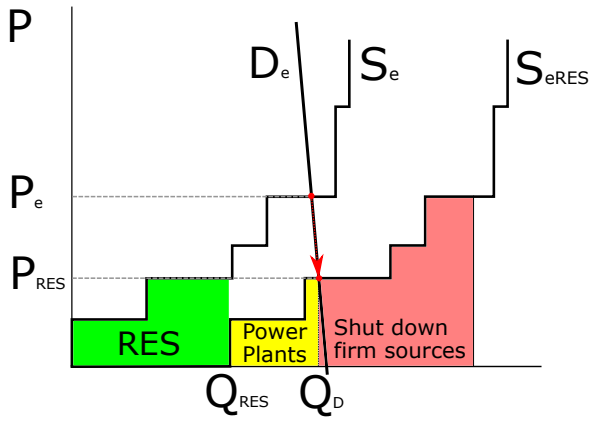

Figure 3.6: Incorporation of RES. Incorporation of intermittent sources and shutting down firm sources.

the level of their public support in a form of subsidies per produced MWh.

The high share of RES in electricity supply, despite its advantage, cannot provide a firm source of energy as the classic plants. So a high penetration of intermittent RES in electricity systems must go hand in hand with the availability of suitable back-up capacity. This back-up capacity is normally provided by thermal units. Thus, a new market failure arises. The capacity which is pushed out of the market by the increasing share of RES is precisely the capacity that can guarantee the secure integration of RES in the electricity system.

Incorporation of capacity mechanisms enables efficient solution of the missing money and the RES problems. First, enough back-up capacity can be used in time of power scarcity to meet power demand. Second, in systems with a high integration of RES, the back-up capacity is able to balance the system in case of an unexpected power imbalance. The thorough description of most commonly used capacity mechanisms is presented in Appendix B.

3.2. ANCILLARY SERVICES

The potential market failures described in Section 3.1.2 represent a problem specific to electricity markets. Back-up capacity is able to overcome these market inefficiencies. There can be different types of capacity which vary, e.g., in the purpose of use, activation time, or in ramp time. In this section, types of back-up capacity denoted as ancillary services are introduced. There are various methods to acquire back-up capacities. The most commonly used mechanisms for capacity acquisition are presented in Appendix B.

Unlike other markets, the produced energy cannot be efficiently stored, it has to be consumed at the same time. Energy markets themselves in a form available today are not able to achieve power system equilibrium in times of extreme demand or supply. As mentioned in Section 3.1, TSOs are responsible for maintaining voltage quality and equilibrium of market supply and demand. To maintain power system security, TSOs reserve a specified amount of generator capacities or scheduleable loads in given locations of the network for a given price. The tools that are used by TSOs to achieve network security goals are called the ancillary services.

Ancillary services are special services provided by participants of the electric grid that facilitate and support a continuous flow of electricity so that supply will continually meet demand. The term ancillary services is used to refer to a variety of operations beyond generation and transmission that are required to maintain grid stability and security. These services generally include, frequency control, spinning reserves and operating reserves. Traditionally ancillary services have been provided by generators, however, the integration of intermittent generation and the development of smart grid technologies have resulted in a shift in the equipment that can be used to provide ancillary services.

There are several types of ancillary services each designed to meet specific TSO requirements. The main types of ancillary services are the frequency containment reserve (FCR), frequency restoration reserve that can have an automatic (aFRR) or a manual (mFRR) form, and replacement reserve (RR). Types of ancillary services are described next.

Note, the standard definitions of the ancillary services are taken from the ENTSO-E

Network Code on the Electricity Balancing [3].

3.2.1. FREQUENCY CONTAINMENT RESERVE

Frequency Containment Reserve (FCR) means operating reserves necessary for constant containment of frequency deviations (fluctuations) from nominal value in order to constantly maintain the power balance in the whole synchronously interconnected system.

Activation of these reserves results in a restored power balance at a frequency deviating from nominal value. This category typically includes operating reserves with the activation time up to 30 seconds. Operating reserves of this category are usually activated automatically and locally.

3.2.2. FREQUENCY RESTORATION RESERVE

Frequency Restoration Reserve (FRR) means operating reserve used to restore frequency to the nominal value and power balance to the scheduled value after sudden system imbalance occurrence. This category includes operating reserves with an activation time typically up to 15 minutes. Operating reserves of this category are typically activated centrally and can be activated automatically or manually.

3.2.3. REPLACEMENT RESERVE

Replacement Reserve (RR) means operating reserve used to restore the required level of operating reserves to be prepared for a further system imbalance. This category includes operating reserves with activation time from 15 minutes (in Continental Europe) up to hours.

Hereby presented ancillary services represent a tool to control power systems in situations in which the market is unable to find an equilibrium. There are various capacity mechanisms requiring a specified amount of ancillary services or provide remuneration to firm sources. The most commonly used capacity mechanisms are presented in the next section.

[3] http//:www.acer.europa.eu/Official_documents/Acts_of_the_Agency/ANNEXES_TO_RECOMMENDATION_032015/Annex%20II%20-%20Proposed%20amendments%20to%20the%20Network%20Code.pdf

4

POINT OPTIMIZATION IN POWER SYSTEMS

Based on information given in Chapters 2 and 3, two main eras of power system optimization methods can be defined. The first is the classical era that begin with the definition of the OPF by Carpentier in 1962 [18]. The structure of power network remains unchanged, the generation is concentrated in power plants and the consumption is distributed in the network. The modern era of the power network optimization starts in early 1990s with the first RES installations. The former power network structure has had to adapt to changing conditions in the power network and had develop new methods of treating the integration of intermittent power injections.

4.1. CLASSIC ERA

Since the foundation of power system optimization in 1960s, the mainstream of optimization techniques is focused on point-wise optimization of a given criteria with respect to a defined set of constraints on controllable and state variables of the problem, i.e., the OPF Problem which will be the main topic of this section.

4.1.1. OPTIMAL POWER FLOW

The following notation is used in this chapter. Let $\mathcal{G}$ be a set containing all PV buses and the slack bus and has cardinality g. Let $\mathcal{L}$ be a set containing all PQ buses and has cardinality l. The set of nodes described as $\mathcal{N} = 1...n$. Note, $n = g + l$. The set of branches is defined as $\mathcal{B} \subset \mathcal{N} \times \mathcal{N}$. Recall, the PV bus represents a node with connected generator supplying a known amount real power with a given voltage magnitude, the PQ bus represents a node with connected load drawing a defined amounts real and imaginary powers from the network, and the slack bus represents a balancing node supplying or drawing power from the network to maintain the total balance. General form of the OPF formulated by Dommel and Tinney [19] is the following:

Problem 1 (Optimal Power Flow)

$$min\ f(x,u), \tag{4.1}$$

subject to,

$$g(x,u,p)=0, \tag{4.2}$$

$$u^- \le u \le u^+,\ x^- \le x \le x^+. \tag{4.3}$$

Vector x is the vector of state variables, i.e., voltage magnitude and voltage phase angle on PQ nodes, voltage phase angle on PV node, u is the vector of control variables, i.e., real and imaginary powers on the slack bus, real and imaginary powers on PV buses and p is the vector the control parameters, i.e., voltage magnitude on PV buses, real and imaginary powers on PQ buses, and voltage magnitude and voltage phase angle at the slack bus. In (4.1) and (4.2) f,g are chosen criteria function and equality constraint functions that can be non-linear, u^+ and u^- are the limits on elements of u.

In newer literature [46], equation 4.3 can be rewritten as a general inequality expression

$$h(x,u,p)\le 0. \tag{4.4}$$

The most important difference between load flow and optimal power flow is the criteria function. The first algorithmic solutions of OPF [19] were solving the problem itteratively using load flow by the Newton method [10] or by the Modified gradient method with Karush-Kuhn-Tucker conditions.

The equality conditions (4.2) represent power balance conditions of the network yielding the OPF equations which are usually stated in the polar power-voltage form

$$P_i^G - P_i^L = V_i \sum_{j=1}^{n} V_j (G_{ij} cos(\theta_i - \theta_j) + B_{ij} sin(\theta_i - \theta_j)), \tag{4.5}$$

$$Q_i^G - Q_i^L = V_i \sum_{j=1}^{n} V_j (G_{ij} sin(\theta_i - \theta_j) - B_{ij} cos(\theta_i - \theta_j)). \tag{4.6}$$

Using the notation from [25], at each node $i \in \mathcal{N}$ the generation P_i^G,Q_i^G must meet nodal power demands P_i^L,Q_i^L and line flows (Right hand side of (4.5) and (4.6))). Variables V_i and θ_i correspond to voltage magnitude and nodal voltage phase angle at node i, respectively. Parameters G_{ij} and B_{ij} stand for conductance and susceptance of branch $b=(i,j)$.

The inequality constraints introduced in (4.3) can have the following form. Parameters P_i^{G-}, P_i^{G+}, Q_i^{G+}, Q_i^{G-}, V_i^-, and V_i^+ represent the maximum or minimum elements of vectors of real and imaginary powers and voltage magnitude at node i. Then the inequalities can be described as

$$V_i^- \le \|V_i\|_2 \le V_i^+,$$

where $\|\cdot\|_2$ denotes the Euclidean norm and

$$P_i^{G-} \le P_i^G \le P_i^{G+},\ \ Q_i^{G-} \le Q_i^G \le Q_i^{G+}. \tag{4.7}$$

4.1.2. EXAMPLE OF THE OPF SOLUTION BY THE NEWTON METHOD

In this section, a brief example of the OPF solution technique using Newton method is given. It serves as a demonstration of the OPF complexity.

Let p (a vector of network parameters) be incorporated into u, the Newton method applied on (4.2) yields

$$g(x^0, u^*) + \frac{dg}{dx}\Delta x + \mathcal{O}(\Delta x) = 0. \tag{4.8}$$

In (4.8), x^0 denotes an initial guess of the solution x and u^* is a chosen value of u. The term dg/dx is the Jacobian matrix evaluated at x^0, u^* and $\mathcal{O}(\Delta x)$ is the neglected higher order part of Taylor polynomial. The first order correction Δx is given by

$$\Delta x = -\left(\frac{dg}{dx}\right)^{-1} g(x^0, u^*), \tag{4.9}$$

and the iteration follows by addition of the correction to the initial guess

$$x^1 = x^0 + \Delta x. \tag{4.10}$$

The optimality condition is that the gradient of the criteria function (4.1), i.e., dF/du is zero. First the u^0 is selected, then the gradient is computed and finally the improved point u^1 is selected s.t.

$$u^1 = u^0 - k\left(\frac{df}{du^0}\right), \quad f(u^1) \leq f(u^0). \tag{4.11}$$

Lets have a look at the main difficulties in solving the general problem defined by (4.1), (4.5), (4.6), and (4.7).

1. Computation of (4.9) represents a time consuming process since an inversion of the Jacobian matrix is needed to compute a new state.

2. Parameter $k > 0$ is chosen and represent the gradient step size. Large values of k yield bigger steps but may cause oscillation of the algorithm around the optimal point. Small values of k lead to a convergent state but at the low speed. Choosing the right value of k is essential for efficient computations of OPF by this method. Algorithm of choosing the value of k was presented by Wu in [52].

3. The new control variable u^i selected in (4.11) may lead to a state x^i which violates some of its bounds (4.3). This was solved by two methods:

   - adding penalty function to the criteria function. When the variable is on its bounds the value of the function is zero and rises with increasing violation distance.
   - Second solution deals the problem the following way. Whenever x_k reaches its bound, it becomes an independent variable u_k and formerly independent variable becomes a dependent variable. This new dependent variable is chosen so that it is free to move, at least during the next iteration.

4.1.3. EXTENSIONS OF THE CLASSICAL OPF

The classical definition of OPF was published in 1962 represented by equations (4.1), (4.5), (4.6), and (4.7). This set of equations represent a general OPF model which can be enriched and modified to meet desired purposes. In this chapter, possible forms of criteria function, new elements, and constraints are presented. These equations can be appended to Problem 1.

Various techniques to solve OPF problem were proposed in review papers [21], [22], and [23]. Development of new methods in late 1980s ,e.g. interior point method and other advanced optimization techniques [21] and [22] finally allowed effective solution of the OPF problem even on large systems.

CRITERIA FUNCTION

Criteria function (4.1) can represent various desired network scenarios or behaviors. In [27], various types of criteria functions are presented, e.g.:

- transmission loss minimization,
- economic cost minimization,
- voltage deviation minimization,
- possible power transfer maximization.

There are other types of criteria functions, e.g. minimization of control actions, reactive power minimization, criticality criterion [53], and many others. In this work, we will describe only the most widely used criteria functions denoted by J_1, J_2, and J_3.

The first introduced criteria function is the transmission loss minimization [54]. It penalizes total loss of energy in the power system due to losses in electrical wiring.

$$J_1 = \min \sum_{\forall i \in \mathscr{B}} \|I_i\|_2^2 r_i. \tag{4.12}$$

In (4.12), for a given branch $i \in \mathscr{B}$, I_i represents the branch flowing current and r_i the line resistance. Loss minimization is a typical optimization criteria of the OPF problem. The criteria penalizes both real and reactive powers in the power system. The criteria function is convex and minimization of convex function represents a tractable convex optimization problem.

Economic cost minimization is generally used in the economic dispatch problem [55]. The criteria penalizes the energy generation costs by a defined cost parameter $c_j, \forall j \in \mathscr{G}$ and takes the following form

$$J_2 = \min \sum_{\forall j \in \mathscr{G}} c_j P_j^G, \tag{4.13}$$

which is a linear program.

Another form of linear program criteria function used in the voltage control is the voltage deviation minimization criteria function [54]. This function minimize the total

deviation of the power system from a defined nominal voltage point V_k^{ref}, it can be written as

$$J_3 = \min \sum_{\forall k \in \mathcal{N}} (V_k - V_k^{ref}). \tag{4.14}$$

The maximization of available power transfer capability (ATC) is a non-trivial problem in which we try to maximize possible energy transfer between defined areas A and B. The idea is to increase the generation in the sending area and do not violate power system limits. More information about ATC maximization can be found in [56]. This criteria function is mentioned here because the computation ATC is one of the few interval optimization methods in power system optimization as will be mentioned in chapter 5.

POWER DEMAND

In classical LF and OPF, loads P^L, Q^L are given by an empirically computed load profile, i.e. represent time varying constants. As proposed in mid 1970s by Borkovska [37], the loads can be modeled as random variables appended to (4.2). Another methods were published in 1980s using multilinearization [57] or Monte Carlo simulation [58]. However, efficient implementation of probabilistic principles to OPF was not able due to insufficient optimization techniques and lack of computation speed. The practical use of probabilistic LF and then probabilistic extension of OPF are being used in the modern era of power network optimization.

ENERGY STORAGE

Starting in mid 1980s the academic interest has focused on the problem of energy storage. Effort has been put to formulate an optimization method considering an energy storage [59] and some application reviews were done in late 1980s in [60]. Despite of the effort put into energy storage implementation, its practical application remains unused due to its high operation and construction costs. However, with increasing energy storage efficiency and increasing RES penetrations, the energy storage installations can help to increase power system safety and robustness.

Incorporation of an energy storage into OPF can be achieved by defining storage energy injections into the system to node $i \in \mathcal{N}$ by P_i^S, Q_i^S and appending them to (4.5) and (4.6). Note, terms P_i^S, Q_i^S can be positive or negative depending on desired behaviour. Storage device at node $i \in \mathcal{N}$ has defined capacity limits P_i^{S+}, P_i^{S-}, Q_i^{S+}, Q_i^{S-} and state P_i^{S0}. The capacity limits P_i^{S+}, P_i^{S-}, Q_i^{S+}, Q_i^{S-} cannot be surpassed and the storage cannot supply more power than it has in its reserves represented by current state. The mathematical expression can be stated as

$$P^{S-} \leq P^S + P^{S0} \leq P^{S+},$$

$$Q^{S-} \leq Q^S + Q^{S0} \leq Q^{S+},$$

$$P^S \leq P^{S0} \quad Q^S \leq Q^{S0}.$$

These inequalities are appended to (4.3). Penalization of storage utilization is appended to criteria function (4.1).

FLOW CONSTRAINTS

The line flows constraints (usually denoted as line thermal limits) can also be added imposing the limits either on apparent or real powers flowing through network branches. Denote P_{ij}, Q_{ij} as the real and reactive power flowing through branch $b = (i, j)$ connecting nodes i and j, P^+_{ij} and S^+_{ij} as the real and apparent branch flow limits, the inequality equations appended to (4.3) have the form of line limits imposed on the real power P_{ij}

$$P_{ij} \leq P^+_{ij},$$

on the current I_{ij}

$$I_{ij} \leq I^+_{ij},$$

or on the apparent power S_{ij}

$$\sqrt{P^2_{ij} + Q^2_{ij}} \leq S^+_{ij}.$$

VOLTAGE CONSTRAINTS AND DC APPROXIMATION

Line flow constraints can also be rewritten as voltage angle constraints since power flowing over branch $b \in \mathscr{B}$ is approximately equal to the sine of the voltage phase angle difference at the receiving and transmitting ends. The voltage angle difference can be constrained as follows

$$\theta^{min}_{ij} \leq \theta_i - \theta_j \leq \theta^{max}_{ij}. \tag{4.15}$$

We can either use the voltage phase angle difference constraint (4.15) or the DC approximation line flow constraint (4.16).

$$B_{ij}(\theta_i - \theta_j) \leq P^+_{ij}, \tag{4.16}$$

recall, B_{ij} corresponds to the susceptance of the branch $b(i, j) \in \mathcal{B}$. More information about DC OPF approximation which is computationally tractable and has proven economic value can be found in [61].

UNIT COMMITMENT CONSTRAINTS

Additional conditions can also be appended to deterministic generation P^G_i,Q^G_i. The generators can have its spinning reserve requirements, ramping up/down limits, minimum up/down time limits, and other constraints like fuel or emission limit constraints. These limits can be used as a refinement of the OPF but are rather used in in economic dispatch or unit commitment problems [55].

4.2. MODERN ERA

OPF algorithms from 1990s have become reliable enough for practical use and has become a standard power analysis tool [62]. With faster and more efficient computation hardware, the power system optimization tools begin to develop rapidly allowing solution of more complex problems, e.g., Security-constrained optimal power flow.

4.2.1. SECURITY-CONSTRAINED OPTIMAL POWER FLOW

The original OPF problem was reformulated into a new problem denoted by Security Constrained Optimal Power Flow (SCOPF) [45]. The problem finds an optimal power system setting with respect to a given set of possible network contingencies represented by a given set of deviations from nominal system topology. The basic problem can be formulated as follows

Problem 2 (Security-Constrained Optimal Power Flow)

$$\min_{u_0,\dots,u_t,x_0,\dots,x_t} f(x_0,u_0), \tag{4.17}$$

subject to,

$$g_0(x_0,u_0)=0, \tag{4.18}$$

$$h_0(x_0,u_0)\leq 0, \tag{4.19}$$

$$g_k(x_k,u_k)=0, k\in\mathscr{C} \tag{4.20}$$

$$h_k(x_k,u_k)\leq 0, \forall k\in\mathscr{C}, \tag{4.21}$$

where $\mathscr{C}$ is the set of defined contingencies with t elements, subscript k refers to variables of k-th post-contingency state, subscript 0 refers to the base state, x and u are the state and control variables, $f(x,u)$ is the objective function, $g(x,u)$ and $h(x,u)$ denote the equality and inequality constraint functions. Note, the same notation as in Problem 1 is used. In addition, the variables representing the contingency state have a subscript k and the variables representing the base state have a subscript 0.

Some papers add the maximum number of corrective actions that can be performed in a post-contingency state. These constrains can be appended to Problem 2 and have the following form used in [63]

$$-s_{ki}\Delta P_i^G \leq P_{ki}^G - P_{0i}^G \leq s_{ki}\Delta P_i^G,$$

$$\sum_{\forall i\in\mathscr{G}} s_{ki}\leq N_k, \forall k\in\mathscr{C},$$

$$s_{ki}=\{0,1\}, \forall k\in\mathscr{C}, \forall i\in\mathscr{G}.$$

Variable s_{ki} is a binary variable describing the status of the generator in post contingency state $k\in\mathscr{C}$. If $s_{ki}=1$, the generator is used in post-contingency corrective strategy. If $s_{ki}=0$, the generator remains on its pre-contingency value. Variable ΔP_i^G is the maximum amount of power that a generator can redispatch following a contingency. N_k is the maximum number of allowed corrective actions.

Foundations and basic methodology of the SCOPF problem were defined and reviewed by Scott in [45], other great paper reviewing the state of art was written by Capitanescu in [47]. Despite the effort put into development of real-time SCOPF methods, its real-time application on large systems was not yet accomplished. The most ambitious way to real-time SCOPF published in [30] is denoted as Iterative Security-Constrained Optimal Power Flow with Network Compression (ISCOPF-NC). This algorithm is using standard Security analysis module, then the contingencies are filtered by a Contingency Filtering technique described in [64]. The contingencies size is then reduced by a Network Compression module. This algorithm was able to compute the network containing 15000 buses, 4500 generators, and 11265 contingencies. The computation time of a one run of the optimization problem was 663 seconds.

4.2.2. DEMAND SIDE MANAGEMENT

The demand side of the energy market was also studied intensively. Various techniques were developed to obtain power demand profile models [65], [66]. Techniques like load shedding, peak shaving, and load shifting have become fundamentals of demand-side management (DSM) tools [67]. Tools comprised in DSM focus on reduction of energy consumption in peak periods by shifting the consumption to a non-peak period. The example of DSM on load profile can be seen on Figure 4.1. This is economically desired behavior since the price of electricity is higher during the peak hours. Application of DSM can be achieved by installing smart controllers to control shiftable household devices, e.g., washing machine, tumble drier, boiler, and mainly plug-in hybrid electric vehicles [68], [69]. This problem is closely connected with development of smart grids which aims to make the power industry more economically, environmentally and socially efficient [70].

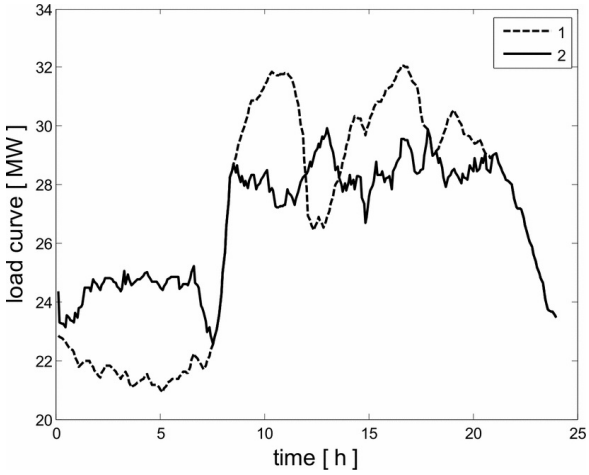

Figure 4.1: Power demand in a power system during hours. Dashed line shows the load profile without using DSM. It can be seen that there are peaks around 12 and 16. The solid line represents the load demand profile using DSM. The peaks at 12 and 16 are shaved, the volatility of the load between 10 and 24 is decreased and more load is demanded between 0 and 7. Source: [71]

4.2.3. RENEWABLE ENERGY SOURCES

The influence of renewable energy began to rise in 1990s. As stated in Section 2.2, connecting intermittent distributed supply to the power network caused many difficulties but has potential benefits that cannot be ignored. From theoretical work in mid 1980s to 1990s, first effective solutions were proposed on the brink of the 21st century [72],[73] using linear programming. The load flow incorporating RES was published in [74]. No uncertainty is considered in the first methods, they have only used the wind power as a scheduled supply injected to the network according to the observations [72],[73] or used the wind speed as an input to the deterministic load flow model [74]. This leads to the development of probability extensions of classical LF and OPF problems.

4.2.4. PROBABILISTIC LOAD FLOW

Probabilistic extension of deterministic load flow yields more accurate description of power network behavior under effects of uncertainty injected by RES. The problem called Probabilistic load flow (PLF) first introduced by Borkovska in 1974 [37] has proven to be effective with RES incorporated into the power system. Complete review of used PLF methods was done by Chen [40]. Solution techniques are divided into 4 categories:

- Simulation based methods using Monte Carlo analysis [75], this method is often used as a benchmark method, the computation complexity for large networks becomes prohibitive.
- Approximate methods based on linearization using various approximations. Linearization is often used in PLF computation [76], however, linearization perturbations are large and are prone to significant errors. The quadratic PLF methods attain some non-linear structure by keeping the second order Taylor series terms [77].
- An alternate approximation can be done by point estimate methods (PEM) [78], which first solves the deterministic load flow at several sample points and then weighs them to estimate the output moments. A third order Taylor series is used to derive the point locations and their weighs.
- Backward/Forward LF method proposed by [41] is applicable for LF analysis of radial and weekly meshed networks [79].

4.2.5. PROBABILISTIC OPTIMAL POWER FLOW

The probabilistic version of OPF (POPF) has also been developed recently and represents an effective solution of OPF incorporating uncertainties in power demand and supply. The probabilistic optimal power flow solution techniques can be divided into following categories:

- Monte Carlo simulation is a traditional and reliable approach solving POPF [75]. However, many simulations runs are required to obtain accurate results. This computational burden may prove to be excessive in many situations.

- Point-estimate methods have proven to be effective solving the POPF problem [80] obtaining accurate probabilistic power system simulations in a computationally efficient manner [78].
- The cumulant based method solving POPF introduced in papers [81], [82] using the logarithmic barrier interior point method [42]. The method was further enhanced by Tamtum in 2009 [83].

4.2.6. PROBABILISTIC OPTIMAL POWER FLOW FORMULATION

In the following section, an example of POPF comprising an energy storage and RES having intermittent nature is given. Note that it represents the DC approximation of the AC POPF problem. This definition of the POPF was presented in [84] applying the uncertainty immunized solution using the duality principle from [85].

The uncertainty injected by the RES in POPF is modeled by the random variable Δ that takes values in $\Omega \subseteq \mathbb{R}^N$ with a zero mean and defined covariance matrix $\langle\langle\Delta\rangle\rangle$. The variable Δ can be described by any chosen probability distribution. The set $\Omega = \mathsf{X}_{i\in\mathcal{N}}\Omega_i$, where $\Omega_i = \{\delta_i \in \mathbb{R} | S\delta_i \leqq h_i, S = [1,-1]^T, h_i = [\delta_i^+, -\delta_i^-]^T \in \mathbb{R}^2\}$ and δ_i^+, δ_i^- are pre-defined bounds.

Problem 3 (POPF) *Let $\delta \in \Omega$, and Γ_g, Γ_s, and Γ_l be the penalization matrices for P^G, P^S, and L, respectively. The problem is to*

$$Min\ (P^G)^T\Gamma_g P^G + L^T\Gamma_l L + trace\left(\Gamma_s^T P^S \langle\langle\Delta\rangle\rangle (P^S)^T\Gamma_s\right),$$

subject to, $\forall b \in \mathscr{B}$ and $\forall n, m \in \mathcal{N}$,

$$P^{G-} \leqq P^G \leqq P^{G+},\ P^{S-} \leqq P^S\delta \leqq P^{S+},$$

$$f^- \leqq e_f + D_f\delta \leqq f^+,$$

$$0 = P_d(n) + \sum_{b\in I_n} e_f(b) - e_l(b) - \sum_{b\in O_n} e_f(b), \tag{4.22}$$

$$0 = P_u(n)\delta + \sum_{b\in I_n} (D_f(b) - D_l(b))\delta - \sum_{b\in O_n} D_f(b)\delta, \tag{4.23}$$

$$e_f(b) = \frac{1}{x(b)}\left(e_\theta(n) - e_\theta(m)\right), \tag{4.24}$$

$$D_f(b)\delta = \frac{1}{x(b)}\left(D_\Theta(n)\delta - D_\Theta(m)\delta\right),\ \forall\delta \in \Omega. \tag{4.25}$$

In Problem 3, vector L denotes the transmission loss vector $\forall b \in \mathscr{B}$. Parameters f^+ and f^- are the vectors of line flow limits. Vectors P_d and P_u represent the deterministic and uncertain net injection vectors, respectively. Power balance condition originally defined as (4.2) is separated into deterministic and stochastic parts (4.22) and (4.23). The

same was done for line flow definition (4.24) and (4.25). Line flows have the form of the affine function $e_f + D_f\Delta$, where e_f is the deterministic part and D_f is the stochastic part. Line losses are also split into its deterministic part e_l and stochastic part D_l. From each node $k \in \mathcal{N}$, the set of outgoing branches O_k is defined as $\{b \in \mathcal{B} | b = (k, j), j \in \mathcal{N}\}$ and the set of incoming branches I_k as $\{b \in \mathcal{B} | b = (j, k), j \in \mathcal{N}\}$. Finally, x is a vector of line reactances.

The problem is that the POPF problem requires solving an infinite number of optimization problems (since the problem has to be solved $\forall \delta \in \Omega$) which is a robust optimization problem. One of the possible solutions of the POPF was presented in [84] applying the uncertainty immunized solution using the duality principle from [85]. The computationally tractable form of the problem presented in [84] is computed as a convex optimization problem and is solved in matter of seconds.

5

INTERVAL OPTIMIZATION IN POWER SYSTEMS

In Sections 4.1 and 4.2, point optimization methods forming the mainstream of power network optimization are presented. But what if the system operator does not want only the knowledge of the optimal point, he could also want to know whether the area around the optimal point given by standard LF/PLF, OPF/SCOPF, or POPF meets the power network constraints.

5.1. CLASSIC ERA

Interval optimization was not the main subject of interest. The main focus was placed on transmission line capacity determination due to the need of replacements or repairs. However, important theoretical work has been done in the area of steady state security regions.

5.1.1. POWER TRANSFER CAPACITY

The maximum transfer capacity of the power line can be increased by various factors, e.g., re-tensioning, re-conducting, using different conductor types, or modification of tower design. Relevant topic considering transmission branches transfer capacity has been studied in [86], [87],[88]. The problem of line sag and ampacity prediction and therefore the power line transfer capacity was studied in [89]. To determine the transfer capacity in real time, ampacity monitoring with PMUs [90] can be used. However, the power transfer capacity problem is based on monitoring of the network state and weather conditions with no optimization performed.

5.1.2. STEADY-STATE SECURITY REGIONS

The problem of finding power injection security regions was first published in [91] and [92]. Steady-state security region is a set of real and reactive power injections (load demands and power generations) for which the power flow equations and the security con-

straints imposed by equipment operating limits are satisfied. However, important simplifications have been done that limit the potential application of the method close to the neighborhood of the nominal network state. Security region based approach has been used in applications for security monitoring, planning and risk assessment of power systems [93]. In [94] and [95], the decoupled power flow equations and DC power flow equations are used respectively. For recent steady state security region tools, see [96] and [97].

5.2. MODERN ERA

In this section, the recently developed interval based optimization methods are presented. Recently developed methods correspond to the TSO needs. The system operator requires information regarding the maximum transfer capabilities, currently available transfer capabilities, reactive supply capacity of the wind generators. To allow fast and efficient computation of proposed methods, various approximation techniques are implemented and its exactness is tested.

5.2.1. AVAILABLE / TOTAL TRANSFER CAPABILITY

The problem concerning the transmission line capacity is denoted as Available Transmission / Transfer Capability (ATC) or Total Transmission / Transfer Capability (TTC) which can provide system operators useful information regarding the power power transfer possible between two nodes of the system without violating the security or system limits. This tool is very important in situations when the system operator wants to know the limits of possible power transmission between two lines, e.g., in case of an unexpected power injection from an intermittent source and the power needs to be directed to the customers without violating some of network limits.

The ATC problem is the determination of the largest additional amount of power above some base case value that can be transferred in a prescribed manner between two sets of buses: the source, in which power injections are increased, and the sink, in which power injections are decreased by an offsetting amount. Increasing the transfer power increases the loading in the network, and at some point causes an operational or physical limit to be reached that prevents further increase. The effects of contingencies are taken into account in the determination. The largest value of transfer power that causes no limit violations, with or without a contingency, is used to compute the TTC and ATC. As shown in Figure 5.1, network limits may be variable in time. ATC / TTC solution techniques are discussed in next paragraph

ATC solution algorithms The methods of computing ATC are using either power transfer distribution factors (PTDF)[99], [100] based on derivatives around the given operating point and may lead to unacceptable results when used at different operating points to calculate ATC. The second approach to calculate ATC is the continuation power flow [101],[102] requiring repeated solution of OPF. These methods yield accurate solution because they consider system non-linearity at control changes. The disadvantage is the repeated use of OPF resulting high computation times and inability to use in real-time. The third approach used to calculate ATC is optimal power flow as shown in [103]. The solution of a large OPF problem, however, can also be time consuming. A new approach

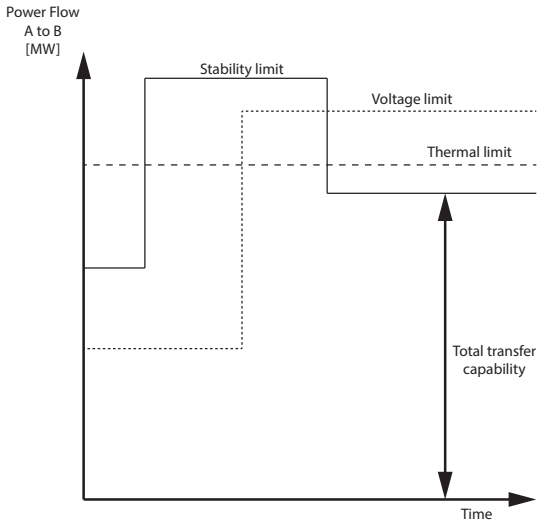

Figure 5.1: Determination of TTC. All network limits are transformed in power flow limits between points A and B. The dotted line represents voltage limitations, the dashed line represents thermal limits, and the solid line represents stability limits [98].

using the Newton-Raphson Load Flow Jacobian matrix overcoming the computational burden of repeated OPF computation was presented in [104].

ATC / TTC sensitiviy Further improvements were done considering the power system ATC sensitivity to network constraint modification. The usefulness of computed ATC can be enhanced if the sensitivity of each computed ATC is also computed [105].

5.2.2. GEOMETRY OF INJECTION REGIONS

Recently, an effort has been put into the determination of the geometry of power injection regions. The power flow injection region is the set of all vectors of feasible real power injections (both generations and withdraws) at the various buses that satisfy the given network and operation constraints. The limits on power flow injection regions are called the Pareto-front; these are the points on the boundary of the region for which one cannot decrease any component without increasing another component. In [106] and [107], Pareto-Fronts are convexified and the zero duality gap of a convex OPF relaxation is studied for tree networks. However, injection regions are formulated to yield a tractable convex formulation of the OPF problem. The intention of the authors is not the determination of optimal injection regions size. An illustration of power injection region for a line in a 2 node network with angle, thermal, and flow constraints under the assumption of fixed voltage magnitude is shown in Figure 5.2.

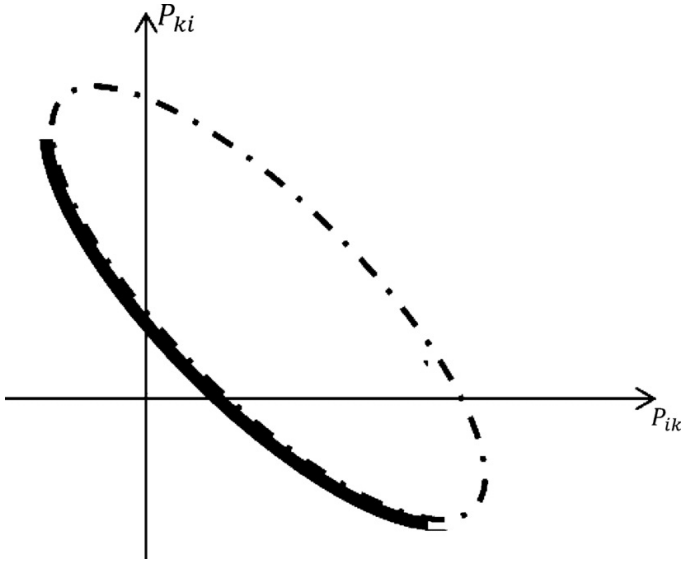

Figure 5.2: Power injection regions for two flows between nodes i and j of the system. Under the assumption of fixed voltage magnitudes, the admissible powers flowing through line are function of phase angles. The injection region is an elipse. The resulting Pareto-front is represented by the thick line. Source: [107]

5.2.3. POWER CAPABILITY

Another use of interval based methods in power network computation is called the power capability (PC). The reactive power requirements are defined, in grid code of several countries, with respect to the power factor as a function of the voltage at the point of common coupling (PCC) with the main grid. In some of the grid code requirements for wind farms, it is required that a wind farm owner should supply a P-Q diagram showing the regulation capability (steady state capability) for reactive power of the installation at the connection point. The system operator would like to know whether a wind turbine is able to fulfill transmission system reactive power requirements and how much it is able to provide reactive power support as an ancillary service. Intervals of reactive power capability available for ancillary services are making the wind turbines an important part of power networks enabling the frequency and bus voltage control [108], [109]. Figure 5.3 show a PQ diagram of a wind turbine.

5.2.4. POWER SUPPLY CAPACITY

In distribution systems, the power supply capacity (PSC) problem has been recently solved by Wang [110], Li [111], and Liu [112]. However, their work is not based on optimization methods but rather on empirical observations and a set of parameters determining the capacity of distribution network. The authors [110] use the N-1 criterion imposed on the substations supplying load to the customers. The method presented in [110] propose an arithmetic way to compute the power supply capacity in distribution system used in a district of Shanghai. An EMS collecting large amounts of data and assessing the power supply capacity is presented in [111].

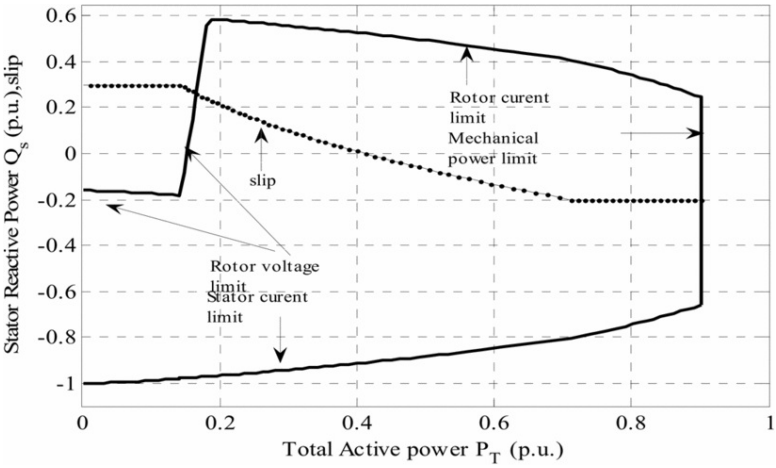

Figure 5.3: PQ diagram of a wind farm. The three limitations (rotor voltage, rotor current, and stator current) of doubly fed induction generator system for reactive power production/consumption have been considered. Source: [108]

5

5.2.5. CAPACITY-LOAD RATIO

In [112] the rational Capacity-Load ratio is computed using empirical methods and assessments. Capacity-Load ratio is a macro-technical indicator used to reflect total power supply capacity. Li [111] is using the Capacity-Load ratio with total load distribution in the network to asses total capacity of the distribution network.

6

REVIEW OF CURRENT OPTIMIZATION TOOLS

In Chapters 4 and 5, thorough review of most widely used point based and interval based optimization tools is given. This chapter summarizes the review process and assesses the current state of the art.

6.1. POINT OPTIMIZATION METHODS

Used tools in power network operation represent the main area of focus of academic and industry intelligence in power system optimization since 1968. New methods and elements were developed with regard to the topological, environmental, and social requirements. From the original OPF presented as Problem 1, the optimization methods have changed incorporating new elements, e.g., power storage, RES, or DSM. New requirements have also been imposed on security assessment of the power network defining Problem 2. Uncertainties can also be imposed on the demand side which comprises the DSM tool or on the supply side representing the RES. Problem 3 shows the possible implementation of POPF problem comprising energy storage and RES with an intermittent nature. It can be seen that the basic Problem 1 formulation has remained unchanged but new variables, model enhancements, and probabilistic or security extensions can be appended to OPF making the model more realistic with respect to changes in power network operation.

6.2. INTERVAL BASED OPTIMIZATION METHODS

Interval based optimization tools are not among the most widely used in the area of power system computation. The only method ordinarily used in many commercial packages is the ATC/TTC and the computations of ATC/TTC sensitivity. The steady state security region method has recently been adjusted but its drawbacks remain unsolved which prevents its use as a network operation tool. Other tools like PC, PSC, power transfer

capacity, and capacity load ratio are based on empirical methods and are rather used for power system monitoring and predictions.

6.3. CURRENT POWER NETWORK OPTIMIZATION TECHNIQUES

According to current state of information,

- main focus of the power system professional public is put on the research of point optimization methods giving only an optimal point without any additional knowledge about possible nearby violations,
- current developments in area of RES is making point optimization more difficult due to rise of uncertainties in power supply and create possible uncertain power flows in real-time operation,
- security and safety is becoming an important criteria of power network operation,
- point optimization methods are dealing with the uncertainty by introducing probabilistic and security extensions of the classical OPF problem, however, they provide no additional knowledge about the neighbourhood the optimal point,
- interval optimization methods have a limited importance in area of power network optimization. Using recent discoveries in semidefinite programming, computationally tractable formulation of interval based optimization problems is possible and allows definition of a new family of optimization problems.

The disadvantages of the classical OPF problem stated in previous sections making the system operator a blind follower of a complex algorithm, has led to an idea to develop an interval method giving the system operator an enhanced view on the power network. Moreover, the interval optimization method is giving him a choice from a secure set of points. The operator can then choose a point within the interval according the his expert knowledge. In this principle the interval optimization method would serve as a decision support rather than a one point solution given by OPF methods.

According to the knowledge of the power system operators this functionality would be desired. The system operator would like to know how far is the current operating point from the network operating limits and eventually how could he change the power injections at each node while maintaining power system security. Assessing the most critical parts of the power network could be also achieved by finding the nodes of the system with the smallest distance from the network operating limits.

As can be seen in Chapter 5, this description corresponds most closely to the Steady-state security regions method. However, this method is limited only to network states that lie in the neighbourhood of the nominal voltage since significant simplification were made. There is no formulation of a power system optimization tool focused on computing intervals of secure power injections of a defined power network that would determine the solution analytically.

7

INTERVAL OF SECURE INJECTIONS

Chapters 2 and 4 introduced historical development and most widely methods used in power network computation. Interval based method have been review in Chapter 5. The summary current state of the art is presented in Section 6. It has been emphasized that the present day transmission systems are operated closer to their security limits. Methods based on OPF/POPF used to clear intraday and spot electricity markets use models to price individual dispatch scenarios but fail to incorporate actual system safety, locational availability of regulation, and flexibility of corrective actions [113], [114]. Problem SCOPF presented in Section 4.2 gives answer how to plan efficient and secure redispatch and limited reconfiguration actions but do not consider nearby regions in the operating space [47]. Recently, fundamentals of social security cost evaluation weighed with system failure probability appended to SCOPF were proposed in [115].

7.1. INTRODUCTION

In this chapter, the fundamentals of an interval based method to compute intervals of necessary secure power injections are presented. The interval solution is chosen for the computational and practical reasons. In real world applications, network operation represent very complex multicriterial problem. Solution of a multicriterial problem gives a pareto-optimal solution which is not a single point. However, solution of SCOPF is giving only one optimal solution. This does not comply with the TSOs expectations. The idea is not to solve a complex optimization problem (OPF) with high computation time giving only a single optimal solution. Moreover, power networks are changing continuously therefore the real-time computation of a very complex problem would be needed. This shows to be computationally intractable [30].

The idea of this new method called Interval of Secure Injections (ISI) is based on an interval optimization principle and provide decision support for transmission system operators (TSOs). Chapter 5 describe the most cited and used interval optimization methods. This method represent an original way to compute power system nodal injection sets in which the injections are necessarily secure in terms of physical constraints. According to current state of knowledge, no similar methods were published.

This method computes intervals of secure nodal injections for each node of a given power system. The injections are limited by network operating conditions, i.e., nodal voltage limits and line current limits. Note, the following text was published in ENERGYCON 2016 [116] and extends the original ISI article presented in IFAC 2014 [117].

7.2. USED NOTATION

The following notation is used throughout. Capital letters are used to denote matrices and vector variables. Lower case letters are reserved for constants and parameter vectors. Script letters are reserved for sets. Any vector $x \in \mathbb{R}^n$ can be written as $(x_1, \ldots, x_n)$, as $(x_k)_{k\in\{1,\ldots,n\}}$, or as $x_{\{1,\ldots,n\}}$. The set of real numbers is denoted by $\mathbb{R}$ and the set of complex numbers is denoted by $\mathbb{C}$. Real and imaginary parts of a complex vector y are given by $Re(y)$ and $Im(y)$, respectively. The letter i is reserved for the imaginary unit. Transpose and complex conjugates of a complex vector y are given by y^T and y^*, respectively. The absolute value of a complex number y is given by $|y|$ and the p-norm of a vector x is given by $||x||_p$. For a set $\mathcal{X}$, the volume of the set is given by $\mu(\mathcal{X}) = \int_{\mathcal{X}} dx$, the cardinality is given by $|\mathcal{X}|$, and for two sets $\mathcal{X}_1, \mathcal{X}_2 \subseteq \mathcal{X}$ and mappings $T_1, T_2 : \mathcal{X} \to \mathcal{Y}$, $T_1\mathcal{X}_1 + T_2\mathcal{X}_2 = \{y \in \mathcal{Y} | y = T_1x_1 + T_2x_2, x_1 \in \mathcal{X}_1, x_2 \in \mathcal{X}_2\}$. An n-dimensional closed interval, a Cartesian product of 1-dimensional closed intervals from x_k^- to x_k^+, is denoted by $[x_k^-, x_k^+]$. A vector of ones with dimension of n is denoted by $\mathbf{1}^n$. The operator $\otimes$ is reserved for the Kroenecker product.

The network is described by a directed graph where each node harbours a potential load or a generator unit and each branch corresponds to a power line or a transformer. The set of nodes is given by the finite set $\mathcal{N} = 1, \ldots, n$ and the set of branches is defined by the set $\mathcal{B} \subset \mathcal{N} \times \mathcal{N}$. Possible network topologies are given by the finite set $\mathcal{T} = 0, 1, \ldots, t$. For a given $\tau \in \mathcal{T}$, $\mathcal{B}_\tau \subseteq \mathcal{B}$. The index $0 \in \mathcal{T}$ denotes the nominal network topology. Node 1 is reserved for the slack bus, where the voltage is held constant and the injected power is adjusted to meet the network demand. The set of nodes with controllable injections (e.g. generators providing ancillary services) but excluding the slack is denoted by $\mathcal{G} \subset \mathcal{N}$ and has the cardinality g. The set of nodes with uncontrollable injections (e.g., standard loads or renewable energy sources) is denoted by $\mathcal{L} \subset \mathcal{N}$. The two sets $\mathcal{G}$ and $\mathcal{L}$ satisfy $\mathcal{L} \cap \mathcal{G} = \emptyset$, $\mathcal{L} \cup \mathcal{G} = \mathcal{N} \setminus \{1\}$. The network admittance matrix is denoted by $Y \in \mathbb{C}^{n\times n}$.

7.2.1. NETWORK VARIABLES

It is assumed the network is operating under normal conditions under which the single phase model is applicable. Each node $k \in \mathcal{N}$ is associated with a voltage $V_k \in \mathbb{C}$ and an injected power $P_k + iQ_k$. It is often more convenient to list the real and imaginary parts of V separately in a real vector $X = (Re(V), Im(V))$ and the real and imaginary parts of the injected powers in a real vector $Z = (P, Q)$. Each branch $b \in \mathcal{B}$ is associated with a power flow $I_b \in \mathbb{C}$.

Distinction is made between free injections (those that are not controllable) and controllable injections. Uncontrollable injections at nodes in $\mathcal{L}$ are assumed to be contained in a set

$$\mathcal{Z}_L = \{(P_\mathcal{L}, Q_\mathcal{L}) \,|\, (P_k, Q_k) \in T_k[z_k^-, z_k^+], k \in \mathcal{L}\},$$

where the bounds $z_k^-, z_k^+ \in \mathbb{R}^2$ as well as the orthonormal matrix $T_k \in \mathbb{R}^{2\times 2}$ are known.

Definition 1 (Nominal Operating Point) *The network has a nominal operating point x_0 that is fixed for all topologies and represents the expected network state for the planning horizon. The realised state at the end of this horizon is defined in terms of deviations from this operating point, $X = x_0 + \Delta$. By the definition of the slack bus, $\Delta_1 = \Delta_n = 0$.*

Definition 2 (Network Operating domain) *Let the state of the network be described by $X = (Re(V), Im(V))$. The network operating domain is the set $\mathcal{Y}_S \subseteq \mathbb{R}^{2n}$ such that the network satisfies the following voltage quality constraints constraints*

$$x_k^- \leq X_k \leq x_k^+, \forall k \in \{1, \ldots, 2n\}. \tag{7.1}$$

The network operating domain represents a set of admissible nodal voltage deviations. In practice, system operators hold the system within given voltage limits $x^-, x^+ \in \mathbb{R}^{2n}$ to prevent voltage quality issues.

Definition 3 (Network Security Domain) *Let the state of the network be described by $X = (Re(V), Im(V))$. The network security domain is the set $\mathcal{X}_S \subseteq \mathbb{R}^{2n}$ such that, for all $X \in \mathcal{X}_S$, the network satisfies the following physical constraints:*

$$|I_b| \leq i_b^+, \forall b \in \mathcal{B}. \tag{7.2}$$

The exact formulation of the network security domain is not important for the results of this paper. Hence, the above defined conditions can be easily expanded to account for other physical constrains or contingency scenarios.

7.3. PROBLEM DEFINITION

Power injections, for all $k \in \mathcal{N}$, are computed from X by the formula from [118]

$$P_k = Z_k = X^T Y_k X, \tag{7.3}$$

$$Q_k = Z_{k+n} = X^T Y_{k+n} X, \tag{7.4}$$

where the matrices Y_k are defined as

$$Y_k = \begin{pmatrix} e_k Re(y_k) & -e_k Im(y_k) \\ e_k Im(y_k) & e_k Re(y_k) \end{pmatrix}, \tag{7.5}$$

$$Y_{k+n} = \begin{pmatrix} -e_k Im(y_k) & -e_k Re(y_k) \\ e_k Re(y_k) & -e_k Im(y_k) \end{pmatrix}, \tag{7.6}$$

with $\{e_k\}_{k \in \mathcal{N}}$ being the set of standard basis vectors in $\mathbb{R}^n$ and y_k being the kth row of the admittance matrix Y.

The general formulation of an interval method addressed at the beginning of the chapter is defined in this section. First, the definition of a general problem is introduced. It will be shown that the solution of General ISI Problem is NP-hard therefore a simplified version of the problem is formulated to achieve computationally tractable solution.

7.3.1. GENERAL PROBLEM

The General ISI problem is defined next.

Problem 4 *Consider the network security domain $\mathcal{X}_S$, the network operating domain $\mathcal{Y}_S$, and the set of injections from the free buses $\mathcal{Z}_L$. Find a set of secure injections $\mathcal{Z}_G^*$ satisfying*

$$\begin{aligned}
&\mathcal{Z}_G^* = \text{argmax}\,\mu(\mathcal{Z}_G), \text{ subject to} \\
&\mathcal{Z} = \left\{(P,Q) \,|\, \left(P_\mathcal{G}, Q_\mathcal{G}\right) \in \mathcal{Z}_G, (P_\mathcal{L}, Q_\mathcal{L}) \in \mathcal{Z}_L\right\}, \\
&\mathcal{Z}_G = \left\{\left(P_\mathcal{G}, Q_\mathcal{G}\right) \,|\, (P_k, Q_k) \in T_k[z_k^-, z_k^+], k \in \mathcal{G}\right\}, \\
&\mathcal{Z} \subseteq \{Z | \exists X \in \mathcal{Y}_S, Z_k = X^T Y_k X, \\
&\quad k \in \{1,\ldots,2n\}\} \implies \\
&\mathcal{Z} \subseteq \{Z | \exists X \in \mathcal{X}_S, Z_k = X^T Y_k X, k \in \{1,\ldots,2n\}\},
\end{aligned} \tag{7.7}$$

under the following assumptions:

A1: $\mathcal{X}_S = \{X | X = x_0 + \Delta, D\Delta \leq d\}$: the network security domain is taken to be a bounded convex polytope, where the slack bus constraint $\Delta_{\{1,n\}} = 0$ holds,

A2: the network operating domain $\mathcal{Y}_S$ is described by the Cartesian product of intervals $[x_k^-, x_k^+]$, $\forall k \in \{1,\ldots,2n\}$. The system operator holds nodal voltages inside the network operating domain,

A3: the transformation mappings $T_k, k \in \mathcal{G}$, are orthonormal and fixed,

The set $\mathcal{Z}_S = \left\{(P,Q) \,|\, \left(P_\mathcal{G}, Q_\mathcal{G}\right) \in \mathcal{Z}_G^*, (P_\mathcal{L}, Q_\mathcal{L}) \in \mathcal{Z}_L\right\}$ is referred to as the interval of secure injections.

The input to the ISI problem is the network security domain $\mathcal{X}_S$, the network operating domain $\mathcal{Y}_S$, and the admittance matrix Y. The output is the set of secure injections $\mathcal{Z}_G^*$, defined by the Cartesian product of intervals $[z_k^-, z_k^+] \subset \mathbb{R}^2$, for all $k \in \mathcal{G}$ in the range space of the orthonormal matrix T_k. Hence, $\mathcal{Z}_G^*$ is itself an interval in $\mathbb{R}^{2g}$. The choice of intervals for the set of secure injections has both computational and practical reasons. Generators may be renewable energy sources, whose power injections are influenced by environmental conditions. Generators may be ancillary service providers or sources redispatched in preventive or corrective actions, whose operation is limited by complex physical constraints dependent on internal hardware limitations. Coordination of such actions in real power systems is performed by advanced systems, e.g., SCADA/EMSs that increase the coordination capability. The intervals are not defined in the standard basis. Instead, they are defined in a rotated coordinate frame to capture potential power factor settings of different devices.

Above, the optimization is carried out over the variables $z_k^+, z_k^-, T_k, k = \{1,\ldots,2n\}$. The resulting problem seeks to find the limits of injection in all directions and hence is more general than the well known AC OPF problem with a linear criterion, which seeks to maximise injections projected in a single direction. The AC OPF problem is known to be NP hard [118] suggesting the ISI problem is not easily solvable without introducing simplifying assumptions A1-A3 that are described next.

The first main simplification is in A1. In practice, one may consider unions of polytopes covering the actual domain with some level of accuracy and repeat the analysis for each polytope separately. A2 represents another important simplification. To maintain voltage quality and system safety, system operators hold nodal voltages within known limits represented by $\mathcal{Y}_S$. The voltage quality is not guaranteed by the solution of the ISI problem but remains in competence of the system operator. A3 includes the third considerable simplification. Coordination of active and reactive power outputs provided by SCADA/EMSs is commonly performed through power factor settings, whose limits are known. In the case study, the nominal power factor is used to a priori compute the matrices T_k.

7.3.2. ISI

In the next section, an approximate solution of Problem 4 is presented. The solution involves two basic steps each solving one of the subproblems defined below.

The approximate solution requires a definition of the convex envelope for power injections that contains upper and lower bounds on power injections with respect to a given network operating domain $\mathcal{Y}_S$. Then for all $k \in \{1,\dots,2n\}$, the power injection Z_k is constrained by lower and upper bounds represented by $\ell \in \{1,\dots,l\}$ inequalities satisfying

$$b^-_{k,\ell} + A^-_{k,\ell}\Delta \le Z_k \le b^+_{k,\ell} + A^+_{k,\ell}\Delta, \forall \Delta \in \mathcal{Y}_S,$$

The convex envelope is described by a matrix

$$A^{\pm} = [A^-, -A^+]^T \in \mathbb{R}^{a\times 2n}, a = 4nl. \tag{7.8}$$

Matrices A^- and A^+ together with b^- and b^+ represent a collection of lower and upper bounds on power injections in an affine form and are only valid for $\Delta \in \mathcal{Y}_S$. The exact method for the computation of the power injection bounds is not important for results in this paper.

The convex envelope is used to derive sufficient conditions for (7.7). For all $k \in \{1,\dots,2n\}$ and $\ell \in \{1,\dots,l\}$

$$\Delta \in \{\Delta | A^{\pm}\Delta \le z^{\pm}\} \implies \Delta \in \mathcal{X}_S, \tag{7.9}$$

where $z^{\pm} = [-b^-, b^+]^T + [z^+ - z_0, -z^- + z_0]^T \otimes \mathbf{1}^l$.

Using Assumption 1, the implication in (7.9) can be rewritten as

$$A^{\pm}\Delta \le z^{\pm} \implies D\Delta \le d. \tag{7.10}$$

The dual formulation is as follows. If there exists a Lagrange multiplier $\alpha \ge 0$ such that

$$\alpha A^{\pm} = D, \tag{7.11}$$
$$\alpha z^{\pm} \le d, \tag{7.12}$$

then the (7.10) holds. Note, since both α and $z^{\pm}$ are optimization variables, the resulting dual problem is non-convex.

To solve the non-convex problem defined in (7.12), a two-step heuristic solution is presented. In step 1, the below problem is solved to compute the Lagrange multiplier α. To reduce the number of optimization variables, optional sets $\mathscr{I}$ and $\mathscr{J}_i$ are introduced. The sets will be further defined in the next section as a part of the modular solution.

Problem 5 *Consider the convex envelope described by the matrix $A^{\pm}$, a convex bounded polytope $\mathcal{D}$ described by the pair $(D,d), D \in \mathbb{R}^{m\times 2n}, d \in \mathbb{R}^m$. Find the Lagrange multiplier $\alpha^* \in \mathbb{R}^{m\times 4nl}$ that solves the following optimization problem.*

$$\begin{aligned} &\min_{\alpha} \sum_{i}^{m}\sum_{j}^{a} \alpha_{ij}, \text{ subject to} \\ &\alpha A^{\pm} = D, \\ \\ &\alpha_{i,j} \geq 0, \text{ if } i \in \mathscr{I}, j \in \mathscr{J}_i, \\ &\alpha_{i,j} = 0, \text{ otherwise.} \end{aligned} \tag{7.13}$$

The problem is similar to the family of basis selection problems [119] it is a linear program and can be either solved as a one optimization problem or a set of optimization problems such that each row of α is computed separately.

In step 2, the below problem is solved to compute limits on the power injections z^+ and z^- for the Lagrange multiplier $\alpha = \alpha^*$.

Problem 6 *Consider a set $\mathcal{G} \subset \mathcal{N}$, the Lagrange multiplier α, a convex bounded polytope $\mathcal{D}$ described by the pair (D,d), and a nominal injection point z_0. Suppose the parameters z_k^- and z_k^+ are given for all nodes $k \in \mathcal{N}\setminus\mathcal{G}$. Then find the injection limits $z_{\mathcal{G}}^{-,*}, z_{\mathcal{G}}^{+,*}$ that solve the following optimisation problem:*

$$\begin{aligned} &\max_{z_{\mathcal{G}}^-, z_{\mathcal{G}}^+} \prod_{k\in\mathcal{G}} \mu([z_k^-, z_k^+]), \text{subject to,} \\ &\quad \alpha z^{\pm} \leq d, \\ &\quad z^- \leq z_0 \leq z^+. \end{aligned} \tag{7.14}$$

Given the Lagrange multiplier α^* from Problem 5, the non-convex constraint is transformed into a system of linear equations. Subsequently, if we take the logarithm of the utility function, Problem 6 is then converted into a convex optimization problem.

7.3.3. LINEAR ISI

This section focuses on computing of ISI for a special case in which the network operating domain $\mathcal{Y}_S$ comprises only the nominal state X_0, i.e. $x^- = x^+ = x_0$ and $\mathcal{Y}_S = \{x_0\}$. The convex envelope in $\mathcal{Z}$-space (7.8) comprises a single point x_0. Considering this assumption, Lemma 1 is used to obtain the optimal solution α^* and hence controllable injection limits $z_{\mathcal{G}}^{-,*}, z_{\mathcal{G}}^{+,*}$ in Problem 7.

Problem 7 *Consider a given set of controllable nodes $\mathcal{G} \subset \mathcal{N}$, a convex bounded polytope $\mathcal{D}$, matrix A, the nominal point x_0, injection limits z^- and z^+ for all nodes $k \in \mathcal{L}$. Then the*

task of finding controllable injection limits $z_{\mathcal{G}}^{-,*}, z_{\mathcal{G}}^{+,*}$ is given by the following optimization problem

$$\begin{aligned} & \max_{z_{\mathcal{G}}^{-}, z_{\mathcal{G}}^{+}} \prod_{k \in \mathcal{G}} \mu([z_k^-, z_k^+]), \\ s.t. \quad & (D(A)^{-1})^+ z^+ - (D(A)^{-1})^- z^- \le d, \\ & z^- \le z_0 \le z^+. \end{aligned} \tag{7.15}$$

The motivation for this simplification is similar to the traditional DC PF analysis, which is based on the idea that real power dispatch and power market analysis require limited accuracy but lay the great emphasis on computational speed [4]. The application of this method in the area of ancillary services is shown in Chapter 10.

Lemma 1 *Let $A^- = A^+ = A$ be the full rank square matrix and $b = 0$. The optimal solution α_i^*, $i = 1, \ldots, 4nl$, minimizing the utility function of Problem 5 subject to the equality constraints (7.13) is given as*

$$\alpha^* = \begin{bmatrix} (DA^{-1})^+ \\ (DA^{-1})^- \end{bmatrix}, \tag{7.16}$$

where $(DA^{-1})^+ = \max(DA^{-1}, 0)$ and $(DA^{-1})^- = -\min(DA^{-1}, 0)$.

Proof of Lemma 1: If $A^+ = A^- = A$ is regular matrix, then there exists maximally one solution of eq. (7.13). Let the vector α be divided into α^+ and α^-, corresponding to matrix A^+ and A^-, respectively, the equality constraint (7.12) can be expressed as

$$[\alpha^+, \alpha^-] \begin{bmatrix} A \\ -A \end{bmatrix} = D. \tag{7.17}$$

or equivalently

$$pA = D. \tag{7.18}$$

where $p = \alpha^+ - \alpha^-$.

The solution of this matrix equation is

$$p = DA^{-1}. \tag{7.19}$$

For each element of p,

$$p_i = \alpha_i^+ - \alpha_i^-, \quad c = 1, \ldots, m. \tag{7.20}$$

Let the $\hat{\alpha}^+$, $\hat{\alpha}^- > 0$ be a feasible solution of (7.19). Then, for each $i \in 1, \ldots, m$ there exists a positive value $\epsilon > 0$ such that

$$\tilde{\alpha}_i^+ = \hat{\alpha}_i^+ - \epsilon \ge 0, \tag{7.21}$$

$$\tilde{\alpha}_i^- = \hat{\alpha}_i^- - \epsilon \ge 0. \tag{7.22}$$

Since we are minimizing, the minimum value of utility function is reached if the value of ϵ is maximum feasible. From (7.21) and (7.22), the optimal value is therefore equal to

$$\epsilon_{max} = \min(\hat{\alpha}_i^+, \hat{\alpha}_i^-). \tag{7.23}$$

Consequently, either $\tilde{\alpha}_i^+$ or $\tilde{\alpha}_i^-$ becomes equal to 0 and from (7.20)

$$(\alpha_i^+)^* = \max(p_i, 0), \tag{7.24}$$
$$(\alpha_i^-)^* = -\min(p_i, 0). \tag{7.25}$$

Finally, substituting to p_i from (7.19) and rewriting the relations in matrix form

$$\alpha^+ = \max\left(DA^{-1}, 0\right), \tag{7.26}$$
$$\alpha^- = -\min\left(DA^{-1}, 0\right), \tag{7.27}$$

which completes the proof. ■

Additionally, if the utility function has a form of sum of logarithms, Problem 7 becomes convex.

The calculated bounds $z_{\{k\}}^-$ and $z_{\{k\}}^+$ ensure that any injection $z_{\{k\}}$, $z_{\{k\}}^- \leq z_{\{k\}} \leq z_{\{k\}}^+$, $\forall k \in \mathcal{G}$, does not cause an unsafe network state, as long as the injections at the other nodes are also within their prescribed bounds.

7.4. TESTING AND RESULTS

The proposed ISI method will be demonstrated on two widely used test networks. In both cases, the slack bus is located at node 1 and all other nodes are taken to be controllable. Obviously, allowing all nodes is exaggeration. However, it makes possible to carry out a comprehensive study providing properties of all nodes in the network. Test networks are considered in the per unit scale with the base apparent power of 100 MVA. Nodal voltage constraints are approximated by ±10% intervals around the nominal state x_0, which is calculated by the MATPOWER [15]. For simplicity, orthonormal matrix $\mathbf{T}_k$ will not be considered in examples

Note, all computations are performed in MATLAB using the SDPT3 solver [120].

For sake of clarity, a simple 4-bus test network shown in Figure 7.1, taken from [121], is used to illustrate the impact of selected NOD on computed ISI.

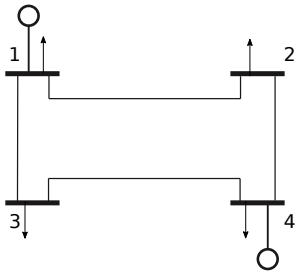

Figure 7.1: The 4-bus test system.

Figure 7.2 shows the computed ISI for the 4-bus test network. While cyan rectangles represent sets of secure injections calculated considering point-wise NOD, the blue rectangles denote the solution of ISI in case of NOD given by ±10% intervals around the nominal state x_0, i.e. $x^+ = 0.1|x_0|$ and $x^- = -0.1|x_0|$. These rectangles provide to the operator information about range of possible secure corrective actions, which will not cause instability of network, and distance of operating point from security margin.

It can be seen, that increasing NOD causes reduction of the resulting network security domain. This phenomenon is connected with expanding the area, where the validity of results is guaranteed. The point-wise NOD is applicable mainly for the needs of trading on power markets, where the limited validity of results is not crucial.

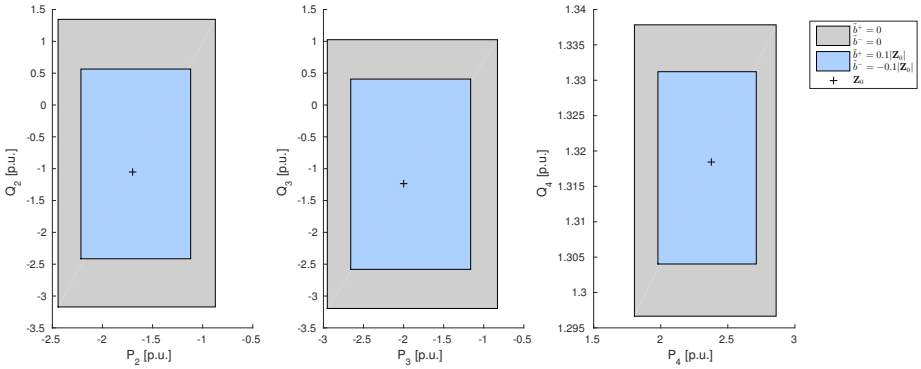

Figure 7.2: Computed intervals of secure power injections for controllable nodes of the 4-bus test network.

The IEEE 30-bus test system, see Figure 7.3, is used in order to demonstrate the applicability and computation tractability for a medium sized power network. Power injections, impedances, line flow constraints and topology of the system are taken from [122].

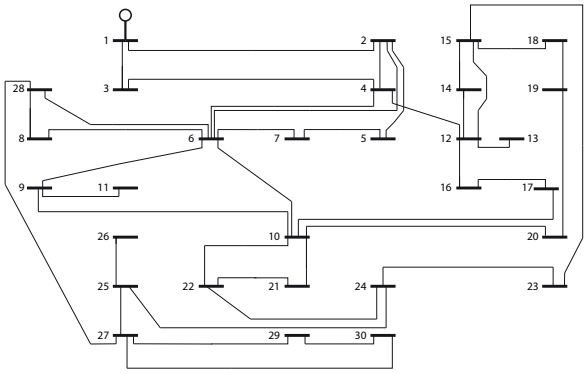

Figure 7.3: The IEEE 30-bus test system.

Finally, time requirements for different power networks are compared in Table 7.1.

Table 7.1: Comparison of computational time of the ISI method.

System	Branches	Time [s]
4-bus test network	4	0.06
IEEE-30 bus	40	0.65
IEEE-118 bus	186	1.44
Illinois-200 bus [123]	245	63.39

The comparison was performed on PC with processor Intel Core i5-4300U CPU @ 1.90GHz×4 and 16GB RAM.

8

ISI ENHANCEMENTS AND APPLICATIONS

The ISI method introduced in Section 7 represents a general interval optimization tool usable in power system operation. Information given in this section show possible enhancements of the ISI method increasing its scalability and robustness making it applicable in real time power system operation.

Additionally, possible new applications of the ISI method in power system operation are presented. The ISI method can be reformulated to yield results on multiple network topologies and can be potentially used as a power network reconfiguration tool with a chosen security criterion.

8.1. SUITABLE ISI ROTATION AND NODE COORDINATION

As defined in Chapter 7, Problem 6, Assumption A3, the rotation matrix $\bar{T}$ is fixed in the simplified ISI problem. Recall, the expression for real and imaginary power injection $P_k, Q_k, k \in \{1,\dots,2n\}$ is given by

$$\begin{pmatrix} Z_k \\ Z_{k+n} \end{pmatrix} = \begin{pmatrix} P_k \\ Q_k \end{pmatrix} = T_k \begin{pmatrix} X^T Y_k X \\ X^T Y_{k+n} X. \end{pmatrix},$$

where $T_k = \bar{T}_{\{k,k+n\},\{k,k+n\}}$ .However, the form of the rotation matrix $\bar{T}$ determines the final volume of ISI. Therefore, $\bar{T}$ is also to be determined to obtain sufficiently large and robust injection intervals. Figure 8.1 shows ISI solutions with different rotation matrices $\bar{T}$ for chosen buses of the IEEE 14 bus test system. It can be seen that each rotation yields different ISI solution. This phenomena requires further attention and will be studied further.

Another important fact is that current rotation matrix $\bar{T}$ is block diagonal suggesting the coordination between nodes is not considered. The inter-node coordination could be potentially achieved by coupling of the blocks in $\bar{T}$.

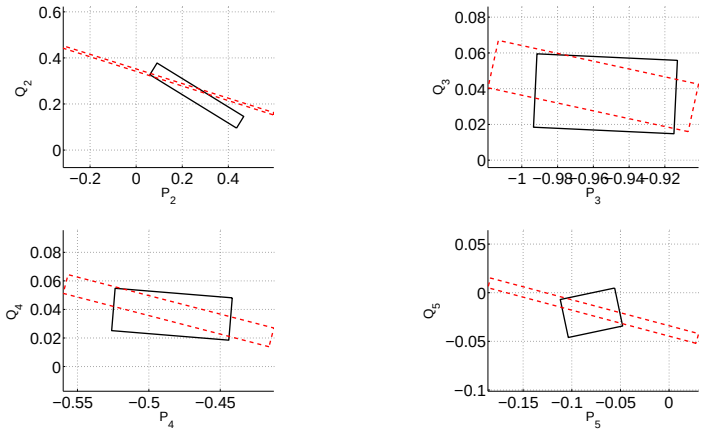

Figure 8.1: ISI for nodes 2,3,4, and 5 of the IEEE 14 bus test system. Two types of rotation are considered. The black line represents rotation with respect to the power factor, the red dashed line represents rotation with respect to derivation of the nominal power injection to the nodal voltage amplitude. It can be seen that the red dashed rotation yields ISI with higher volume but the robustness of ISI is limited (e.g. reactive power at node 2).

8.2. EXTENDING ISI WITH PQ DIAGRAMS

In real world power network operation, PQ diagrams [124] are commonly used to define the area of generators operation limits. The ISI Problem could be extended to account for these limitations and search for the injection intervals within PQ diagrams given by system operators. The limits imposed on real and imaginary powers are assumed to be contained in a known set

$$\mathcal{Z}_Z = \{Z | D_Z Z \leq d_Z\},$$

where D_Z and d_Z are known, such that,

$$\mathcal{Z}_\mathcal{G}^* \subseteq \mathcal{Z}_Z.$$

8.3. TOOLS FOR COMPUTING N-1 SECURE REDISPATCH AND RECONFIGURATION ACTIONS

The ISI method can be reformulated as a tool for a fast and secure network redispatch or reconfiguration. Current methods dealing with network reconfiguration are using the mixed integer linear programming [125] or mixed inter non-linear programming [126]. These methods show to be very time consuming and enable only limited number of reconfiguration layouts. Moreover, the current methods are not dealing with the transition between the states. Existing computation tools in power system operations evaluate individual scenarios for power injection and network configuration but fail to consider

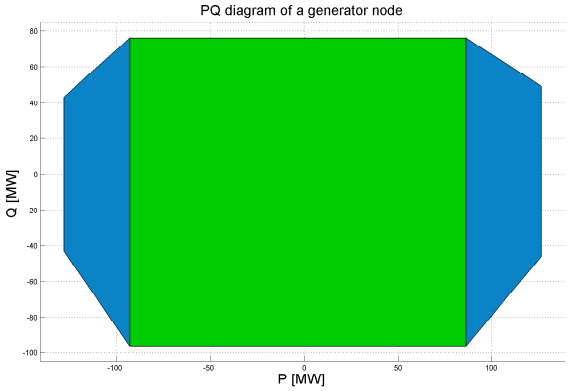

Figure 8.2: Example of PQ diagram for a node in the 843 bus CEPS system. The PQ diagram is comprised of three parts, two trapezoids shown in blue, and a rectangle shown in green. The ISI rectangle for this $\mathcal{G}$-node must lie inside this polytope.

nearby regions in the operating space. The only given information is that the reconfiguration is or is not possible. The transition can, however, lead to temporary dangerous voltages close to or even surpassing the borders of the network security domain. The interval based ISI method can be reformulated to a security oriented form potentially applicable in power system redispatch and reconfiguration.

Above the standard ISI network model, we define possible network topologies which are given by the finite set $\mathcal{T} = 0, 1, \ldots, m$. For a given $\tau \in \mathcal{T}$, $\mathcal{B}_\tau \subseteq \mathcal{B}$. The index $0 \in \mathcal{T}$ denotes the nominal network topology. For a topology $\tau \in \mathcal{T}$, the network security domain is written as $\mathcal{X}_{S,\tau}$ and the network admittance matrix is denoted by Y_τ. The ISI problem which solves the network reconfiguration problem is defined next.

Problem 8 (General $\mathcal{T}$-ISI) *For all $\tau \in \mathcal{T}$, consider the network security domain $\mathcal{X}_{S,\tau}$ and the set of injections from the free buses $\mathcal{Z}_L$. Find a set of secure injections $\mathcal{Z}_G^*$ satisfying*

$$
\begin{aligned}
\mathcal{Z}_G^* &= \underset{z_{\mathcal{G}}^-, z_{\mathcal{G}}^+}{\operatorname{argmax}} \mu(\mathcal{Z}_G), \text{ subject to} \\
\mathcal{Z} &= \left\{(P,Q) \middle| \left(P_{\mathcal{G}}, Q_{\mathcal{G}}\right) \in \mathcal{Z}_G, (P_{\mathcal{L}}, Q_{\mathcal{L}}) \in \mathcal{Z}_L\right\}, \\
\mathcal{Z}_G &= \left\{\left(P_{\mathcal{G}}, Q_{\mathcal{G}}\right) \middle| (P_k, Q_k) \in T_k[z_k^-, z_k^+], k \in \mathcal{G}\right\}, \\
\mathcal{Z} &\subseteq \{Z | \forall \tau \in \mathcal{T}, \exists X_\tau \in \mathcal{Y}_{S,\tau}, Z_k = X_\tau^T Y_{\tau,k} X_\tau, \\
&\quad k \in \{1, \ldots, 2n\}\} \implies \qquad (8.1) \\
\mathcal{Z} &\subseteq \{Z | \forall \tau \in \mathcal{T}, \exists X_\tau \in \mathcal{X}_{S,\tau}, Z_k = X_\tau^T Y_{\tau,k} X_\tau, \\
&\quad k \in \{1, \ldots, 2n\}\}. \qquad (8.2)
\end{aligned}
$$

The set $\mathcal{Z}_S = \left\{(P,Q) \middle| \left(P_{\mathcal{G}}, Q_{\mathcal{G}}\right) \in \mathcal{Z}_G^*, (P_{\mathcal{L}}, Q_{\mathcal{L}}) \in \mathcal{Z}_L\right\}$ is referred to as the interval of secure injections. The matrices T_k are rotation matrices satisfying $T_k^T T_k = I$.

One of the possible $\mathcal{T}$-ISI application is the reconfiguration planning with the N-1 security criterion. The problem definition, computationally tractable solution, and testing

on the IEEE 14 bus test system was thoroughly described in [127].

An example of $\mathcal{T}$-ISI performed on IEEE 14 bus test system [128] is given in Figure 8.3. The intervals of secure injection are plotted for the set of controllable nodes $\mathcal{G} = \{2,3,6,8\}$. Additional information about the parameters of the network can be found in [127].

Figure 8.3 shows the intervals of secure injection with the certificate of N-1 security, i.e., if the system operator redispatches generator outputs at controllable nodes into these intervals, the network will be N-1 secure.

Given a nominal operating point, the method parametrises a set of injections that necessarily comply with a general network security criteria for AC systems as well as with the N-1 security criteria. The advantage of security constrained optimal point methods (represented for example by SCOPF) lie in their ability to find a better solution (e.g., in terms of economic cost or loss minimization) that may not be included in the injection intervals given by $\mathcal{T}$-ISI. Advantages of ISI compared with known operation support tools (based on point optimization) are potential enhancement of network robustness and broader decision support.

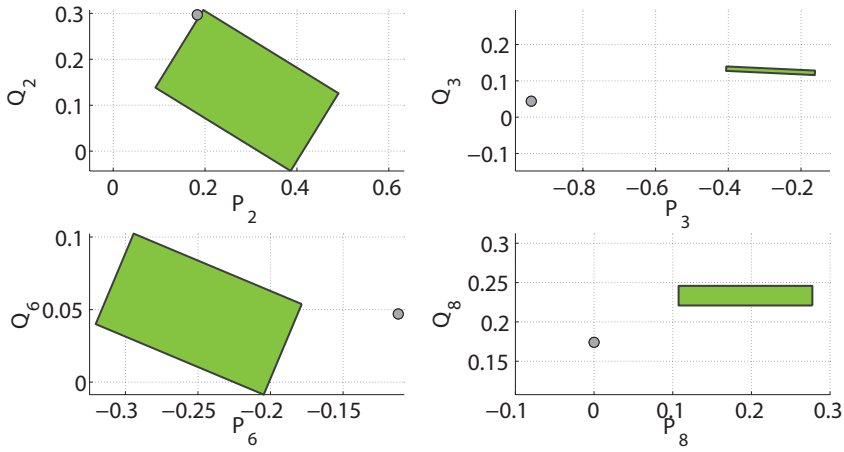

Figure 8.3: Intervals of secure injections with the certificate of N-1 security for the nominal topology 0 of the IEEE 14 bus test system for the set of controllable nodes $\mathcal{G} = \{2,3,6,8\}$. Nominal power injection points are represented by a grey shaded circle. The nominal injection points lie out of the interval of secure injections. Any redispatch to the green coloured injection intervals yields the N-1 secure solution. It is guaranteed that the redispatch from nominal injection point to injection intervals does not violate the physical constraints of the system.

9

MODULAR EXTENSION OF INTERVALS OF SECURE INJECTION

In this section a modular extension of the ISI method is formulated. Suppose, the system operator wants to perform marginal changes in the network, i.e., opening transmission lines or connecting nodes with a transmission line. The ISI method computes intervals of secure injection with respect to a given network topology. According to current definitions, the ISI method has to be recomputed to obtain a new solution for the reconfigured system. Computation of the intervals of secure injection can be time consuming in case of large scale transmission systems and the recalculation of the whole network in case of a marginal change in network topology is ineffective.

In this chapter, a new modular method which is able to track the marginal changes between nominal and reconfigured network topologies and adjust the nominal interval of secure injections is formulated. In order to comply with this methodology, we define a set $\mathcal{A}$ that contains nodes affected by the reconfiguration, i.e., if the system operator opens branch $b = (k, \ell) \in \mathcal{B}$ between nodes k and $\ell \in \mathcal{N}$, then $\mathcal{A}$ contains all nodes affected by this change (i.e., in terms of adjusted injection intervals). The set of unaffected nodes $\mathcal{U}$ comprises nodes with injection intervals unchanged. Note, the exact definition of the set $\mathcal{A}$ will be given further. We use the definition of network topologies $\mathcal{T}$ introduced in Section 8.3. In this problem, only the nominal topology 0 and reconfigured topology 1 are considered, i.e., $\mathcal{T} = \{0, 1\}$. For a topology $\tau \in \mathcal{T}$, intervals of secure injection are denoted by $\mathcal{Z}_{S_\tau}$, the network security domain by $\mathcal{X}_{S,\tau}$, the linear transformation matrix by A_τ, and the admittance matrix by Y_τ.

The idea is that the modular method denoted by Mod-ISI does not use the ISI method to recalculate the whole network but only performs changes in a relevant part of it, since most of the topology remains unchanged. We can track changes in topologies as a difference between admittance matrices and network security domains. This leads to a problem described in Section 9.1.

9.1. PROBLEM DEFINITION

Problem 9 (General Mod-ISI) *Suppose we have intervals of secure injection $\mathcal{Z}^*_{S_0}$, i.e., the Cartesian product of intervals $\left[\hat{z}_k^-, \hat{z}_k^+\right] \subset \mathbb{R}^2, k \in \mathcal{N}$ in the range space of the orthonormal matrix T_k computed by ISI for a given topology 0, then for a new topology 1, the set of injections from the free buses $\mathcal{Z}_L$, the set of affected nodes $\mathcal{A}$, and the set of unaffected nodes $\mathcal{U}$, we define $\mathcal{A} \cup \mathcal{U} = \mathcal{N} \setminus \{1\}$ and $\mathcal{A} \cap \mathcal{U} = \emptyset$. Find a set of secure injections $\mathcal{Z}_{S_1}$ satisfying*

$$
\begin{aligned}
\mathcal{Z}^*_A &= \underset{z^-_{\mathcal{A}}, z^+_{\mathcal{A}}}{\operatorname{argmax}}\, \mu(\mathcal{Z}_A), \textit{subject to} \\
\mathcal{Z}^*_{S_0} &= \left\{(P,Q) \,|\, (P_k, Q_k) \in T_k \left[z_k^-, z_k^+\right], k \in \mathcal{N}\right\}, \\
\mathcal{Z}_{S_1} &= \left\{(P,Q) \,|\, (P_k, Q_k) \in T_k \left[z_k^-, z_k^+\right], k \in \mathcal{U}, (P_{\mathcal{A}}, Q_{\mathcal{A}}) \in \mathcal{Z}_A\right\}, \\
\mathcal{Z}_A &= \left\{(P_{\mathcal{A}}, Q_{\mathcal{A}}) | \, (P_k, Q_k) \in T_k \left[\hat{z}_k^-, \hat{z}_k^+\right], k \in \mathcal{A}\right\}, \\
\mathcal{Z}_{S_1} &\subseteq \left\{Z | Z_k = X^T Y_{1,k} X, X \in \mathcal{Y}_S, k \in \{1, \ldots, 2n\}\right\} \implies \qquad (9.1) \\
\mathcal{Z}_{S_1} &\subseteq \left\{Z | Z_k = X^T Y_{1,k} X, X \in \mathcal{X}_{S,1}, k \in \{1, \ldots, 2n\}\right\}. \qquad (9.2)
\end{aligned}
$$

The input to the general Mod-ISI problem is the set of secure injections $\mathcal{Z}^*_{S_0}$, network topologies 0 and 1 (i.e., $\mathcal{T} = \{0, 1\}$) given by the admittance matrices Y_0 and Y_1, the network operating domain $\mathcal{Y}_S$, and the set of affected nodes $\mathcal{A}$. The output is the set of adjusted secure injections $\mathcal{Z}^*_A$, the Cartesian product of intervals $\left[\hat{z}_k^-, \hat{z}_k^+\right] \subset \mathbb{R}^2, k \in \mathcal{A}$ in the range space of the orthonormal matrix T_k.

In further text, the following assumptions are formulated.

Assumption 1 *Suppose, the system operator is allowed to perform only the reconfigurations that yield feasible network behavior (in terms of convergent load flow), i.e., the network is operated within its physical limits.*

Assumption 2 *The system operator does not change the settings of nodal voltage constraints.*

Note, all assumptions are realistic since the system operator will not willingly reconfigure the system to an insecure state. The maximum and minimum allowed voltage levels are usually predefined by legislative and corporal norms and cannot be manipulated by the system operator.

9.2. SOLUTION PROPOSAL

The illustration of problem solution using Mod-ISI is shown in Figure 9.1. The complexity of the Mod-ISI problem is significantly reduced when compared with ISI since

- Mod ISI does not require to compute Problem 5 for nodes in $\mathcal{U}$.
- ISI is computed at all nodes in $\mathcal{N}$, the ModISI method is developed adjusting the injection intervals only at the affected nodes $\mathcal{A}$ which speeds up the computation significantly.

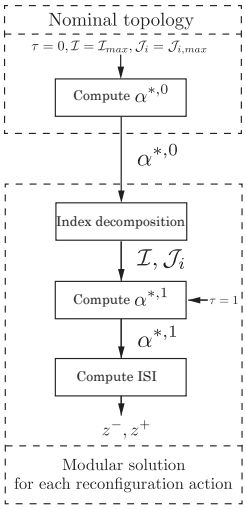

Figure 9.1: Flowchart for mod-ISI solution algorithm.

- Problem 5 is computed only for the set of affected nodes $\mathcal{A}$ which again speeds up the computation when compared with the ISI method.

9.3. MODULAR METHODS USING DUALITY PRINCIPLES

As shown in Section 7.3.2 and Chapter 9, computation of Problem 6 requires knowledge of constraints at all nodes of the system. But under assumptions stated in this Chapter, i.e., a marginal change in the power system is performed, it might be suitable not to work with intervals of secure injection at all nodes of the network but only at nodes affected by the reconfiguration. This would speed up the computation time and reduce the complexity of the problem.

In this section, the Mod-ISI Problem is solved under the set of assumptions given in Problem 6. We have a known power system with controllable nodes $\mathcal{G}$, free nodes $\mathcal{L}$, and topologies $\tau \in \mathcal{T} = \{0,1\}$, we define matrices $\hat{T} \triangleq A^{-1}_{\mathcal{N}\setminus\{1\},\mathcal{N}\setminus\{1\}}$, $\bar{D} = D_{\mathcal{N},\mathcal{N}\setminus\{1\}}$, $\tilde{D} \triangleq \bar{D}\hat{T}$, the vector of RHS d, nominal power injections z_0, and limits on free injections $\bar{z}^+_{\mathcal{L}}, \bar{z}^-_{\mathcal{L}}$. We define $\tilde{D}^+ \triangleq \max(\tilde{D}, 0)$ and $\tilde{D}^- \triangleq \min(\tilde{D}, 0)$. Mod-ISI Problem is computed for topology 1 and the ISI problem has already been solved for topology 0, i.e., intervals of secure injection at controllable nodes $\mathcal{G}$ for topology 0 are known.

We begin the derivation of Mod-ISI by recalling Problem 7 formulated in Chapter 7.

$$\max_{\bar{z}^+_{\mathcal{G}}, \bar{z}^-_{\mathcal{G}}} \prod_{i \in \mathcal{G}} \mu([\bar{z}^+_i - \bar{z}^-_i]), \tag{9.3}$$

subject to,

$$\tilde{D}^+(\bar{z}^+ - z_0) + \tilde{D}^-(\bar{z}^- - z_0) \leq d,$$
$$\bar{z}^+ \geq \bar{z}^-.$$

In further text, the criteria function (9.3) is approximated by a sum of injection intervals weighed by a parameter w. The new criteria function is shown in (9.4)

$$\max_{\bar{z}^+_{\mathcal{G}}, \bar{z}^-_{\mathcal{G}}} \sum_{i \in \mathcal{G}} w_i (\bar{z}^+_i - \bar{z}^-_i). \tag{9.4}$$

To study individual constraints of the network, the dual problem of ISI_1 is formulated. The Lagrangian takes the form

$$L(\bar{z}^+, \bar{z}^-, \lambda, \eta) = \left(w^T + \eta^T\right)\left(\bar{z}^+ - \bar{z}^-\right) - \lambda^T\left(\tilde{D}^+\bar{z}^+ + \tilde{D}^-\bar{z}^- - \tilde{D}z_0 - d\right).$$

We now collect the like terms

$$\left(w^T + \eta^T - \lambda^T\tilde{D}^+\right)\bar{z}^+ = 0,$$
$$\left(-w^T - \eta^T - \lambda^T\tilde{D}^-\right)\bar{z}^- = 0.$$

The dual problem is defined as

Problem 10 (d-ISI_1)

$$\min_{\lambda} \lambda^T\left(\tilde{D}z_0 + d\right), \tag{9.5}$$

subject to

$$w^T - \lambda^T\tilde{D}^+ \leq 0,$$
$$-w^T - \lambda^T\tilde{D}^- \geq 0,$$
$$\lambda \geq 0.$$

The purpose of using dual problem formulation is a suitable decomposition of the network to affected and unaffected parts of the network. Note, the ISI problem has been already solved for topology 0, the dual problem solution is therefore known as well. In the Mod-ISI Problem, the values of λ in the unaffected part of the network remains unchanged and recomputed in the affected part. This allows the following decomposition.

The dual variable λ is split into two parts such that $\lambda = [\lambda_{\mathcal{A}}, \lambda_{\mathcal{U}}]$. The part $\lambda_{\mathcal{A}}$ corresponds to the affected part of the network and stands for a variable, $\lambda_{\mathcal{U}}$ corresponds to the unaffected part of the network and is constant with values obtained from ISI for topology 0. In further text, for $\tau \in \mathcal{T}$, matrices $\tilde{D}$, $\bar{D}$, and $\hat{T}$ have been given topology subscript (e.g., for topology 1, the corresponding matrix is equal $\tilde{D}_1 = D_{1,\mathcal{N},\mathcal{N}\setminus\{1\}}$). The dual variable λ is split such that if

$$\tilde{D}_\tau \triangleq \begin{bmatrix}\tilde{D}_{\tau,\mathcal{A}} \\ \tilde{D}_{\tau,\mathcal{U}}\end{bmatrix}, \text{ then } \tilde{D}_\delta \triangleq \begin{bmatrix}\tilde{D}_{\delta,\mathcal{A}} \\ \tilde{D}_{\delta,\mathcal{U}}\end{bmatrix} \triangleq \begin{bmatrix}\tilde{D}_{1,\mathcal{A}} - \tilde{D}_{0,\mathcal{A}} \\ \tilde{D}_{1,\mathcal{U}} - \tilde{D}_{0,\mathcal{U}}\end{bmatrix}. \tag{9.6}$$

We now examine the structure of difference between $\tilde{D}_1$ and $\tilde{D}_0$ to determine the decomposition of the network to $\mathcal{A}$ and $\mathcal{U}$ parts.

The difference between matrices $\bar{D}_1$, $\bar{D}_0$ is defined as

$$\bar{D}_1 \triangleq \bar{D}_0 + \bar{D}_{\mathcal{D}}. \tag{9.7}$$

Rewriting (9.6), the difference is equal to

$$\begin{bmatrix} \tilde{D}_{\delta,\mathcal{A}} \\ \tilde{D}_{\delta,\mathcal{U}} \end{bmatrix} = \begin{bmatrix} \bar{D}_{1,\mathcal{A}}\,\hat{T}_1 \\ \bar{D}_{1,\mathcal{U}}\,\hat{T}_1 \end{bmatrix} - \begin{bmatrix} \bar{D}_{0,\mathcal{A}}\,\hat{T}_0 \\ \bar{D}_{0,\mathcal{U}}\,\hat{T}_0 \end{bmatrix}. \tag{9.8}$$

Using (9.7), the expression for difference can be written as

$$\begin{bmatrix} \tilde{D}_{\delta,\mathcal{A}} \\ \tilde{D}_{\delta,\mathcal{U}} \end{bmatrix} = \begin{bmatrix} \bar{D}_{\mathcal{D},\mathcal{A}}\,\hat{T}_1 \\ \bar{D}_{\mathcal{D},\mathcal{U}}\,\hat{T}_1 \end{bmatrix} + \begin{bmatrix} \bar{D}_{0,\mathcal{A}}\left(\hat{T}_1 - \hat{T}_0\right) \\ \bar{D}_{0,\mathcal{U}}\left(\hat{T}_1 - \hat{T}_0\right) \end{bmatrix}. \tag{9.9}$$

The difference shown in (9.9) is important for the definition of $\mathcal{A}$ and $\mathcal{U}$ sets. The idea of Mod-ISI is that the difference $\tilde{D}_{\delta,\mathcal{U}}$ is equal zero. To achieve this, the following equation must hold

$$\bar{D}_{\mathcal{D},\mathcal{U}}\,\hat{T}_1 + \bar{D}_{0,\mathcal{U}}\left(\hat{T}_1 - \hat{T}_0\right) = 0. \tag{9.10}$$

The first term can be easily set to zero since the structure of $\bar{D}$ is known. The term $\bar{D}_{\mathcal{D},\mathcal{U}}\,\hat{T}_1$ is zero, if the nodes on which the reconfiguration is performed are in the set $\mathcal{A}$. In this case $\bar{D}_{\mathcal{D},\mathcal{U}} = \mathbf{0}$. To make the second term equal to zero requires knowledge of the difference between $\hat{T}_1$ and $\hat{T}_0$. Note, $\hat{T}_\tau$ is equal to inverse of the matrix and its structure cannot be easily determined. However, the differences can be tracked and the set $\mathcal{A}$ can be expanded to obtain solution close to zero. In Section 9.4, the problem of determining the set of affected nodes is examined in detail and will require more attention. For further derivation, it is assumed that $\tilde{D}_{\delta,\mathcal{U}} \approx \mathbf{0}$. The determination of the set $\mathcal{A}$ should be constructed as a trade-off between the size of $\mathcal{A}$ (computation complexity) and the accuracy of the approximation error of the $\tilde{D}_{\delta,\mathcal{U}} \approx \mathbf{0}$ term (method accuracy).

We now continue with the derivation of Mod-ISI Problem under the assumption $\tilde{D}_{\delta,\mathcal{U}} \approx 0$. We use the decomposition of λ and $\tilde{D}$ introduced in (9.6) to rewrite Problem 10 to the form

$$\min_{\lambda_{\mathcal{A}}} \lambda_{\mathcal{A}}^T\left(\tilde{D}_{\mathcal{A}}\,z_0 + d_{\mathcal{A}}\right) + \lambda_{\mathcal{U}}^T\left(\tilde{D}_{\mathcal{U}}\,z_0 + d_{\mathcal{U}}\right), \tag{9.11}$$

subject to

$$\begin{aligned} w^T - \lambda_{\mathcal{A}}^T\tilde{D}_{\mathcal{A}}^+ - \lambda_{\mathcal{U}}^T\tilde{D}_{\mathcal{U}}^+ &\le 0, \\ -w^T - \lambda_{\mathcal{A}}^T\tilde{D}_{\mathcal{A}}^- - \lambda_{\mathcal{U}}^T\tilde{D}_{\mathcal{U}}^+ &\ge 0, \\ \lambda_{\mathcal{A}} &\ge 0. \end{aligned}$$

Recall, $\lambda_{\mathcal{U}}$ is a parameter obtained from the solution of the ISI Problem for topology 0 and Mod-ISI Problem is defined for topology 1. Note, the second term in (9.11) can be

omitted since it contains only constants. This problem is now converted back to primal problem using Lagrangian. The Lagrangian takes the form

$$L_D(\lambda_{\mathcal{A}},\kappa^-,\kappa^+,\psi) = \lambda_{\mathcal{A}}^T\left(\tilde{D}_{\mathcal{A}}z_0 + d_{\mathcal{A}}\right) + \left(w^T - \lambda_{\mathcal{A}}^T\tilde{D}_{\mathcal{A}}^+ - \lambda_{\mathcal{U}}^T\tilde{D}_{\mathcal{U}}^+\right)\kappa^+ + \left(w^T + \lambda_{\mathcal{A}}^T\tilde{D}_{\mathcal{A}}^- + \lambda_{\mathcal{U}}^T\tilde{D}_{\mathcal{U}}^+\right)\kappa^- + \lambda_{\mathcal{A}}^T\psi. \tag{9.12}$$

If we collect like terms, we get

$$\lambda_{\mathcal{A}}^T\left(\tilde{D}_{\mathcal{A}}z_0 + d_{\mathcal{A}} - \tilde{D}_{\mathcal{A}}^+\kappa^+ + \tilde{D}_{\mathcal{A}}^-\kappa^- + \psi\right) = 0$$

To express the dual problem properly, the projection matrix $P_{\mathcal{U}}$ is defined such that

$$\kappa^+ = P_{\mathcal{U}}\kappa^+ + (I - P_{\mathcal{U}})\kappa^+,\ \kappa^- = P_{\mathcal{U}}\kappa^- + (I - P_{\mathcal{U}})\kappa^-.$$

The projection matrix is constructed to separate affected and unaffected parts in κ^+ and κ^-. The dual problem of Problem 10 is then

Problem 11 (p-ISI$_1$)

$$\max_{\kappa^+_{\mathcal{N}\setminus\mathcal{U}},\kappa^-_{\mathcal{N}\setminus\mathcal{U}}} \left(w^T - \lambda_{\mathcal{U}}^T\tilde{D}_{\mathcal{U}}^+\right)(I - P_{\mathcal{U}})\kappa^+ + \left(w^T + \lambda_{\mathcal{U}}^T\tilde{D}_{\mathcal{U}}^-\right)(I - P_{\mathcal{U}})\kappa^-, \tag{9.13}$$

subject to

$$\tilde{D}_{\mathcal{A}}z_0 + d_{\mathcal{A}} - \tilde{D}_{\mathcal{A}}^+(I - P_{\mathcal{U}})\kappa^+ + \tilde{D}_{\mathcal{A}}^-(I - P_{\mathcal{U}})\kappa^- - \tilde{D}_{\mathcal{A}}^+P_{\mathcal{U}}\kappa^+ + \tilde{D}_{\mathcal{A}}^-P_{\mathcal{U}}\kappa^- \le 0,$$
$$\kappa^+ \ge 0,\ \kappa^- \ge 0.$$

Then the following definitions are made

$$\bar{z}^+ \triangleq \kappa^+,\ \bar{z}^- \triangleq -\kappa^-,$$

$$w_{\mathcal{M},1}^T \triangleq \left(w^T - \lambda_{\mathcal{U}}^T\tilde{D}_{\mathcal{U}}^+\right)(I - P_{\mathcal{U}}),\ w_{\mathcal{M},2}^T \triangleq \left(w^T + \lambda_{\mathcal{U}}^T\tilde{D}_{\mathcal{U}}^-\right)(I - P_{\mathcal{U}}).$$

Finally, we can formulate Mod-ISI Problem with linear criterion as

Problem 12 (ℓMod-ISI)

$$\max_{\bar{z}^+_{\mathcal{N}\setminus\mathcal{U}},\bar{z}^-_{\mathcal{N}\setminus\mathcal{U}}} w_{\mathcal{M},1}^T\bar{z}^+ - w_{\mathcal{M},2}^T\bar{z}^-, \tag{9.14}$$

subject to

$$\tilde{D}_{\mathcal{A}}^+(I - P_{\mathcal{U}})\bar{z}^+ + \tilde{D}_{\mathcal{A}}^-(I - P_{\mathcal{U}})\bar{z}^- + \tilde{D}_{\mathcal{A}}^+P_{\mathcal{U}}\bar{z}^+ + \tilde{D}_{\mathcal{A}}^-P_{\mathcal{U}}\bar{z}^- - \tilde{D}_{\mathcal{A}}z_0 \le d_{\mathcal{A}},\tag{9.15}$$
$$\bar{z}^+ \ge \bar{z}^-.$$

Above defined Problem 12 represent a consistent formulation of the modular ISI method. Recall, in the derivation, instead of the non-linear product criterion from Problem 6, we use the linear criterion, therefore, the resulting problem is a linear program (LP). This allows to obtain strong duality in Problems 10 and 11 (Slater constraint qualification [129]). An important goal in implementation of this method is to define the set of affected nodes in order to achieve low computational complexity but also high accuracy. One of possible methods of determining the set of affected nodes is presented in the next section.

9.4. DETERMINING THE SET OF AFFECTED NODES

The definition of the set of affected nodes $\mathcal{A}$ is also to be determined. The set $\mathcal{A}$ is chosen with respect to (9.10). Let us formulate the following hypothesis.

Hypothesis 1 *Suppose the system operator wants to perform a marginal reconfiguration, i.e., opening/closing transmission line/s. The set of affected nodes $\mathcal{A}$ should contain nodes directly affected by the reconfiguration (given by changes in network security domain) and the relevant neighbouring nodes (given by further analysis) respecting the network topology.*

To rationalize this hypothesis, main determinants of the matrix $\tilde{D}_\tau$ are provided. Information regarding nodes influenced by a defined reconfiguration can be found in

- network security domain,
- inversion of the matrix A.

Recall, more information about the construction of intervals of secure injection is given in Section 7.3.2. Network security domain provides a basic overview on the set of affected nodes. It is described by a known polytope with a given structure. For $\tau \in \mathcal{T}$, the matrix A_τ is computed as a product of nominal voltages and admittance matrix (Problem 6), i.e., A_τ is also given explicitly. However, in ISI Problem, the inversion of A_τ is considered. The inversion was defined in Section 9.3 as $\hat{T}_\tau$. The structure of $\hat{T}_\tau$ and differences with respect to topology changes have to be examined to obtain the set of affected nodes $\mathcal{A}$.

In the following text, an example of the difference matrix $\hat{T}_\mathcal{D} = \hat{T}_1 - \hat{T}_0$ is given. Suppose, the system operator wants to perform a change in IEEE 300 bus test system [128]. Transmission line $b = (246, 247) \in \mathcal{B}$ is opened. We want to track the difference between the matrix $\hat{T}_0$ for the nominal and $\hat{T}_1$ for the reconfigured topology. The structure of $\hat{T}_\mathcal{D}$ is shown in Figure 9.2. Hereby presented difference analysis can be a potential tool to determine the set of affected nodes. In Figure 9.2, the nodes yielding the most important differences are colored red. It can be seen that the results are consistent with the logical expectations proposed in Hypothesis 1, i.e., the proposed set of affected nodes contains the neighborhood of the reconfiguration. To confirm the findings, the affected nodes obtained from the analysis are highlighted by red color in Figure 9.3. Note, the problem of determining the set of affected nodes is connected with the settings of the threshold level, i.e., what difference in the $\tilde{D}_{\delta,\mathcal{U}}$ matrix is considered relevant. This problem also needs to be studied further.

9.5. THE MOD-ISI ALGORITHM

In general, the sets $\mathcal{I}$ and $\mathcal{J}_i$ in Problem 5 include all possible indices of α denoted by $\mathcal{I}_{max}$ and $\mathcal{J}_{i,max}$. For large systems, this leads to a time consuming problem not

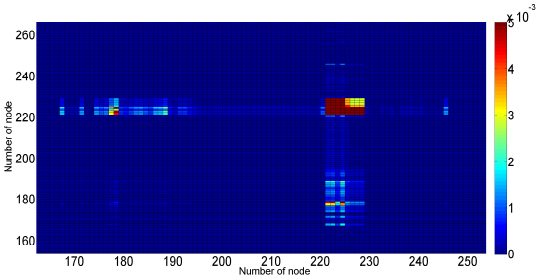

Figure 9.2: Structure of difference matrix $\hat{T}_{\mathcal{D}}$, the values coloured in dark red yield the highest difference and might be included in the set of affected nodes. Dark blue color represent the lowest difference and does not need to be included in the set $\mathcal{A}$.

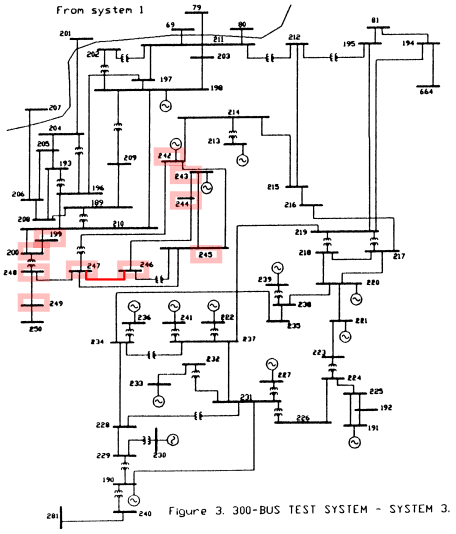

Figure 9.3: Part 3 of IEEE 300 bus test system: Nodes yielding the biggest difference are highlighted in light red color. The reconfigured line is marked in red. The affected nodes are located in the neighbourhood of the planned reconfiguration which is consistent with Hypothesis 1.

tractable in advanced analysis requiring repeated executions, e.g., the contingency analysis. If properly defined, however, the sets $\mathscr{I}$ and $\mathscr{J}_i$ enable modular solutions that are efficient when analysing the effects of local changes in the network, e.g., a line outage.

Suppose $|\mathscr{I}| = m$, then Problem 5 includes m subproblems. Next, consider two topologies $\tau = 0$, $\tau = 1$. If the Lagrange multiplier α for $\tau = 0$ and the i^{th} subproblem is known and if the alternative topology does not change the rows of $A^{\pm}$ that belong to $\mathscr{J}_i$, then the same Lagrange multiplier solves the i^{th} subproblem for $\tau = 1$. This can be stated compactly using the following notation. If $A^{\pm,0}_{\mathscr{J}_i} = A^{\pm,1}_{\mathscr{J}_i}$, then $\alpha^{*,0}_i = \alpha^{*,1}_i$, where $A^{\pm,\tau}_{\mathscr{J}_i}$ are the $\mathscr{J}_i$ rows of $A^{\pm}$ corresponding to topology τ and $\alpha^{*,\tau}_i$ is the Lagrange multiplier solving the i^{th} subproblem of Problem 5 for topology τ. The mod-ISI solution algorithm is outlined in Figure 9.1. The next section describes an efficient algorithm for computing the sets $\mathscr{I}$ and $\mathscr{J}_i$.

9.5.1. INDEX DECOMPOSITION

In this section, an algorithm for computing the sets $\mathscr{I}$ and $\mathscr{J}_i$ is proposed. Results published in this section were published in ENERGYCON 2016 [116]. The sets are computed to balance the trade-off between performance and computation complexity. In other words, the sets are computed to

1. yield a nominal Lagrange multiplier α^0 for which Problem 5 is feasible given an alternative topology $\tau = 1$ and the sets $\mathscr{I}$ and $\mathscr{J}_i$.
2. minimize the cardinality of the sets $\mathscr{I}$ and $\mathscr{J}_i$.

The following distance function is defined for this purpose.

Definition 4 *Consider the set of nodes $\mathcal{N}$ and the set of branches $\mathcal{B}$. For any given $i \in \mathcal{N}$ and $b \in \mathcal{B}$, the distance $d(i,b)$ is defined as*

$$d(i,b) = \frac{sp(i,b_1) + sp(i,b_2)}{2},$$

where for $i, j \in \mathcal{N}$, $sp(i,j)$ denotes the length of the shortest path from i to j.

Find a minimal set of coefficients for the nominal Lagrange multiplier α^0 First note that each row of $A^{\pm}$ corresponds to a node $i \in \mathcal{N}$. Second note that each row of D corresponds to a branch $b \in \mathcal{B}$. Hence, the above defined distance function can be extended in a natural way to operate on rows of $A^{\pm}$ and rows of D.

For each branch constraint and the nominal topology $\tau = 0$, represented by D^0_i, compute $\mathscr{J}_i$ and α^0_i as follows:

1. compute the vector of distances $w^0_{i,j} = d(D^0_i, A^{\pm,0}_j)$,
2. compute $\mathscr{J}_i = \{k | w_{ik} \leq d^0_{min,i}\}$
3. Solve Problem 5 for the single constraint D^0_i, and the computed $\mathscr{J}^0_i$.
4. If a solution has been found, iteration stops with success, otherwise increase $d^0_{min,i}$ and go to step 2.

Compute the index decomposition set $\mathscr{I}$ Next, compute the decomposition set $\mathscr{I}$ as follows. For each branch constraint $i \in \{1,\dots,m\}$, $A^{\pm,\tau}_{\mathscr{J}_i}$ are the $\mathscr{J}_i$ rows of $A^{\pm,\tau}$ corresponding to topology τ, then the decomposition set $\mathscr{I}$ is defined as

$$\mathscr{I} = \left\{ i \middle| A^{\pm,0}_{\mathscr{J}_i} \neq A^{\pm,1}_{\mathscr{J}_i} \right\}.$$

9.5.2. MODULAR SOLUTION

Recall, if the Lagrange multiplier α for $\tau = 0$ and the i^{th} subproblem is known and if the alternative topology does not change the rows of $A^{\pm}$ that belong to $\mathscr{J}_i$, then the same Lagrange multiplier solves the i^{th} subproblem for $\tau = 1$.

Hence, for $\tau = 1$, only the $\mathscr{I}$ rows of α^1 are computed by Problem 5. Given the Lagrange multiplier α^0, the i^{th} row of α^1 is constructed such that

$$\alpha^1_i = \begin{cases} \alpha^{*,1}_i, & \text{if } i \in \mathscr{I}, \text{compute Problem 5,} \\ \alpha^{*,0}_i, & otherwise. \end{cases}$$

Finally, α^1 is used to compute limits on power injections z^- and z^+ for the alternative topology $\tau = 1$. This is done by solving Problem 6.

9.5.3. CASE STUDY

A performance study was carried out on IEEE test systems [122] and on 5 real models of European transmission systems. The purpose of the study is to show potential time reduction between the ISI and mod-ISI methods. Time reduction and scalability was tested on IEEE 14, IEEE 30, 49, 59, 106, 135, and 342 bus systems. All nodes except the slack are taken to be controllable. While, allowing all nodes to be controllable is an exaggeration, it provides a comprehensive study of the proposed method performance and potential scalability.

All systems are considered in the p.u. scale with the base of 100MVA. The line current limits i^+_b, for all branches $b \in \mathcal{B}$ are for the purposes of the case study approximated by the MVA limits provided in [130]. All computation experiments were performed on a standard desktop machine (Intel® Core™i7-4790 @ 3.6 GHz, 32GB RAM) in Matlab using CVX [131].

In the first part of the case study, the construction of network security domain and network operating domain is shown. In the second part, results of the ISI and mod-ISI performance study are presented.

NETWORK DOMAINS MODELLING

The network operating domain $\mathcal{Y}_S$ given in Definition 2 is for each $k \in \{1,\dots,2n\}$ defined as the Cartesian product of intervals $[x^-_k, x^+_k]$, the network operating domain limits are defined as $x^-_k = 0.98x_{0,k}$ and $x^+_k = 1.02x_{0,k}$, i.e., ±2% of the nominal operating point.

The network security domain $\mathcal{X}_S$ given in Definition 3 is defined by a convex polytope represented by the pair (D,d) that includes all line current constraints of the network. For each $b \in \mathcal{B}$, the line current constraints $|I_b| \leq i^+_b$ can be rewritten to the form $|V_k - V_\ell| \leq v^M_b$, where $v^M_b = i^+_b |Y_{k,\ell}|$ denotes the maximum allowed voltage difference. Construction of line current constraints requires to couple nodal voltages of connected

nodes. For each $b \in \mathcal{B}$, the line current constraint is defined in the form of matrix inequalities which are embedded into D and d.

MODULAR NETWORK OPERATION

In this section, ISI and mod-ISI methods are assessed in terms of computation time and scalability. First, ISI is solved for all examined systems. Then a reconfiguration action is performed. The reconfiguration involves opening of one line in the network and both methods are used to compute new injection intervals. The ISI solution algorithm requires recomputation of the whole problem without utilization of the nominal topology solution. The mod-ISI method uses the solution for the nominal topology to compute injection intervals for the new topology. Because of the size of examined networks individual injection intervals and differences between methods are not plotted in this paper.

Table 9.1: Computation time comparison

Network	ISI [s]	m-ISI [s]	Time reduction [%]
IEEE 14	8.1	4.2	48.2
IEEE 30	18.3	2.1	88.5
Real 49	30	10.4	65.2
Real 59	35.5	4.9	86.3
Real 106	81.1	9.6	88.2
Real 342	1645	10.3	99.4

Time consumption and percentage time reduction when using the mod-ISI solution algorithm instead of the ISI algorithm are shown in Table 9.1. The time reduction of the proposed mod-ISI method is substantial and increases with system size resulting 99.4% reduction for the 342 node system.

10

ISI IN ENERGY MARKETS

The ISI method presented in Chapter 7 can be reformulated for application into the area of energy markets. The General ISI problem presented in Section 7 is designed to compute the injection intervals that meet given network security criteria (e.g., N-0 or N-1). In the area of energy markets, the optimization criteria can redefined. In this section, multiple applications of the ISI method into the area of energy markets are presented. It can be shown that ISI can be potentially used as a tool for economically efficient and secure reservation and activation of ancillary services.

The ancillary services (AS) shall be activated as a backup tool for system operators in case of an unexpected network condition. Currently used AS activation and reservation methods are solely price based, i.e., an improper activation of an AS may result in a network congestion. In this chapter, an innovative interval based approach of AS acquisition and activation is proposed using the ISI method defined in Chapter 7. Note, various capacity mechanisms are described in Appendix B.

The following two assumptions are taken into account when using the ISI method in the area energy markets:

1. The criteria function is a linear cost minimization function.

2. Network operating domain $\mathscr{Y}_S = x_0$.

The first assumption states the the volume maximization is replaced by a cost minimization function. The need of an economic criteria instead of a security based criteria is the economic efficiency of activation or reservation of a portfolio of ancillary services. The second simplification deals with adequate level of injection intervals accuracy. For portfolio verification, there is no need to maintain network security for all possible combination within secure injection intervals. This methods focuses on the robustness in the operating point.

The ISI method reformulated for the energy markets is the following:

Problem 13 (BID-ISI)

$$\min_z c^{\mathrm{T}} z \tag{10.1}$$

$$\text{s.t.} \quad \mathbf{M}z \le b, \tag{10.2}$$

$$z \ge 0. \tag{10.3}$$

where

$$\mathbf{M} = \begin{bmatrix} diag(\mathbf{D}_P, \mathbf{D}_N, \mathbf{D}_S) & \mathbf{0}_{n_B \times n_D} \\ -diag(\mathbf{D}_{PD}, \mathbf{D}_{ND}, \mathbf{D}_{SD}) & \mathbf{I}_{n_D \times n_D}, \\ \mathbf{T}_p(:, i_P) \quad \mathbf{T}_n(:, i_N) \quad \mathbf{T}_p(:, i_S) - \mathbf{T}_n(:, i_S) & \mathbf{0}_{n_d \times n_D} \end{bmatrix}$$

$$b = \left[b_P^{\mathrm{T}}, b_N^{\mathrm{T}}, b_S^{\mathrm{T}}, -b_{PD}^{\mathrm{T}}, -b_{ND}^{\mathrm{T}}, -b_{SD}^{\mathrm{T}}, d^{\mathrm{T}}\right]^{\mathrm{T}}, \quad b \in \mathbb{R}^{n_B+n_D+n_d}$$

$$c = \left[c_P^{\mathrm{T}}, c_N^{\mathrm{T}}, 2c_S^{\mathrm{T}}, K_{1\times n_D}\right]^{\mathrm{T}}, \quad c \in \mathbb{R}^{n_B+n_D}$$

$$z = \left[z_P^{\mathrm{T}}, z_N^{\mathrm{T}}, z_S^{\mathrm{T}}, z_A^{\mathrm{T}}\right]^{\mathrm{T}}, \quad z \in \mathbb{R}^{n_B+n_D}$$

$$\mathbf{T}_p = (\mathbf{D}(\mathbf{A})^{-1})^{+},$$

$$\mathbf{T}_n = (\mathbf{D}(\mathbf{A})^{-1})^{-},$$

$(\mathbf{D}(\mathbf{A})^{-1})^{+} = \max((\mathbf{D}(\mathbf{A})^{-1}), 0)$, $(\mathbf{D}(\mathbf{A})^{-1})^{-} = \min((\mathbf{D}(\mathbf{A})^{-1}), 0)$, where $\mathbf{D}$ and d represent a polytope approximation of the network security domain $\mathcal{X}_S$, linearization matrix $\mathbf{A}$ captures a linear transformation between nodal voltages and active and reactive powers and is valid around nominal voltage X_0. Matrices $\mathbf{D}_P$, $\mathbf{D}_N$, $\mathbf{D}_S$ define bid positions within the network. Vectors b_P, b_N, b_S correspond to bid size and c_P, c_N, c_S are the bid cost of n_B bids. Lower index P corresponds to positive bids, N to negative bids and S to symmetric bids.

Matrices $\mathbf{D}_{PD}$, $\mathbf{D}_{ND}$, $\mathbf{D}_{SD}$ assign bids to demanded ancillary services (i.e., bids that correspond to a particular AS have 1 in its columns, zero otherwise). Ancillary services demand is given in vectors b_{PD}, b_{ND}, b_{SD}. Vectors i_P, i_N, i_S define bid positions within the network. In case the accepted power z is lower than the demanded power, slack variables $z_A \in \mathbb{R}^{n_D}$ are used to maintain feasibility of the problem. These variables have high cost, i.e., has non-zero value only in case the demand cannot be satisfied. In this case, acceped bids in z correspond to a best feasible solution.

The next sections show possible applications of the BID-ISI method in selected areas of energy markets.

10.1. BID-ISI APPLICATIONS

Transmission system operators are required to hold a certain portion of power injection flexibility at selected nodes of the system to protect the network from the unexpected imbalances between power demand and supply (ACE - area control error). These capacity reserves are denoted as ancillary services. In a sufficient time before the ancillary services are needed, the TSO pays price for reservation of this flexibility at selected generators or schedulable loads. In general, the ancillary services reservation is solely price based. As shown in Section 10.2.1 and Figure 10.7, the AS are acquired in Damas/MMS

system through year based tenders. However, there can be situations in which the long term reservation of cheap ancillary services might be acquired in a location where the activation may yield unwanted network congestion and therefore result in a costly multilateral redispatch action (MRA). An example of a real network situation in ČEPS Control Area is shown in Figure 10.1. In this case, there was a network congestion that was reduced by aFRR activation from 0:00 until approx. 11:00. Manual FRR and crossborder redispatch actions were used together with aFRR around 11:00.

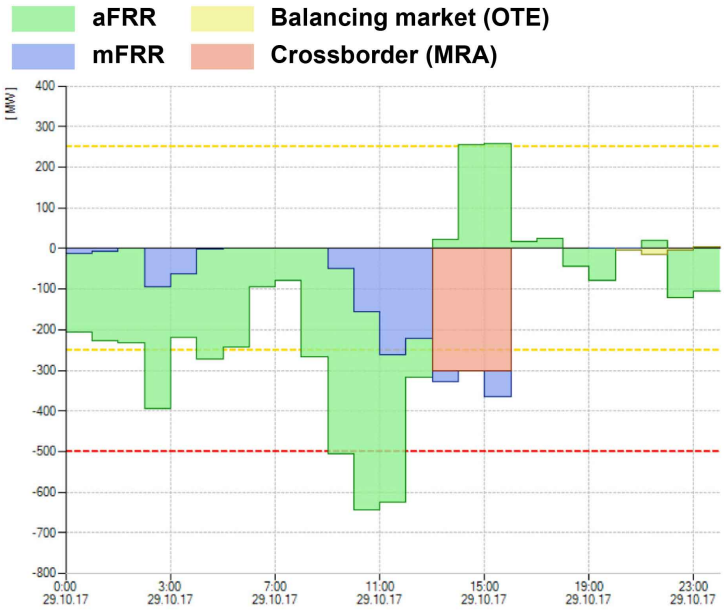

Figure 10.1: ČEPS AS activation chart for 29.10.2017. Note, most of the AS activation is done by aFRR but in case of an emergency state, mFRR are activated. In this scenario, crossborder power exchange was used to reduce network congestion. Minor amount of AS was acquired on the balancing market.

10.1.1. ANCILLARY SERVICES RESERVATION AND ACTIVATION STRATEGIES

The proposed BID-ISI method is compared to the traditional approaches of ancillary services acquisition and activation. The assessment of both AS methods is performed throughout this Chapter.

Suppose the system operator requires reservation of ancillary services for the following calendar year. In this approach, the system operator announces the total ancillary services demand d. The ancillary service providers submit their bids b and reservation prices c which are allocated to specified nodes of the network ($\mathbf{M}$).

PRICE BASED ANCILLARY SERVICES SELECTION

Using the classic ancillary services selection approach, the bids for each individual ancillary service is purchased in order to meed the demand while maintaining a financial budget, i.e., the reservation strategy is solely cost based.

As mentioned in Section 10.2.1, CEPS acquires ancillary services in year ahead public tenders using the Merit order strategy [51] (see Appendix E). The process of AS acquisition is illustrated in Figure 10.2. The results of tenders are available on CEPS website[1]. Other possible form of price based strategy is called Pro-Rata. This strategy is used, e.g., as an activation strategy of aFRR. This strategy can offer potentially lower congestion due to the distribution of power injections. The cost for the distribution is increased cost of activation. Figure 10.4 illustrates the principle of Pro-Rata strategy.

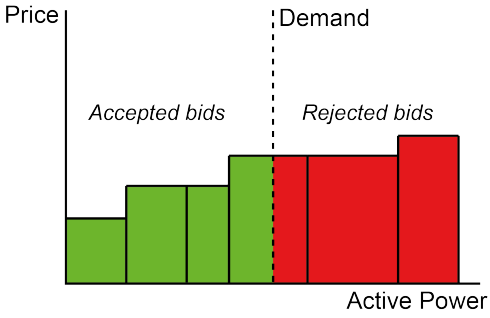

Figure 10.2: Merit order method of AS reservation. Bids are sorted in ascending order and the cheapest portfolio is purchased.

SECURITY VALIDATION USING THE BID-ISI METHOD

Using the portfolio selected by the merit order strategy, BID-ISI can validate the security of selected bids and suggests bid curtailment. The method can show potentially insecure bids that may result in a network congestion as shown in Figure 10.3.

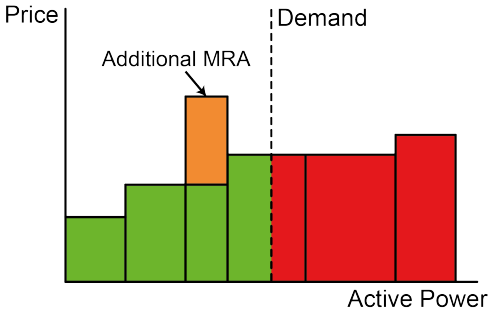

Figure 10.3: The BIS-ISI method validates the reserved bids and proposes a new network secure portfolio.

[1] https://www.ceps.cz/cs/vyberova-rizeni-pps

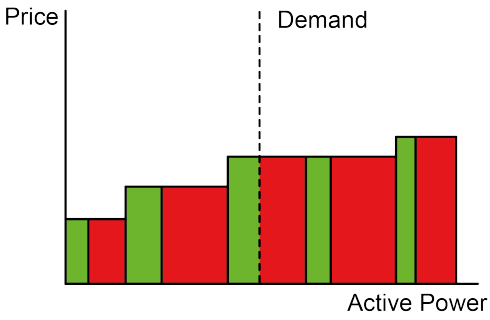

Figure 10.4: Pro-Rata strategy, all reserved bids contribute simultaneously to the activation.

AS-ISI BASED ANCILLARY SERVICES SELECTION

Instead of using the priced criteria in ancillary services reservation, the AS-ISI method is able to select a economic efficient portfolio that satisfies the network security criteria. The secure portfolio is shown in Figure 10.5.

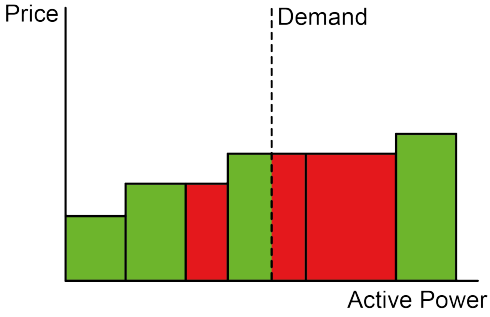

Figure 10.5: ISI based AS acquisition, the AS are acquired w.r.t. network limits.

10.2. REAL APPLICATION - PROJECT ANSVAL

In this section, results of a R&D project realized in cooperation between the University of West Bohemia and Unicorn Systems a.s. are presented. The project was supported by the Technology Agency of the Czech Republic (TACR TA04020320).

The project Ancillary Services Values and Limits (AnSVaL) focuses on the development of advanced methods and decision support tools for purchase and activation of ancillary services. These methods and tools simultaneously consider economic cost and network security criteria. New developed method and tools lead to minimization of additional ancillary services costs caused by redispatch (generation increase/decrease in a bordered area). Main objective of the project was the development of algorithms and decision support tools for purchase and activation of ancillary services considering economic cost and network security criteria.

10.2.1. ANCILLARY SERVICES IN CZ

The capacity mechanisms implemented in the Czech Republic are very close to the form of a capacity auction [51]. The Czech TSO (CEPS) announces annual tenders to supply automatic, manual and restoration reserves. There is a certification process specific for each type of an ancillary service and only certified ancillary service provides may contribute in the tender. The providers are able to define the minimum price and an amount of each ancillary service they wish to sell. Then all ancillary service bids are sorted according to the price and the cheapest amount of energy that satisfies the demand is acquired. This method of obtaining the ancillary services is called the Merit order strategy. The results of the tender are visible to the market participants through the internal platform Damas Energy/MMS [2]. Figure 10.7 shows an activity diagram of an annual tender for ancillary services in 2017.

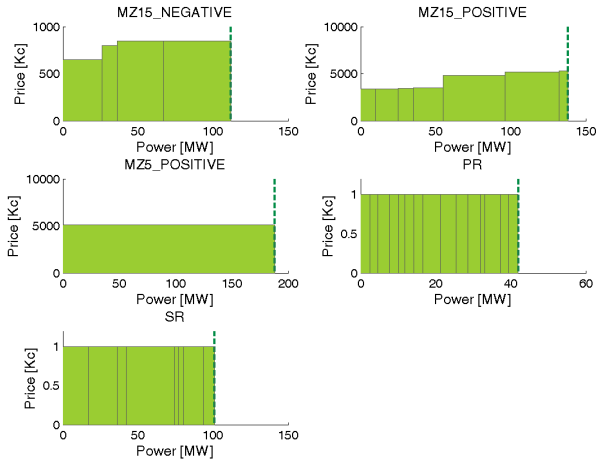

Figure 10.6: Example of merit order tenders for different types of Czech ancillary services.

The tenders described above are used to acquire the major part of the ancillary service demand. To cover the intraday and day ahead discrepancies in the demand and supply, the TSO acquires extra regulation energy from the day ahead and intraday market. This market is operated by the Czech electricity and gas market operator (OTE). OTE provides comprehensive services to individual electricity and gas market players. OTE commenced organizing trading in the day-ahead electricity market in 2002 and the intra-day and block electricity markets in later years.

It can be seen that the Czech electricity market is divided into many individual markets focused on regulation energy, ancillary services, base load, etc. Each energy product is treated differently without a centralized energy market. The absence of a central market that provides relevant information to all market participants increase the energy markets inefficiency due to the "imperfect information" effect. Some types of ancillary

[2] http://www.ceps.cz/cs/damas-energy-a-mms

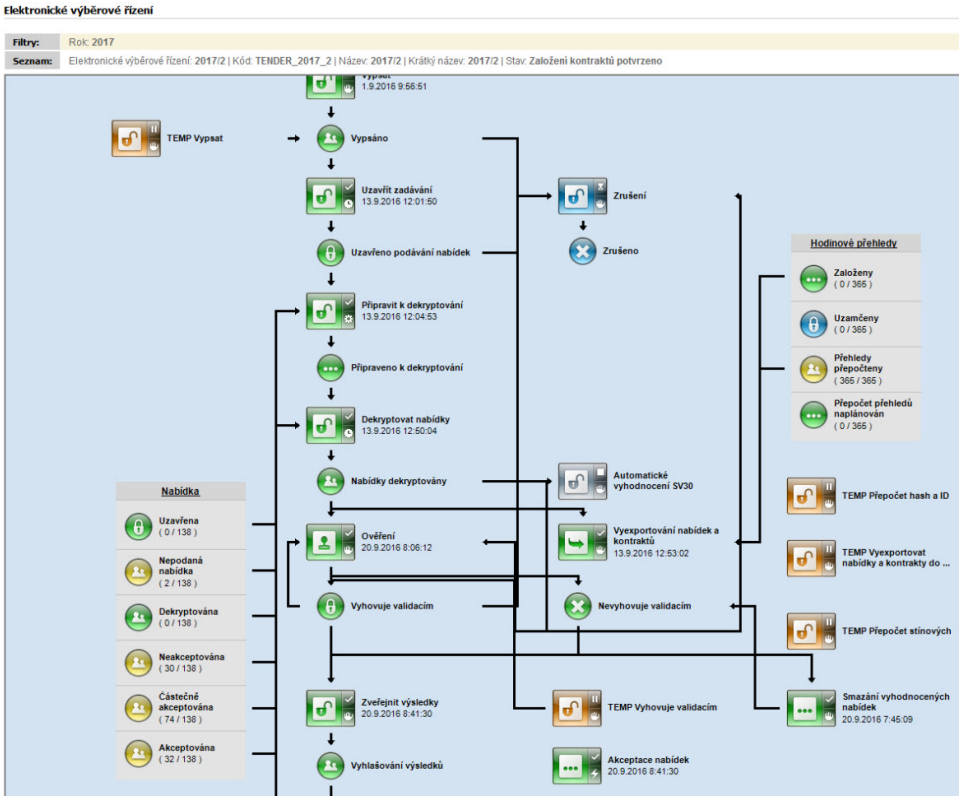

Figure 10.7: Acitivity diagram of an annual tender in Damas Energy. The tender has been called on 1.9.2017. End of acceptation of bids was 13.9.2016. The results of the tender were announced on 20.9.2017.

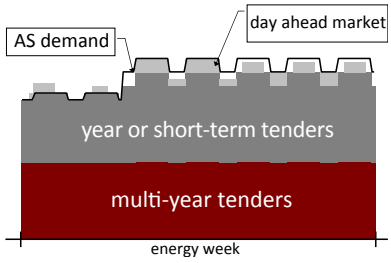

Figure 10.8: Structure of acquired ancillary services during the week. The highest share is obtained from year and multiyear tenders (red, dark grey), minor part is bought in day-ahead and intra-day balancing market.

services, e.g., SRU/Q is, due to the absence of an open market, still acquired using bilateral contracts with selected providers.

Market concentration in the Czech Republic remains very high, but the dominant position of three main power suppliers, ČEZ, E.ON and PRE is gradually decreasing. The three companies covered close to 70% of the market in 2014 down from 85% in 2011 [3].

10.2.2. SOFTWARE ARCHITECTURE

In this project the BID-ISI method was used to compute an economic efficient and secure portfolio of ancillary services. A computational platform created in Matlab, Java and MySQL was used to compute various scenarios of ancillary service reservation and activation in the Czech control area. Picture of developed software packages is shown in Figure 10.9.

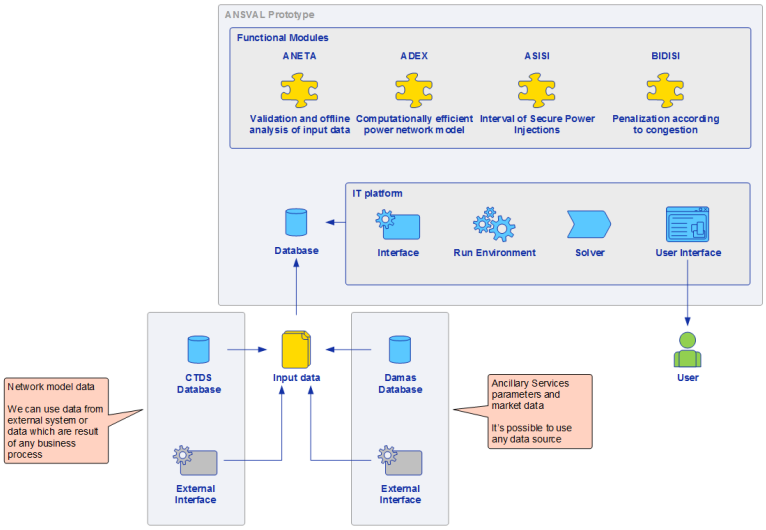

Figure 10.9: Overview of an application package developed in the project AnSVaL. The proposed ISI method and BID-ISI method we integrated in a software prototype which is able to read data from AMICA and MMS (formerly Damas) databases and provide relevant outputs.

The algorithm developed in this project shall be implemented in AMICA 1.3 (formerly CTDS) tool maintained by a Regional Security Coordinator (RSC) called TSCNET[4]. This tool is used by system operators of member TSOs. The potential integration of ISI methods in AMICA is shown in Figure 10.10.

[3] https://ec.europa.eu/energy/sites/ener/files/documents/2014_energy_market_en_0.pdf

[4] TSCNET is based in Munich, Germany, is a joint venture of the thirteen TSOs from ten European countries: Austria (APG), Croatia (HOPS), Czechia (ČEPS), Denmark (Energinet.dk), Germany (50Hertz, Amprion, TenneT, and Transnet-BW), Hungary (MAVIR), the Netherlands (TenneT), Poland (PSE), Slovenia (ELES), and Switzerland (Swissgrid)

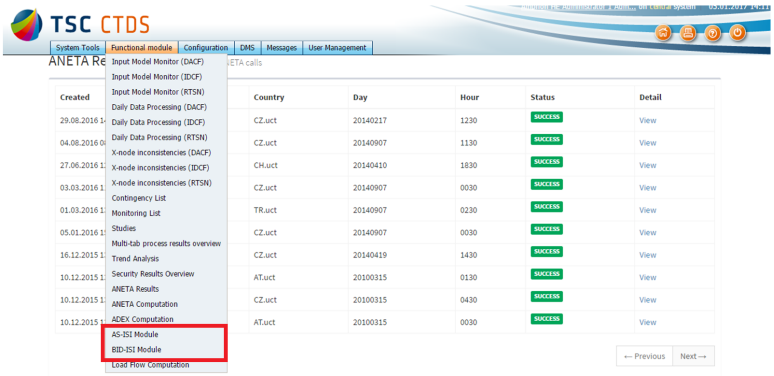

Figure 10.10: Integration of ISI methods within the TSCNET platform AMICA. All the packages developed throughout the project are integrated in the web application.

	Mean	Standard deviation	1% quantile	99% quantile
AS^+	2.62	0.46	1.73	3.53
AS^-	2.29	0.45	1.5	3.14

Table 10.1: BID-ISI computation times for CEPS transmission network

10.2.3. COMPUTATION TRACTABILITY

To test computational tractability of the BID-ISI method, a thorough case study was carried out on 6642 snapshots of the Czech transmission network comprising approximately 260 nodes and 300 branches. The computation was performed on a PC with Intel Core i7-4790 (4 cores @ 3,6 GHz) and 32GB RAM in Matlab 2014b. The results are shown in Table 10.1. Note, the BID-ISI method represents a linear programming optimization problem with linear scaling. Figure 10.11 shows computation time of each examined timestamp colored from light orange to black according to the minimum distance of the nodal voltages from the Network Security Domain. Figure 10.11 clearly confirms the linear scaling of the BID-ISI method.

10.2.4. DETAILED NETWORK ANALYSIS

A thorough case study was performed on one timestamp of the CEPS transmission network from 7.8.2014. The ancillary service bids were taken from Damas database. The network topology and parameters we taken from CTDS (AMICA) database. The load flow computation and network preprocessing was performed in ANETA/ADEX modules. The goal of the study is to validate the purchased portfolio of bids and eventually propose bid curtailment.

The graphical interpretation of the analysed network model was created in a network analysis tool called Gephi. A graph representing the network is shown in Figure 10.12.

To study the efficiency of acquired bid portfolio, the bids were allocated to corresponding generators in the network and a full run of the BID-ISI method was performed.

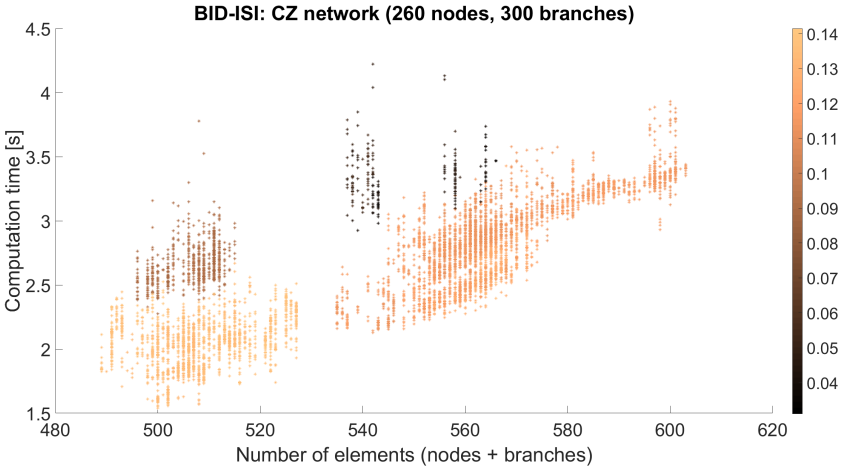

Figure 10.11: Computation time comparison. Each point corresponds to one timestamp. The timestamps are colored w.r.t. the network security, i.e., relative distance distance of the nodal voltages from the Network Security Domain. The black colored timestamps represent the most congested cases.

Figure 10.13 shows the model with colored nodes and lines. The lines are colored from green to red with respect to their loading and their thermal limit TATL (temporary admissible thermal limit). The red colored lines represent the congested branched and activation of more ancillary services may result in violations of TATL. The accepted bids, partially accepted bids and rejected bids are colored in green, orange, and white, respectively. The remaining line capacity is shown in Figure 10.14. The red colored congested area shown in Figure 10.13 resembles to lines 178 and 179 in Figure 10.14.

Figure 10.15 shows bids for each ancillary service ordered by price in ascending order. The dashed line represent the ancillary service demand (red in case the demand is not satisfied, green otherwise). The unaccepted bids have grey color. The results imply that the physical limits of the network do not enable activation of all ancillary services in one moment. Buying this portfolio is ineffective since the activation of one service may result in a need of activation of another type elsewhere in the network. It can also be seen that the pure merit order strategy may result in an extra cost, therefore, buying a more expensive ancillary service but in an uncongested area shall be a preferred option.

10.2.5. ANCILLARY SERVICES ACTIVATION: SENSITIVITY ANALYSIS

In this section, one of timestamps examined in Section 10.2.3 is assessed in terms of different amount of activated ancillary services. The timestamp is from 7.9.2014 at 15:30. Suppose the system operator activates a portion of reserved ancillary services. The amount of reserved and activated AS are shown in Table 10.2. The amount of activated MZ15+ varies from 125 to 250 MW. With increasing amount of activated MZ15+, the BID-ISI method identifies situations in which a classic merit order activation fails.

For lowest level of activated MZ15+, the merit order activation corresponds to BID-ISI activation strategy. This can be seen in Figure 10.16. With increasing amount of acti-

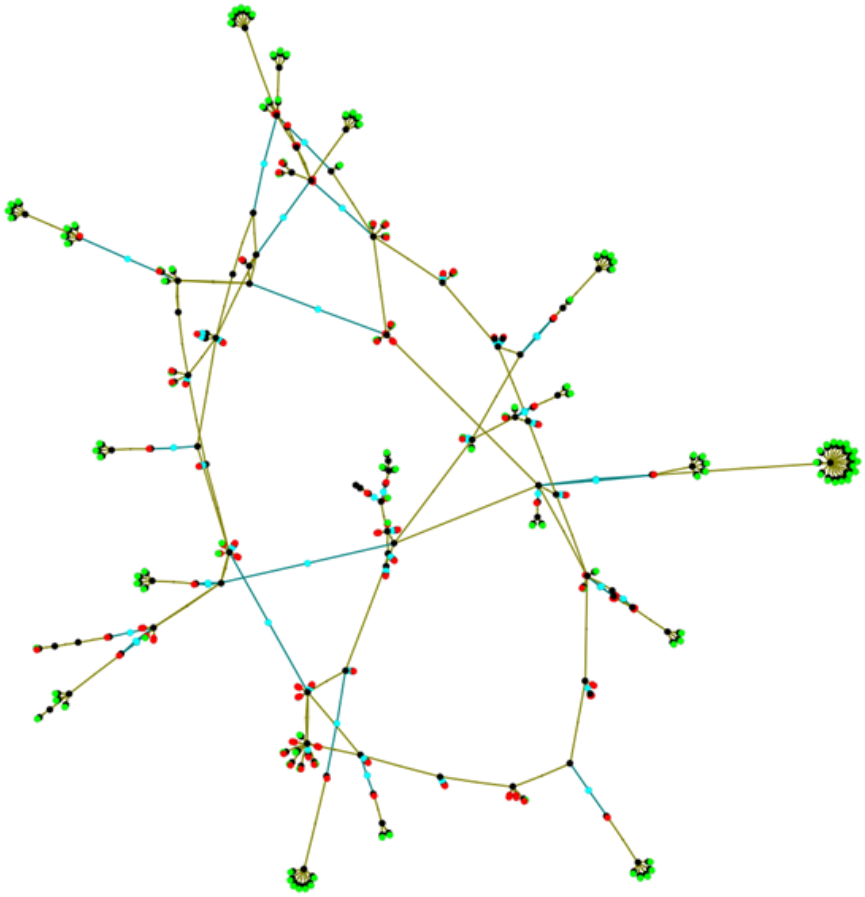

Figure 10.12: CEPS network model with highlighted equipment types. Red - load, blue - generator, teal - power transformer, black - node.

Ancillary Service	Reserved [MW]	Activated [MW]
PR	75.5	42
SR	216	76
MZ15+	245	125-175
MZ15-	196	77
MZ5+	321	100

Table 10.2: BID-ISI reserved and activated ancillary services. Note, activated amount of MZ15+ varies from 125 to 175 MW.

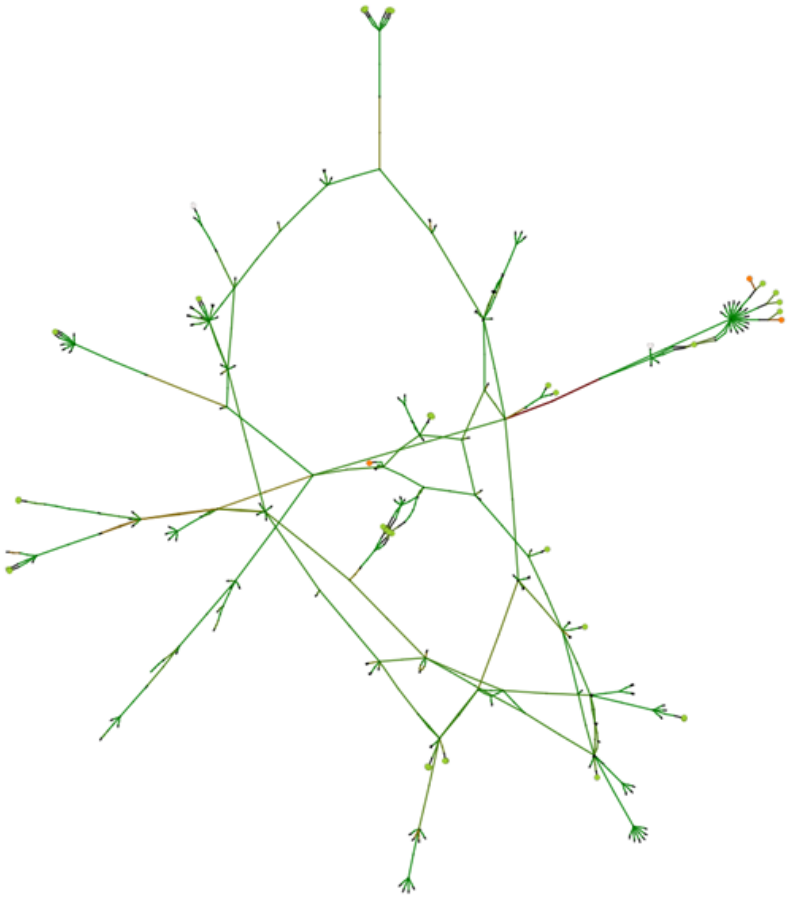

Figure 10.13: CEPS network model colored with respect to a line loading factor and bids acceptance. Green nodes - accepted, orange nodes - partially accepted, white nodes - rejected. The line loading is colored from green (no congestion) to red (network congestion).

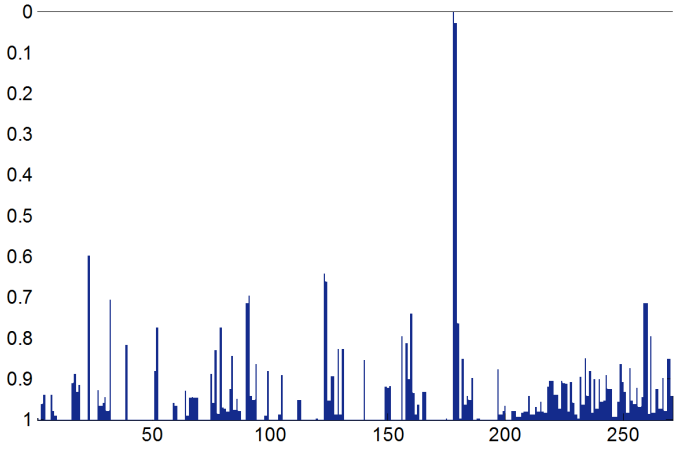

Figure 10.14: CEPS network line capacity. Lines closer zero are more congested. Note, lines 178 and 179 correspond to the red coloured congested area shown in Figure 10.13.

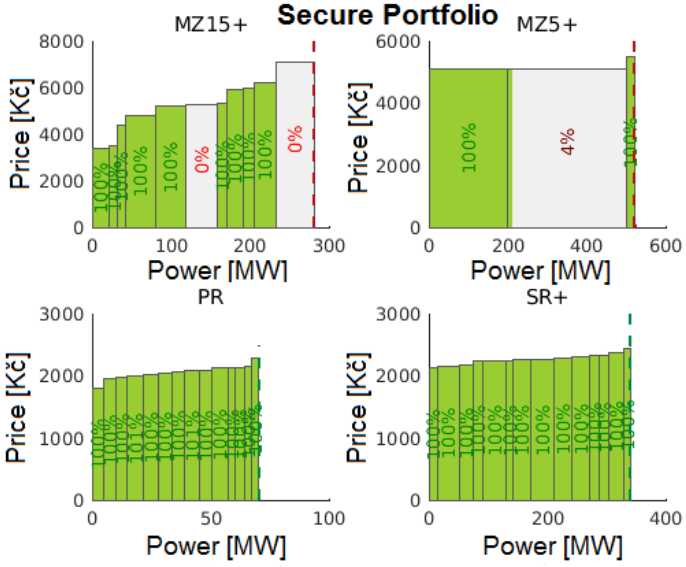

Figure 10.15: Accepted and rejected bids for each ancillary service ordered by price in ascending order. It can be seen that some of the positive MZ15+ and MZ5+ are curtailed.

vated MZ15+, the network becomes congested. The BID-ISI method, identifies the congestion and suggests a different activation strategy to avoid line current limits violations. Figure 10.17 shows the case in which the amount of activated MZ15+ equals to 150 MW. Some of MZ5+ and PR are allocated to more expensive bids to avoid network congestion. By further increasing the amount of activated MZ15+ to 175 MW, the total amount of activated ancillary services cannot be injected into the network without surpassing the current limits. This situation is shown in Figure 10.18.

This section has shown potential benefits of BID-ISI as a decision support tool for ancillary services activation. The BID-ISI method is suitable for cases with network congestion and can be used as an extra validation level with the classic Merit order.

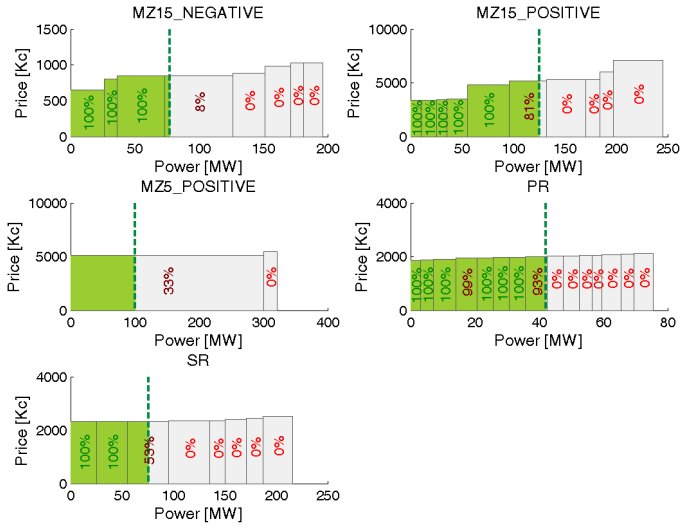

Figure 10.16: MZ15+ activation set to 125MW. Network remains uncongested. Merit order corresponds to BID-ISI.

10.2.6. CROSS-BORDER FLOWS SIMULATION

To further verify results of the BID-ISI method, intermittent cross-border interchanges are added to the CZ network model from 2.1.2014 at 9:30. The interchanges can vary and may result in an imbalance in the network. To study the impact of different amount of cross-border interchanges, the nominal interchanges obtained from statistical data are incremented and its the impact is assessed by the BID-ISI method. Analysis of cross-border interchange data from 2014 are available in Appendix C.

In this scenario, a specific example of crossborder flows is selected. Let us assume that the RES on the north of Germany generate large amounts of intermittent power. This power is injected into the European transmission network. The resulting voltage differences direct the power from the north into the south of Germany and into Austra.

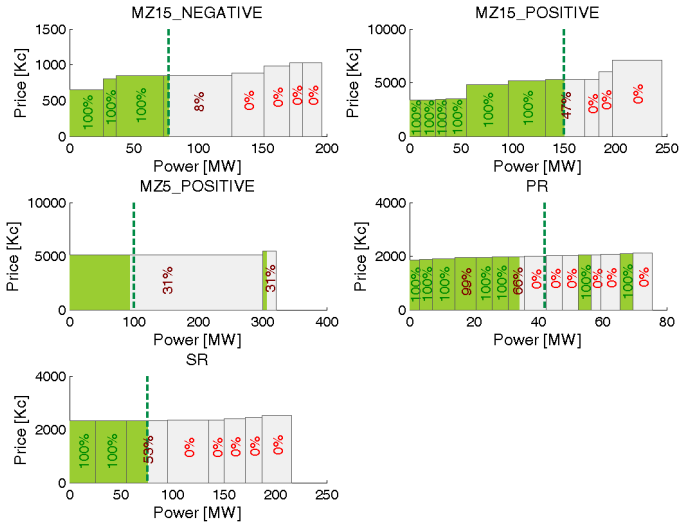

Figure 10.17: MZ15+ activation set to 150MW. Network becomes congested. BID-ISI avoids congestion by activating different bids. The activation strategy differs from Merit order. MZ5+ and PR are not activated according to Merit order.

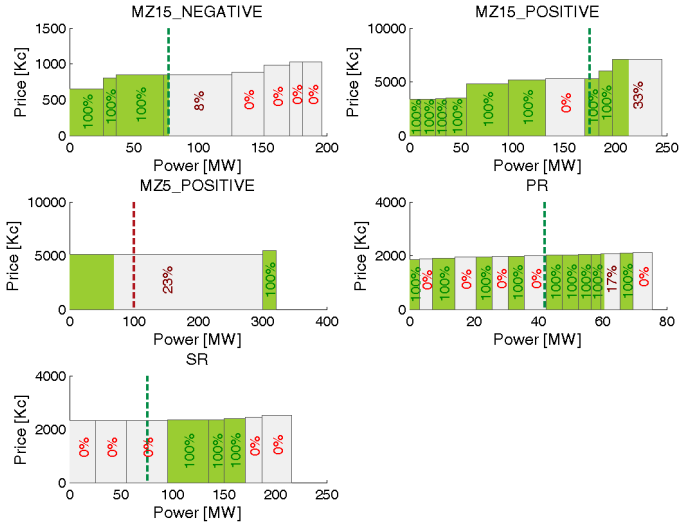

Figure 10.18: MZ15+ activation set to 175MW. Portfolio cannot be activated without surpassing line current limits. Demanded amount of MZ5+ cannot be satisfied. Note, to satisfy AS demand and maintain network security, the BID-ISI method selects different bids for PR, SR, MZ5+, and MZ15+.

Country	Interchange [MW]
50HzT	340
TenneT	-618
PL	585
AT	-667
SK	-539

Table 10.3: Nominal crossborder interchanges used in border flow scenario. CZ area is a net exporter.

In this case, CEPS and PSE are used as a transition counties. An illustration of the orientation of crossborder flows in CZ is given in Figure 10.19.

To simulate different network congestion levels, the nominal border flows from Table 10.3 are multiplied by number $k \in \{0.6, 0.8, 1.0, 1.2, 1.4\}$, i.e., 5 different scenarios are obtained with different congestion levels. In this section, scenarios $k = 1.0$ and $k = 1.2$ are analysed in detail. Complete results of the scenario can be seen in Appendix D.

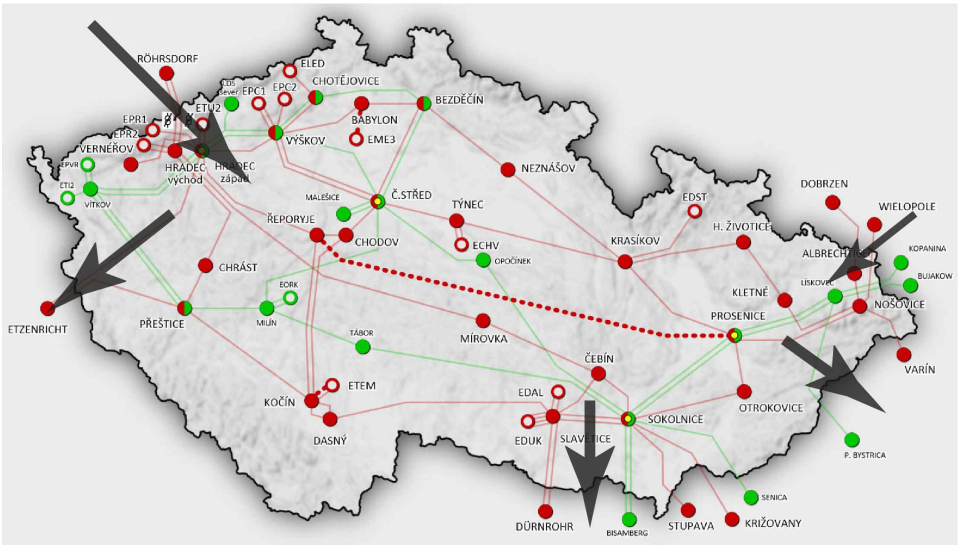

Figure 10.19: Crossborder flows scenario. Increased power flows from 50HzT through substation Hradec; indirectly from PSE through substation Albrechtice and Nosovice. The power flows through the Czech transmission network into TenneT, APG and SEPS.

Considering the nominal interchanges from Table 10.3, the network is able to satisfy de ancillary service demands and the crossborder flows. This can be seen in Figure 10.20. Note, there is a small shift in MZ15+ compared to the merit order. An illustration of network with coloured line congestion is given in Figure 10.22.

Considering a 20% increase in crossborder interchanges, the network congestion prevents the ancillary service activation without violating line current limits. The result-

ing secure portfolio is shown in Figure 10.21. It can be seen that the portfolio selected by the BID-ISI method is significantly different from the merit order. Using merit order strategy to activate ancillary services may result in security limit violations. The increase in line loading can be seen in Figure 10.23.

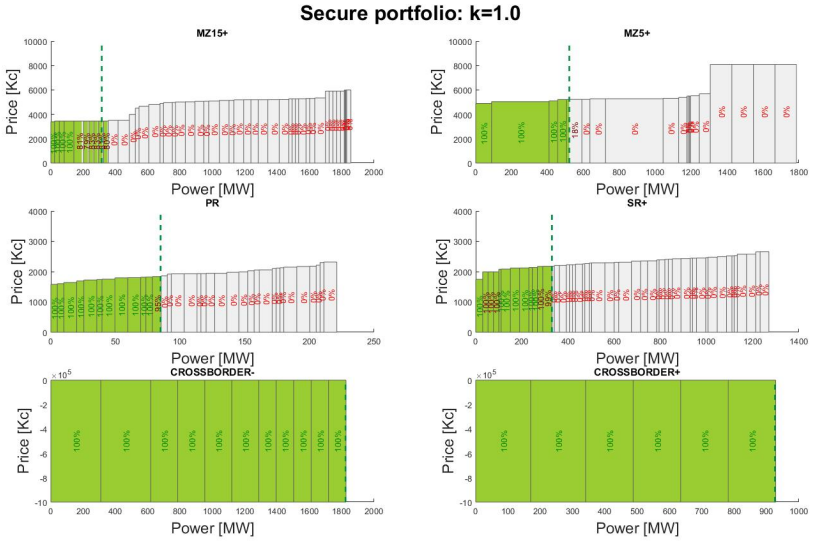

Figure 10.20: Crossborder flows at nominal levels, i.e., $k = 1.0$. AS demand and crossborder flows are satisfied.

10.3. ASSESSMENT OF BID-ISI IN ANCILLARY SERVICE MARKETS

In this chapter, the BID-ISI method has been tested in various network scenarios. Section 10.2.3 has shown the computational tractability and potential scalability. Over 6000 snapshots of CZ network we tested. The computation time for CZ network is between 2.2 and 2.6 seconds which makes it potentially usable in Energy Management Systems. Test implementation in RSC client application called Amica has been shown in Figure 10.10.

Section 10.2.4 has shown a thorough analysis of one selected timestamp. The analysis comprises bid validation usig the BID-ISI method, identification of the weakest part of the network, and a detailed picture of network topology with line loading. The methods shows in this scenario the portfolio of ancillary services is validated by the BID-ISI method. The results show curtailment of MZ15+ and MZ5+ when compared to classic merit order.

Section 10.2.5 has demonstrated the advantage of BID-ISI method when considering activation of a part of reserved ancillary services portfolio. The method has shown its advantage in situations with increased network congestion which is exactly the situation

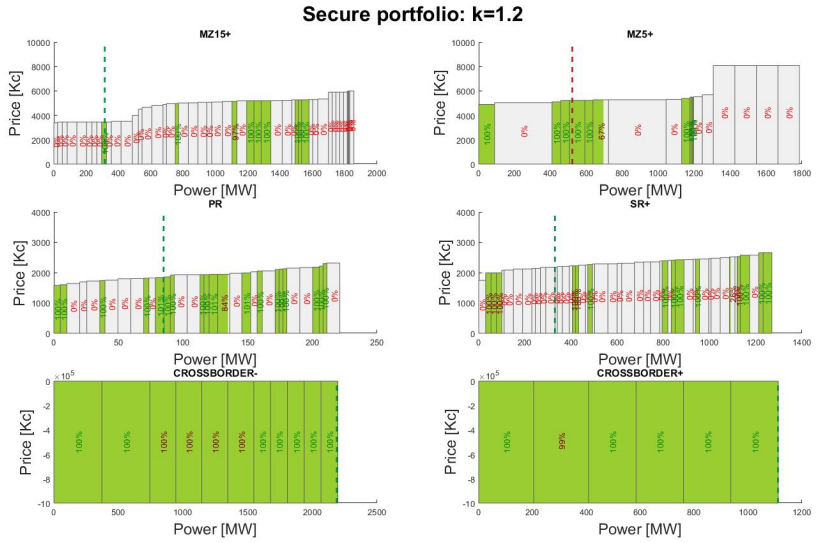

Figure 10.21: Crossborder flows increased by 20%, i.e., $k = 1.2$. MZ5+ cannot be activated in full scale. The demanded amount was curtailed.

which can require addition decision support for system operators. Figure 10.16 shows an uncongested case in which the demanded activated ancillary services can be activated w.r.t. their price. When increasing the MZ15+ demand, the bids obtained by price based criteria may yield network congestion. The BID-ISI method identifies this congestion and selects a different activation strategy. This situation is shown in Figures 10.17 and 10.18.

Crossborder capacity calculation with interchanges are analyzed in Section 10.2.6. Capacity calculation represent an important area in energy markets. The Transmission Reliability Margin and Total Transmission Capacity between each TSO are calculated on weekly basis and a tool for determining the border limits may be desired by operational planning departments in TSOs. Scenario modeled in Section 10.2.6 corresponds to a specific phenomena that has risen in Central Europe. Large amounts of intermittent power injected to the grid by the wind generators in Northern Germany causes massive flows of power flowing through Poland and the Czech Republic into Southern Germany and Austria. A simplified map with major power flows and their orientation in given in Figure 10.19. This scenario captures this behavior and analyses the CZ network and its ability to activate additional ancillary powers. Figure 10.20 shows sorted ancillary service bids for the nominal case in which the crossborder interchanges are satisfied and the bids portfolio can be activated. In case of a further increase o power flows from Germany, the activation of whole demanded ancillary services portfolio wound not be possible. The situation is illustrated in Figure 10.21.

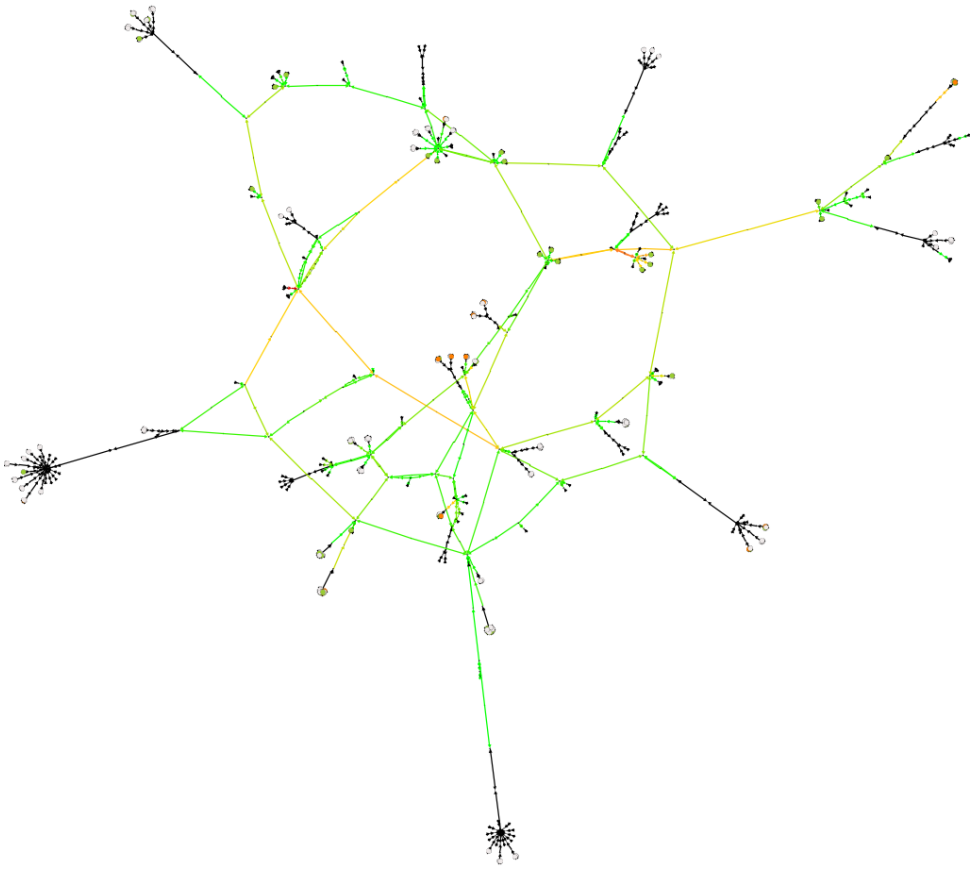

Figure 10.22: Network graph with coloured lines w.r.t. their loading $k = 1.0$.

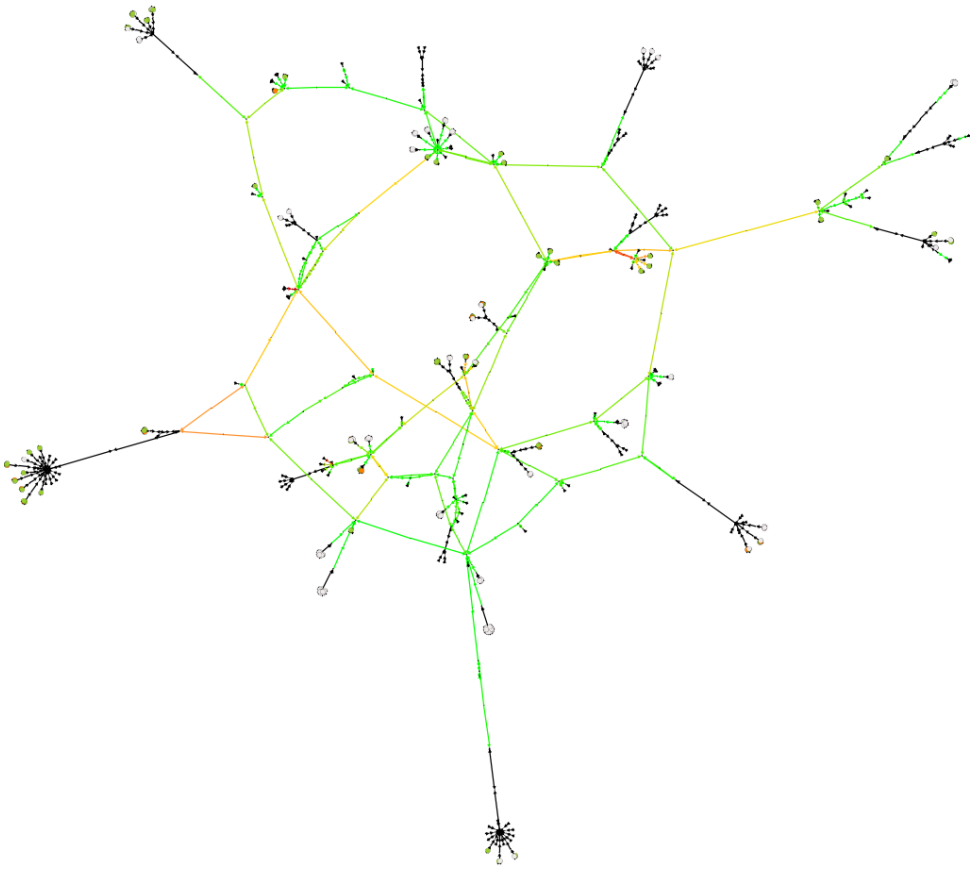

Figure 10.23: Network graph with colored lines w.r.t. their loading $k = 1.2$.

10.4. POSSIBLE BID-ISI APPLICATIONS IN PRESENTED CAPACITY MECHANISMS

The possible applications of the BID-ISI method are not limited to capacity mechanisms used in the Czech Republic. Interval based optimization can play an important role in each type of capacity mechanism described in Appendix B.

German Electricity market 2.0 is going to rely on a significant amount of renewables [132]. One of the important issues of this new market will be development of efficient strategies to manage Area Control Error and a way to prevent local network congestion due to an increased power injections from RES on lower voltage levels. To deal with these problems, two types of reserves were introduced: 1) Capacity reserve and 2) Grid reserve. Capacity reserve corresponds to an ancillary service that will be used in case of insufficient market supply. This reserve should deal with the Missing money problem described in Section 3.1.2. The about 4 GW of installed capacity should be retained in this reserve. The BID-ISI method should be able to give a decision support during the process of selection of the capacity reserve. Moreover during the short-term or intra-day operation planning, the method can help with the selection of activated equipment.

Grid reserve is a new phenomena and their location in the German transmission network will be a subject of research. The installations of firm sources that will form the grid reserve shall be used to balance the network in case of local imbalances. The BID-ISI method can be used when assessing the potential grid capacity locations. The method can verify the amount of installed capacity in terms of network security. Moreover, the method can be used to assess the amounts of secure interchanges between TSO and DSO [133].

France is going to implement the capacity obligation mechanism [134]. Each DSO will have an obligation to obtain a certain amount of capacity certificates by a given date. These certificates will be traded in an open obligation market. Entities that will offer capacity, i.e., firm sources or demand response need to pass a certification process to get capacity certificates that can be further traded. The BID-ISI method can be used during the certification process to assess the capacity potential of the local area. Moreover, the method can be used in Peak periods in which the certified capacities may have to supply contracted power. The method is able determine a cost effective and secure portfolio of certified capacities.

So far the ancillary services acquisition is limits each TSO to purchase AS from its own bidding zone. According to the ENTSOE Energy Balancing Guideline [5], each TSO shall either to create or join an existing Coordinate Balancing Area (CoBA). With the creation of CoBAs, the AS could be acquired from the whole balancing area, i.e., even from a foreign country that shares the same CoBA. The BID-ISI method can be used in a cost benefit analysis for ENTSO-E member states to analyze whether to join an existing CoBA or create a new with the neighboring TSO. Further information regarding ENTSO-E market integration is given in Appendix E.

In January 2018, Capacity Allocation and Congestion Management (CACM) work-

[5] http://eur-lex.europa.eu/legal-content/EN/TXT/?uri=uriserv:OJ.L_.2017.312.01.0006.01.ENG&toc=OJ:L:2017:312:TOC

group has published a final draft of crossborder capacity calculation [6] using Available Transfer Capability (ATC). It can be seen that the methodology is based on Power Transfer distribution coefficients (PTDF) [100] and expected crossborder interchanges. However, the document shows possible extension of this simplified approach using physical network constraints to create an approximate secure domain. This can be achieved using the BID-ISI method.

As mentioned in Chapter 10.1.1, the most common way to activate ancillary services is the Merit order and Pro-rata strategies. The BID-ISI method described in this work can be used for ancillary services activation on Regional but even on European level. The method retains the economical efficiency of the Merit order since the optimization criteria is the cost minimization. Moreover, the method respect physical limits of the network and implicitly avoids network congestion. The main blocking issue for the crossborder testing remains the absence of real economic data about the price of the ancillary service bids.

[6] https://consultations.entsoe.eu/markets/core-da-ccm/user_uploads/explanatory-note-for-core-da-fb-cc-public-consultation_fv.pdf

11

Conclusion

Power system optimization has been in focus of professional public since the second part of 20th century. Optimization techniques used in 20th century were documented in Chapter 2. In this chapter, the theoretical background of economic dispatch, load flow and optimal power flow was presented. Nowadays, a lot of literature is focused on the renewable energy sources which are being widely connected to interconnected power networks. Section 2.2 described problems and advantages of the RES and assessed the future trends in RES penetrations.

Chapter 3 introduced general energy market principles. It defined energy market supply and market demand, and the equilibrium of this imperfect competitive market. Two important issues were addressed in this chapter, the Missing Money problem and the RES incorporation problem. To deal with these market inefficiencies, capacity reserves, that reduce Area Control Error, have to be contracted in advance. This chapter comprises a basic taxonomy of ancillary services and introduces automatic and manual frequency restoration reserve (a/mFRR) and frequency containment reserve (FCR).

The review part of the work given in Chapters 2 and 3 provided an introduction into power system optimization and a brief description of energy markets supported by relevant citations. The practical part of the work began in Chapter 4 that presented the most common tools used in point based power network optimization. This chapter was divided into two sections. In Section 4.1, an overview of the classical era comprising the mathematical definition of the optimal power flow problem with an example of its solution using the Newton method were described. The modern era, described in Section 4.2, presents the advanced tools of power system optimization, i.e., security constrained OPF (SCOPF), probabilistic load flow and probabilistic optimal power flow (POPF). Moreover, a practical contribution to this area was presented in Section 4.2.6, which comprises a mathematical definition of POPF used for assessing various transmission loss models. This innovative method was presented in the proceedings of ECC 2013.

An overview of interval optimization methods was given in Chapter 5. The interval optimization is not a main topic in power system optimization, therefore, literature

sources are limited. Most common methods were cited and summarized in Section 6.2. In this chapter, possible advantages of interval based methods when compared to point optimization methods were provided.

A complete overview of the current state of power network optimization was given in Chapter 6. A comprehensive summary with the advantages and disadvantages of the current point based and interval based power system optimization methods was presented in Sections 6.1 and 6.2. Section 6.3 concluded with findings that there are no interval optimization tools able to compute intervals of secure injection at all nodes of the system. Hence, the proposed principle can be formulated into an innovative interval based power system optimization method.

The work continued with a rigorous definition of Intervals of Secure Power Injection (ISI) together with its possible extensions, and applications. These chapters represent the main contribution of this work.

The ISI method was presented in Chapter 7. The general concept was introduced in Section 7.1, the used notation was defined in Section 7.2. The problem was analytically defined in Section 7.3 where the General ISI and also the simplified ISI methods were defined. An efficient solution of the ISI method was provided in Section 7.3.2. The validity of the presented ISI method was tested on academic and real power systems. Details about the testing and results were given in Section 7.4. Preliminary results were published in the proceedings of IFAC 2014.

The most important challenges that had to be faced were mentioned in Chapter 8. Section 8.1 introduced the problem of determining the rotation matrix and its effects on the size of the secure injection intervals. Section 8.2 proposed an extension of ISI by incorporating the PQ diagrams of generators as an additional constraint in ISI. This extension was used in the BID-ISI method defined in Chapter 10. Section 8.3 presented an adjustment of the basic ISI method allowing reconfiguration planning and contingency analysis. This contribution allowed definition of N-1 secure intervals but the method can be extended to any level of security (N-x). The results were published in the proceedings of ISGT 2014.

Chapter 9 comprises one of the research results of the work, i.e., a modular extension of the ISI method called Mod-ISI. The Mod-ISI method can reduce the computation burden of the ISI problem and enable efficient use of this interval based tool even on larger power systems. Advantages of ISI compared with known operation support tools (based on point optimization) are potential enhancement of network robustness and broader decision support. The computationally efficient implementation of the Mod-ISI method suggests its potential to be applied as a tool in EMS/SCADAs. General Mod-ISI Problem was rigorously formulated in Section 9.1. A comparison between ISI and Mod-ISI in terms of computation complexity was shown in Section 9.2. Simplified Mod-ISI solution proposal was derived in 9.3. The final formulation of the modular ISI method were shown in Section 9.5. This section comprises an approximate solution and presents case studies with computation time reduction. This Mod-ISI method was published in an article presented in the proceedings of ENERGYCON 2015.

A second important contribution of this work is a method called BID-ISI. This method applicable in area of capacity markets was presented in Chapter 10. Note, the testing and development of the prototype tool were accomplished by in collaboration with the

AnSVaL project team. The main contribution of the author lies in the mathematical definition and selection of testing scenarios of the BID-ISI method.

In Section 10.1, applications of BID-ISI in ancillary services reservation and activation were presented. The BID-ISI method was formulated as a linear program with low time consumption and good scalability potential as shown in Section 10.2.3. A real application of the BID-ISI method was demonstrated in Section 10.2. Capacity mechanisms currently used in the Czech Republic were shown in Section 10.2.1. This section was followed by system specification given in Section 10.2.2 and testing scenarios comprising ancillary services reservation and activation in Section 10.2.4. Moreover, a study of crossborder interchanges and its effects on domestic ancillary services activation strategies was included in Section 10.2.5. This can be a valuable tool when assessing the effects intermittent power flows flowing from neighboring TSOs into the Czech Republic. The BID-ISI method has shown that the classic price based strategies (Merit order or Pro-Rata) can be used in scenarios without network congestion. However, in situations with increased line loading, the BID-ISI can give signals not to activate the cheapest portfolio, which may result in an extra cost, but rather a secure one that will avoid network congestion. Section 10.4 concluded the Chapter with more potential applications of the method in other European countries.

Appendices

A

GENERAL MARKET PRINCIPLES

A.1. SUPPLY AND DEMAND ANALYSIS

In this Appendix, fundamentals of the microeconomic analysis of supply and demand is given. Note, the exact derivation of supply and demand curves is out of the scope of this work. For derivations of demand and supply curves for individual or for the whole market, see [49], [50], or [48]. For the purposes of this work, suppose the long run supply and demand curves of a market are modeled as affine functions.

A.1.1. MARKET DEMAND AND SUPPLY CURVES

The demand curve captures relationship between price and demanded quantity of a given commodity. In this work, the price of the commodity (P) is an affine function of its demanded quantity (Q), i.e, $P = aQ + b$, where $a \in \mathbb{R}^-$, $b \in \mathbb{R}^+$. Figure A.1 a) illustrates the affine model of the market demand for a given commodity.

The supply curve captures relationship between price and supplied quantity of a given commodity. In this work, the price of the commodity (P) is an affine function of its supplied quantity (Q), i.e, $P = cQ + d$, where $c \in \mathbb{R}^+$, $d \in \mathbb{R}$. Figure A.1 b) illustrates the affine model of the market supply for a given commodity.

A.1.2. MARKET EQUILIBRIUM AND SURPLUSES

The optimal quantity and price in a model, under the assumption of perfect market competition [50], is determined by the intersection of supply and demand curves.

Figure A.2 shows the market equilibrium. Note, the equilibrium is reached for quantity of goods Q^* and price P^*. Area below the demand and above the supply curve represent the total welfare that comes from the execution of the trade in the market. The area is split in two parts. The area below the demand curve up to the equilibrium price is defined as the consumer surplus. The area above the supply curve up to the equilibrium price is defined as the producer surplus. As we can see, the total welfare produced by the market is on its maximum.

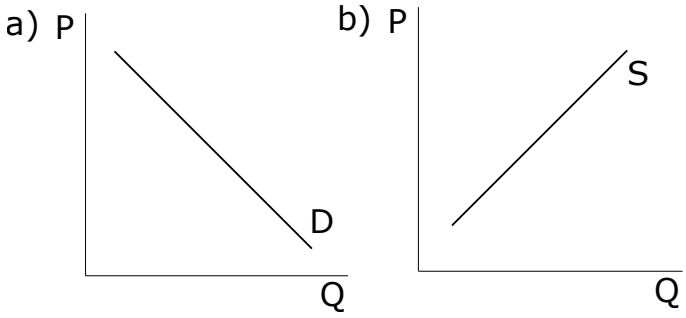

Figure A.1: Market demand and supply

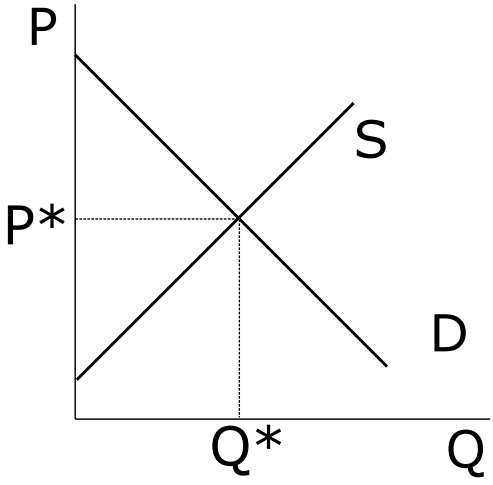

Figure A.2: Market equilibrium

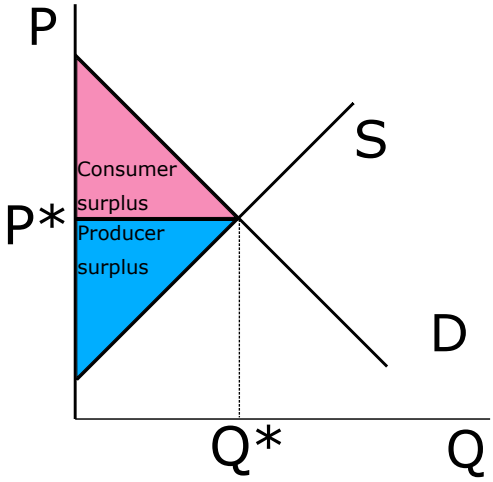

Figure A.3: Consumer and producer surpluses: Blue area represents the producer surplus, pink area represents the consumer surplus

However, in real world markets, there is no perfect competition. The model of perfect competition is based on the following assumptions:

1. Many sellers that are unable to affect the commodity price. Each seller represents a small fraction of all purchases in the market. The seller takes the price as given and decides the amount to produce that will generate the greatest profit.
2. Many buyers that are unable to affect the commodity price (price taker). Each buyer represents a small fraction of all purchases in the market. The buyer accepts the price as given and decides the amount to purchase.
3. There are no barriers to enter the market. Sellers and buyer may enter any time without additional costs as conditions change.
4. The exchanged commodity is homogeneous, i.e., all sellers sell the same product/commodity.
5. All market participants have perfect information. Producers understand the production capabilities known to other producers in the market and have immediate access to any resources used by other producers.

It is obvious that the model of perfect competition is insufficient for further modelling of the energy markets. The main reasons of the perfect competition model insufficiency is presented in the next section.

A.2. MARKETS WITH IMPERFECT COMPETITION

Imperfect competition exists whenever a market violates one or more of the assumptions of the perfect competition model. In practice, all real markets can be classified as imper-

fect. When dealing with imperfect competition the equilibrium price can be influenced by the actions of agents. In imperfect competition the price of goods can increase above their marginal cost and thus have customers decrease their level of purchase (and vice versa), and so reach inefficient levels of production. There are various types of imperfect competition, the most common types are:

- Monopoly / Monopsony,
- Oligopoly / Oligopsony,
- Monopolistic competition.

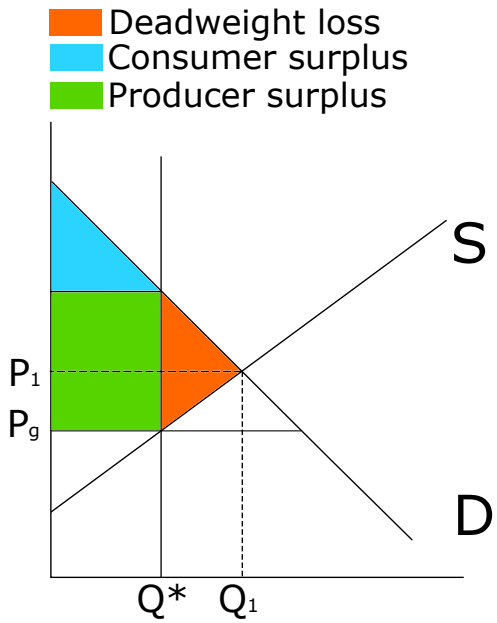

Figure A.4: Deadweight loss represents cost of allocation inefficiency.

More information about special types of imperfect competition can be found in literature [48]. In further text, the monopolistic competition, which is the most common type of market imperfection, is described.

In real markets, the price can deviate from its equilibrium price P^* and quantity Q^*. Figure A.4 shows a situation in which the price P_g is lower than the equilibrium. This can be caused, e.g., by a government regulation (minimum wages, taxation). In this case the resulting quantity supplied Q_g is lower than the equilibrium Q^*. The market surpluses are turned in favor of the producer. Moreover, the red coloured area corresponds to the allocation inefficiency, i.e., the amount of goods that were not produced due to the inefficient market behaviour.

A.2.1. MONOPOLISTIC COMPETITION

One of the most common types of imperfect completion. The main characteristics of monopolistic competition are the following:

- A large number of sellers: The number of firms in monopolistic competition is large. Each firm sells a substitute for the product of other firms in the industry.
- Product differentiation: Under monopolistic competition, the firms sell differentiated products. Product differentiation may be real or imaginary. Real differentiation corresponds to differences in the materials used, design, color etc. Imaginary differences are be created through advertisement, brand name, trademarks etc. The firms producing similar products cannot raise the price of product much higher than the competitors. If they do so, they will lose a part of their sale. In case, they lower the price, the total sale may be increased to a certain extent. How much will the sale increase or decrease by lowering or raising the price will depend upon the product differentiation of the different firms.
- Advertisement and propaganda: Another very important characteristic of the monopolistic competition is that each firm tries to create difference in its product from the other by advertising, propaganda, attractive packing, etc.
- Elasticity of demand: Since the existence of close substitutes limits the monopoly power, the demand curve faced by a monopolistically competitive firm is often very elastic. The degree of elasticity will, depend on the number of firms in the industry. If the number of firms is large and the product of each firm is not very similar, the demand curve of a firm will be quite elastic. In case, there is close competition among the rival firms for the sale of similar products, the demand curve of a firm will be less elastic.
- Barriers of entry: The entry of new firms in the monopolistically competition industry is relatively easy. There are no barriers of the new firm to enter the product group or leave the industry in the long run.
- Non-price competition: In monopolistic competition, the firms make every effort to win over the competitors. The firms may offer after sale service, a gift scheme, discount not declared in the price list and other strategies.

A.2.2. OLIGOPOLY

The Oligopoly market characterized by few sellers, selling the homogeneous or differentiated products. In other words, the Oligopoly market structure represents a market, where few sellers dominate the market and have control over the price of the product.

Features of an Oligopoly market are the following:

- Few sellers: In the oligopoly market, there are few sellers and many customers. Few firms dominating the market enjoys a considerable control over the price of the product.

- Interdependence: One of the most important features of an oligopoly market, wherein, the seller has to be cautious with respect to any action taken by the competing firms. Since there are few sellers in the market, if any firm makes the change in the price or promotional scheme, all other companies in the industry have to comply with it, to remain in the competition. Thus, every company remains alert to the actions of others and plan their counterattack beforehand, to escape the turmoil. Hence, there is a complete interdependence among the sellers with respect to their price-output policies.
- Advertising: In the oligopoly market, every firm advertises their products on a frequent basis, with the intention to reach more and more customers and increase their customer base. This is due to the advertising that makes the competition intense. If any firm does a lot of advertisement while the other remained silent, then he will observe that his customers are going to that firm who is continuously promoting its product. Thus, in order to be in the race, each firm spends lots of money on advertisement activities.
- Competition: There is an intense competition among the sellers. Any move taken by the firm will have a considerable impact on its rivals. Thus, every seller keeps an eye over its rival and be ready with the counterattack.
- Entry and exit Barriers: The firms can easily exit the industry whenever it wants, but has to face certain barriers to entering into it. These barriers could be government licenses, patent, economies of scale, high capital requirement, complex technology, etc. Also, sometimes the government regulations favor the existing large firms, thereby acting as a barrier for the new entrants.
- Lack of Uniformity: There is a lack of uniformity among the firms in terms of their size, some are big, and some are small.

Since there are less number of firms, any action taken by one firm has a considerable effect on the other. Thus, every firm must keep a close eye on its counterpart and plan the promotional activities accordingly.

B

CAPACITY MECHANISMS

B.1. TAXONOMY

There is a variety of capacity mechanism designs, a key difference lies in their competitive or regulated nature. The mechanisms can be divided by the approach that determines the price and volume of the capacity. Generally, there are two types of mechanisms: market based and central/regulation based. Market based mechanisms are usually called 'capacity markets'. There are many different ways to classify capacity mechanisms. It is common to group capacity mechanisms into:

(a) price-based and volume-based,

(b) market-wide and targeted,

(c) centralized and decentralized.

In a price-based mechanism, central authority sets price and let investors decide how much they are willing to participate in capacity markets at a given price. In a volume-based mechanism, central authority decides on the volume of capacity required, then the market determines the price of the demanded volume. Market-wide capacity mechanisms remunerate all capacities, whereas targeted mechanisms reward only specific plants or technologies. In centralized mechanisms, contracts are awarded centrally, as opposed to decentralized mechanisms where contracts are awarded through bilateral arrangements.

This work refers to the taxonomy provided by the Agency for Cooperation of Energy Regulators (ACER), which defines five different types of capacity mechanisms: strategic reserve, capacity obligation, capacity auction, reliability option and capacity payment (see Figure B.1).

Figure B.2 and B.3 provide a snapshot of the five types of capacity mechanisms existing in the EU [1]. While all result from different combinations of the features (a), (b), and (c), each of these five types can have further variants.

[1] ACER, Report on capacity remuneration mechanisms and the internal market for electricity, 30 July 2013

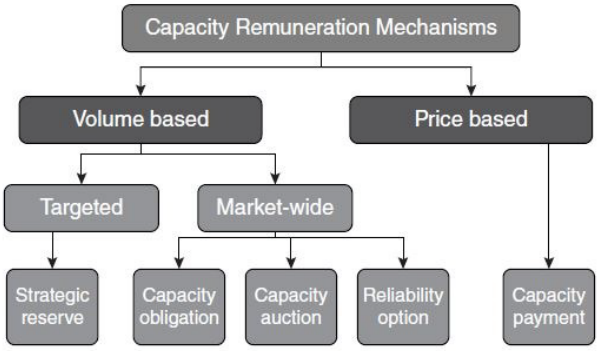

Source: ACER, Report on capacity remuneration mechanisms and the internal market for electricity, 2013 (ACER's Report).

Figure B.1: Taxonomy of capacity models

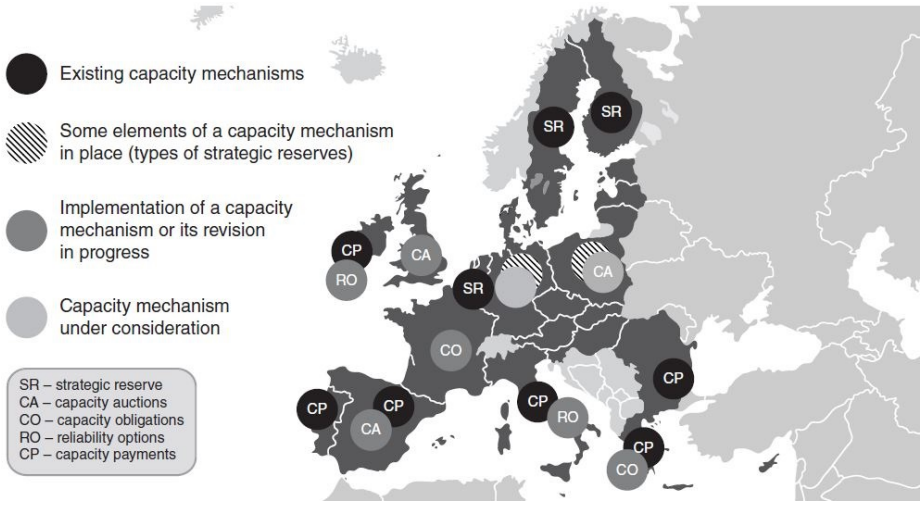

Figure B.2: Capacity models used in EU.

Table II.1.2: **Electricity market characteristics at Member State-level**

Country	Power Exchange	Power Pool	Energy only Market	Capacity Mechanism	Strategic Reserve
Austria	x		x		
Belgium	x				x
Bulgaria			x		
Croatia			na	na	na
Cyprus			na	na	na
Czech Republic	x		x		
Denmark	x				x
Estonia	x		x		
Finland	x				x
France	x			x	
Germany	x				x
Greece		x		x	
Hungary	x			x	
Ireland		x		x	
Italy	x			x	
Latvia	x		x		
Lithuania	x		x		
Luxembourg			na	na	na
Malta			na	na	na
Netherlands	x		x		
Poland	x		x		
Portugal		x		x	
Romania	x		x		
Slovakia	x		x		
Slovenia	x		x		
Spain		x		x	
Sweden	x				x
United Kingdom	x			x	

A Member State is reported as having a capacity mechanism or a strategic reserve whether they are "active", "proposed" or "under consideration".
Source: ACER 2013

Figure B.3: Capacity models used in member states.

B.1.1. GRID RESERVE

In this mechanism, a central agency (e.g. TSOs or a governmental authority) decides the amount of capacity needed a number of years in advance. This capacity is then contracted, usually by means of a public tender based on the lowest price offers. The contracted part of the plants output is then held in reserve and no longer participate in the energy market. Only when capacity shortfalls arise, they are activated according to a pre-defined criterion. This trigger criterion can be, for instance, a certain (high) price level in the energy-only market or possible security violations in the network. As a consequence, strategic reserves are capacities set aside in order to secure supply in certain exceptional circumstances. Given this targeted nature, strategic reserves normally have only a small impact on the prices in the energy-only market. Economic considerations suggest that particularly old plants will be best suited to act as reserve in this regime. Strategic reserve has been implemented in Sweden and Finland, which are hydrodominated and need to ensure enough capacity reserve to meet demand in case of a dry year. In addition, Sweden had to address the lack of sufficient capacity after the decommissioning of a large stock of nuclear generation in the late 1990s. Interim solutions similar to strategic reserve are currently in place in Germany, Belgium, and Poland. Beyond the EU, strategic reserves have also been used in Australia and New Zealand.

B.1.2. CAPACITY AUCTION

The total required capacity is set several years in advance of delivery and centrally procured in an auction by an independent body (usually a TSO). Capacity providers bid to receive a capacity payment. The lowest offers wins the auction, as the TSO is interested in the lowest possible price for the capacity to be sold by generation companies. The new capacity selected at the auction will participate in the energy-only market. As a consequence, there may be a market distortion if the amount of capacity is such that the new capacity may artificially undercut the existing capacity in the energy-only market. In addition, there is a risk of triggering a 'wait-for-the-tender' approach, where investors refrain from responding to the energy-only market price signals for fear of losing the extra remuneration they may reap in capacity auctions.

The UK capacity mechanism recently implemented is based on centralized auctions. Capacity auctions were also discussed in Germany as a long-term option. Beyond the EU, capacity auctions have also been used in the US, Colombia, Brazil, and Panama.

B.1.3. CAPACITY OBLIGATION

This mechanism imposes an obligation on large consumers or suppliers to contract a certain level of capacity linked to their self-assessed future consumption or supply requirements (plus a certain level of reserve margin, established by regulation). The obligation can be fulfilled by owning generation facilities (self-supply) or entering into bilateral agreements with capacity providers. A key design aspect of this system is that suppliers (or consumers) are penalized financially if, in certain situations of capacity scarcity (to be defined by the regulator), they have not procured the required capacity. The expectation is that the threat of such penalties will promote the development of

(ACER's Report) p 5.

a market for capacity contracts that offer an additional (and relatively stable) revenue stream for plant operators. To avoid penalties, suppliers and consumers need to prove that together with their contracted energy they also bought the associated plant capacity. This can be done through certificates, each of which represents a certain amount of capacity made available by a given capacity provider. If they are standardized, they can be traded in a separate market, where prices are set by supply and demand (certificate market). On the supply side, contracted capacity providers are required to make the contracted capacity available to the market in periods of shortage, defined administratively or by market prices rising above a threshold level. Greece adopted a capacity mechanism based on capacity obligations in 2005 (not implemented in practice) and France will follow suit in 2015. Furthermore, this model is strongly favored by the German energy industry. Going beyond European examples, this model can also be found in the US, where regional pools introduced a form of payment for capacity indirectly through capacity obligations imposed on load serving entities. Such capacity mechanisms exist in the Independent System Operator New England (ISO—NE), New York ISO and the Pennsylvania-New Jersey-Maryland Interconnection (PJM) in the District of Columbia.

B.1.4. RELIABILITY OPTIONS

In this model, a TSO or large customers and suppliers are designated by the regulator to enter into option contracts with capacity providers. Such contracts offer TSOs the option to procure power at a strike price. In other words, the option contract obliges the capacity provider to pay the TSO the difference between the price in the energy only market and the strike price, whenever this difference is positive (contracts for difference, CfDs). In exchange for this price guarantee, capacity providers receive an option premium, which is fixed and provides a more stable and predictable stream of revenues (similar to capacity payments). In this regime, capacity providers will continue to participate in the energy market.

The strike price, and the total volume of the reliability options that capacity providers must offer, is set through regulation. In that respect, these mechanisms differ from other risk-hedging instruments available in the market, where both the strike price and the volume are negotiated in the market. Further, reliability options are normally not just financial contracts, but also entail the physical delivery of electricity. In particular, when the price in the energy-only market exceeds the strike price, the capacity provider must be available, otherwise it will pay a penalty. In any case, capacity providers are selected in a competitive tender, which will also set the capacity premium.

Reliability options are being implemented in Italy, through a central auctioning. Beyond the EU, the US and Colombia have also implemented reliability options.

B.1.5. CAPACITY PAYMENT

Capacity payments are pre-determined fees set by the regulator and paid to capacity providers. They have been in place for several years in markets that are less well connected in the periphery of Europe such as Spain, Portugal, Ireland, Greece, and Italy. Capacity payments may be determined in various ways, they can be fixed or variable (e.g., per 'firm' megawatt [MW] and year or simply per month), and awarded to all or part of the eligible capacity declared or actually available. The plants so rewarded will

continue to participate in the energy-only market where they will still benefit from an additional revenue stream. The recipients of capacity payments can be selected through a tender. However, for capacity payments designed to remunerate back-up capacity in systems with a high RES penetration, the feasibility of the tender depends on the proportion between the available firm capacity and the RES capacity. In some cases, such as Spain, the amount of RES may be so high that all existing firm capacity is needed. As a consequence, a tender may not be feasible, and capacity payments are paid out to all the providers of firm capacity. Spain has used capacity payments since 1997, Portugal since 2010, and Ireland and Greece have used this system since 2005. Italy recently decided to move to an auction system and reforms are planned in Spain and Greece, which could lead to a change from the current approach relying on administratively set capacity prices toward a more market based approach. Looking beyond the European experience, capacity payments have been introduced in some South American countries including Argentina, Brazil, Chile, and Colombia.

C

CROSSBORDER INTERCHANGE STATISTICS

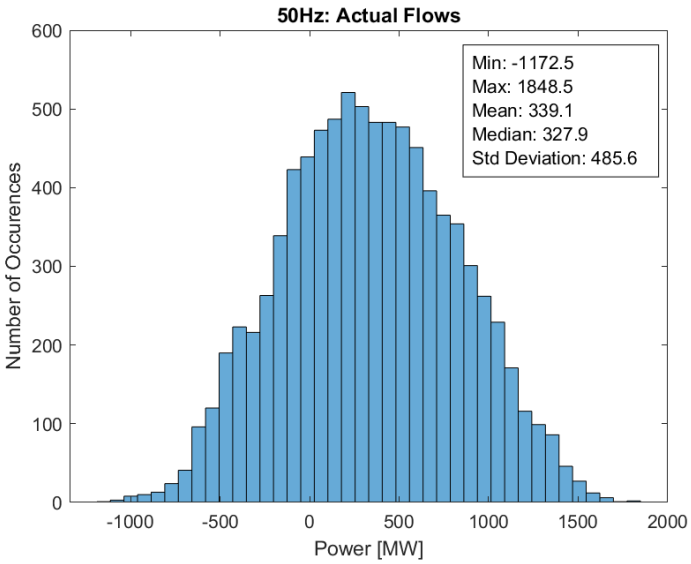

Figure C.1: Interchange statistics from CZ to 50Hz in 2014. Note, positive number represents import of power into CZ area. The typical interchange from 50Hz has a positive sign and mean of 339.1 MW.

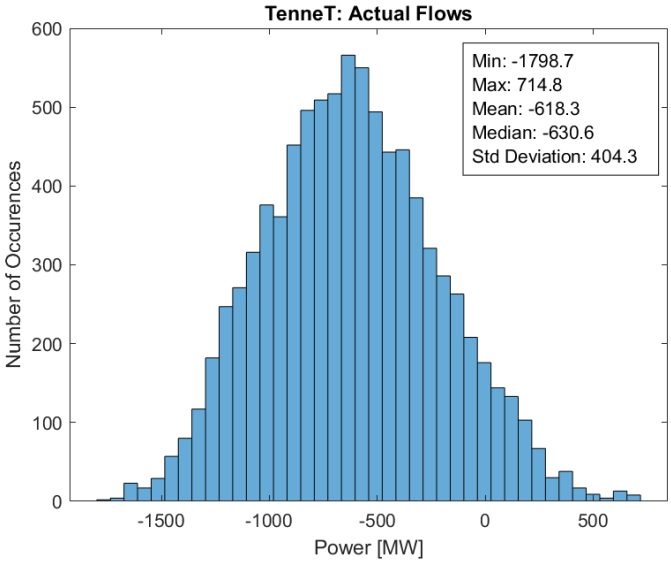

Figure C.2: Interchange statistics from CZ to TenneT in 2014. Note, negative number represents export of power from CZ area. The typical interchange from TenneT has a negative sign and mean of -618.3 MW.

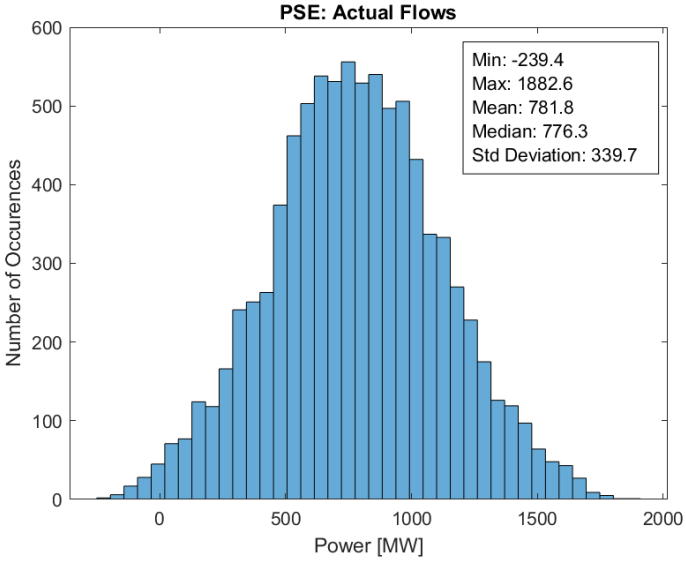

Figure C.3: Interchange statistics from CZ to PSE in 2014. Note, positive number represents import of power into CZ area. The typical interchange from PSE has a positive sign and mean of 781.6 MW.

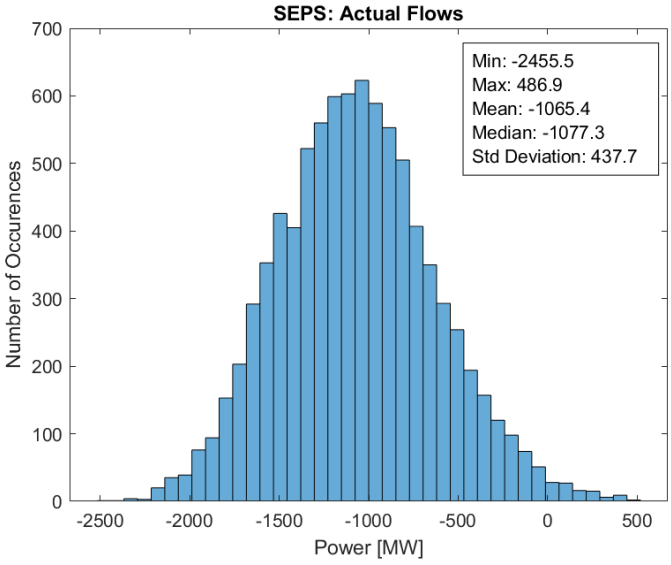

Figure C.4: Interchange statistics from CZ to SEPS in 2014. Note, negative number represents export of power from CZ area. The typical interchange from SEPS has a negative sign and mean of -1065.4 MW.

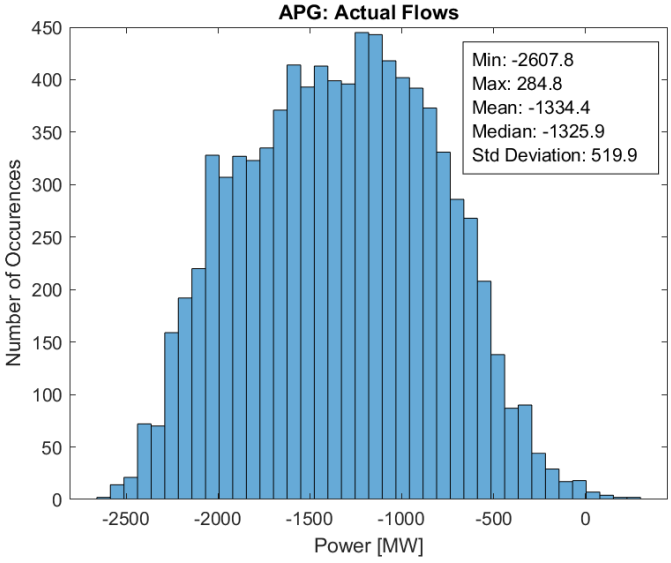

Figure C.5: Interchange statistics from CZ to APG in 2014. Note, negative number represents import of power from CZ area. The typical interchange from APG has a negative sign and mean of 1334.4 MW.

D

CROSSBORDER SCENARIO RESULTS

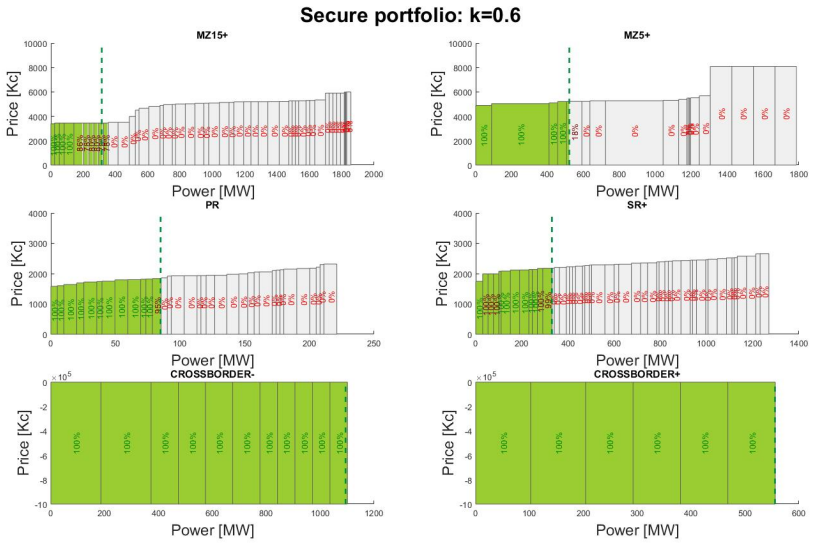

Figure D.1: Crossborder flows belows nominal levels, i.e., $k = 0.6$. AS demand and crossborder flows are satisfied.

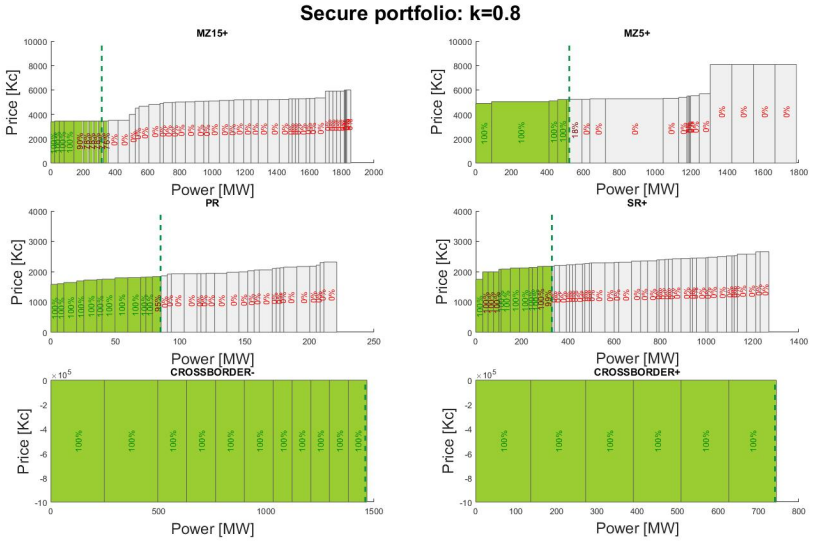

Figure D.2: Crossborder flows belows nominal levels, i.e., $k = 0.8$. AS demand and crossborder flows are satisfied.

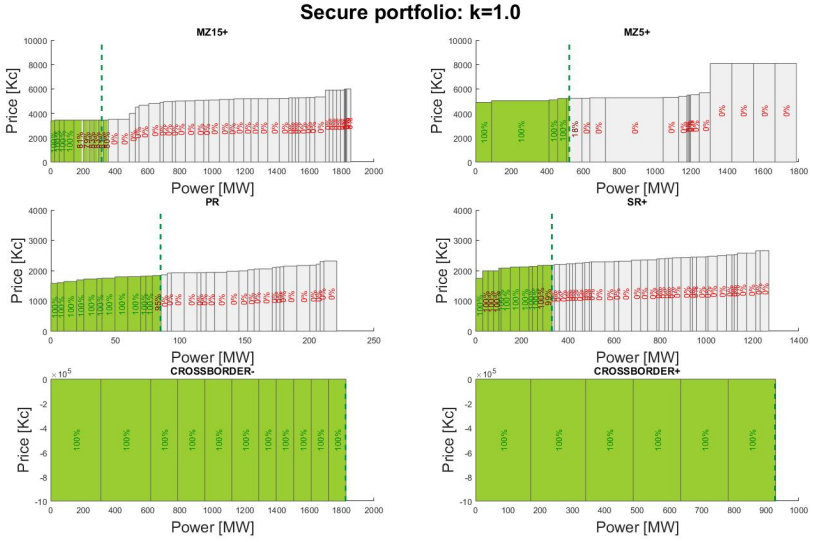

Figure D.3: Crossborder flows at nominal levels, i.e., $k = 1.0$. AS demand and crossborder flows are satisfied.

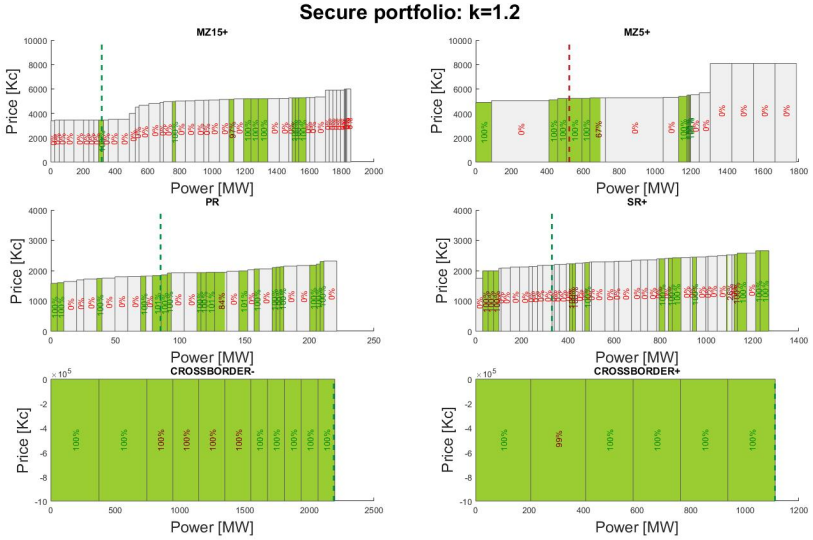

Figure D.4: Crossborder flows increased by 20%, i.e., $k = 1.2$. MZ5+ cannot be activated in full scale. The demanded amount was curtailed.

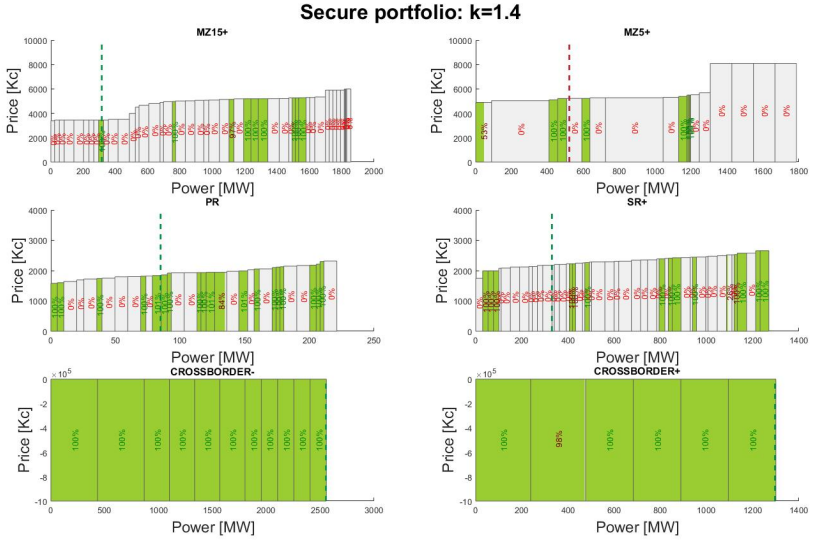

Figure D.5: Crossborder flows increased by 40%, i.e., $k = 1.4$. The demanded amount was curtailed.

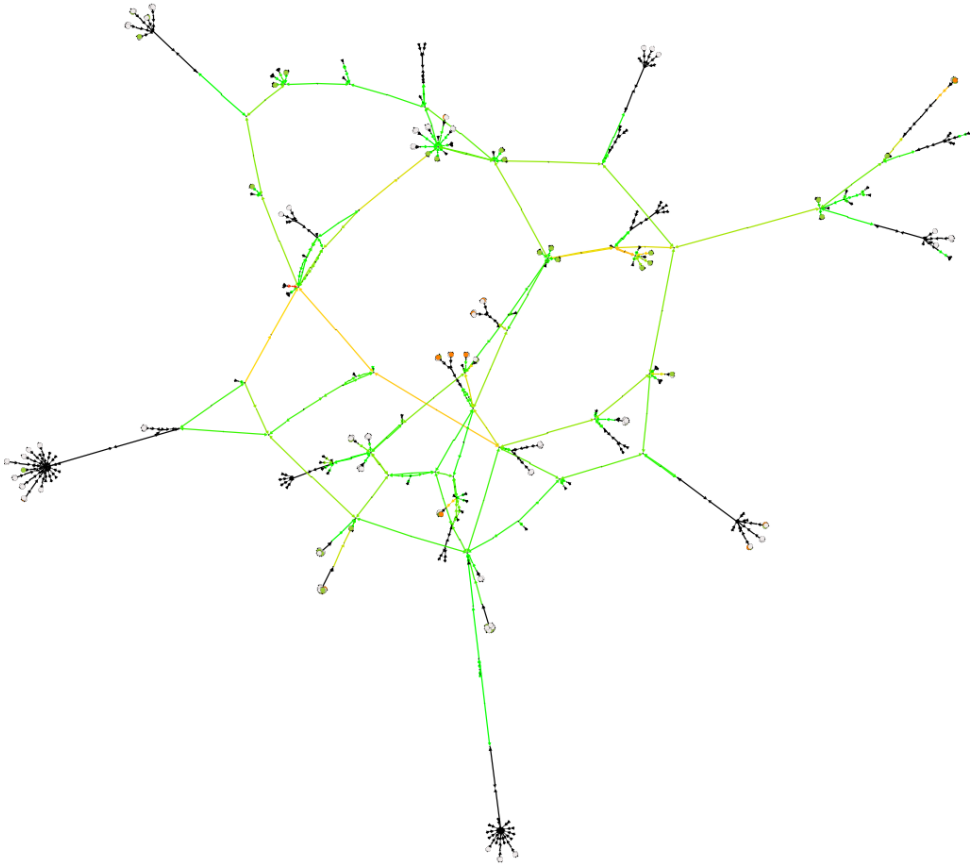

Figure D.6: Network graph with coloured lines w.r.t. their loading $k = 0.6$.

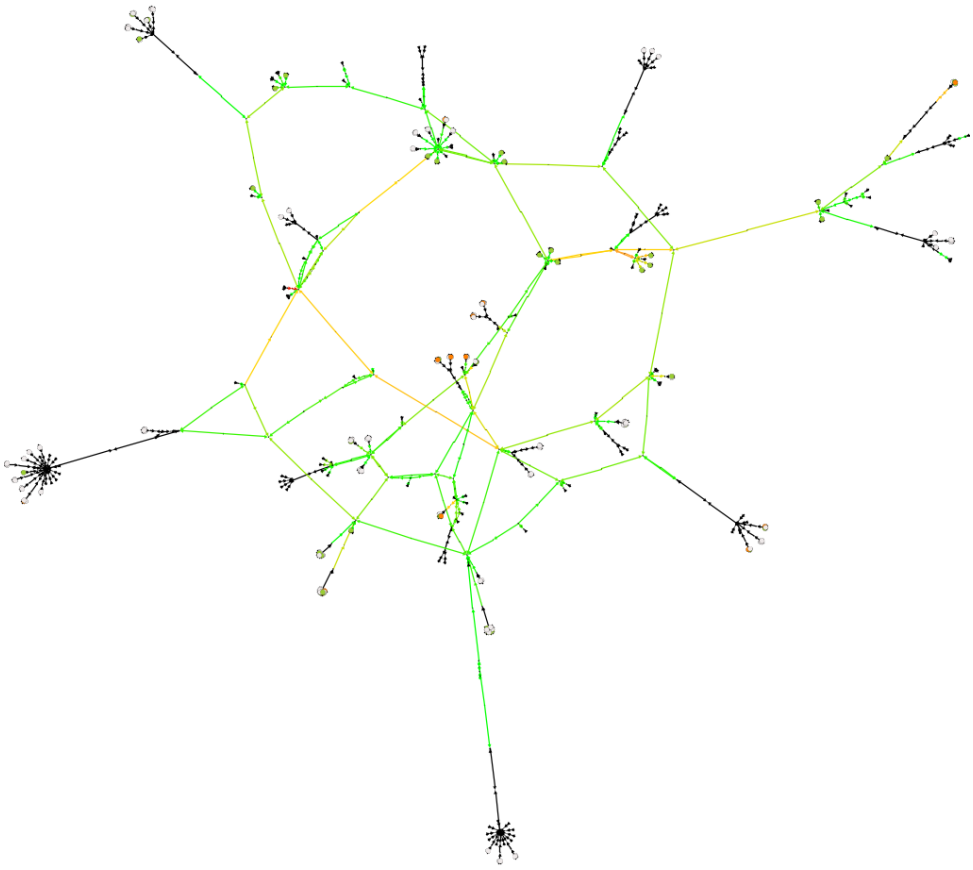

Figure D.7: Network graph with coloured lines w.r.t. their loading $k = 0.8$.

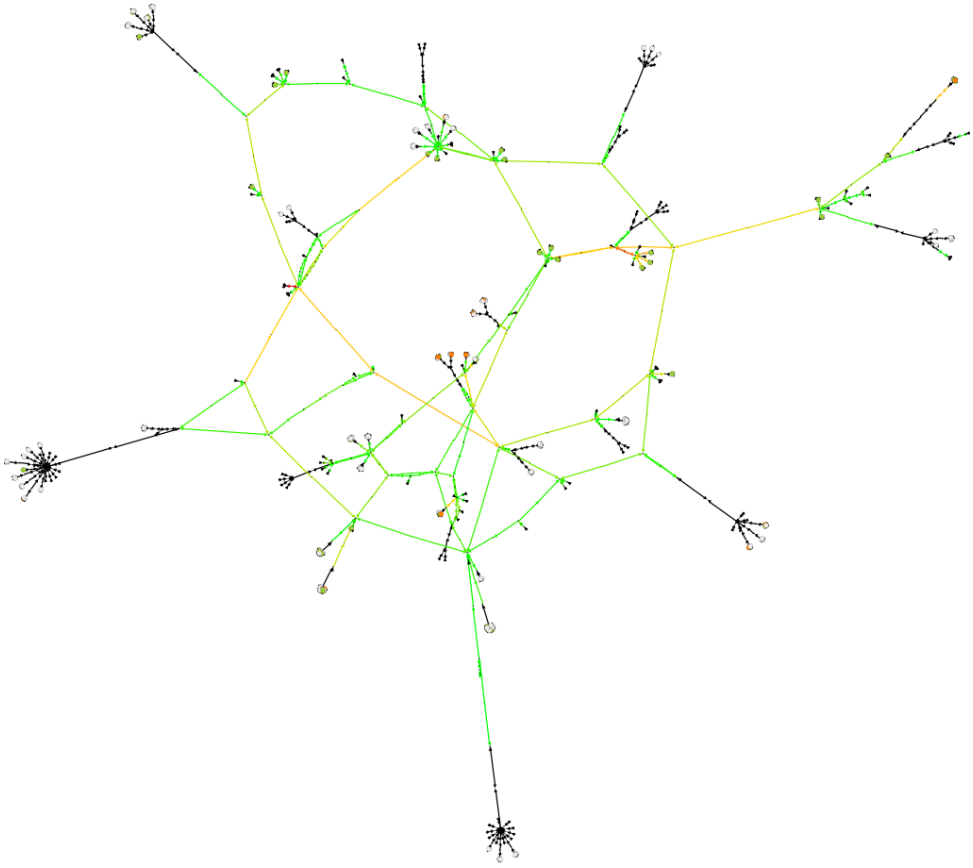

Figure D.8: Network graph with coloured lines w.r.t. their loading $k = 1.0$.

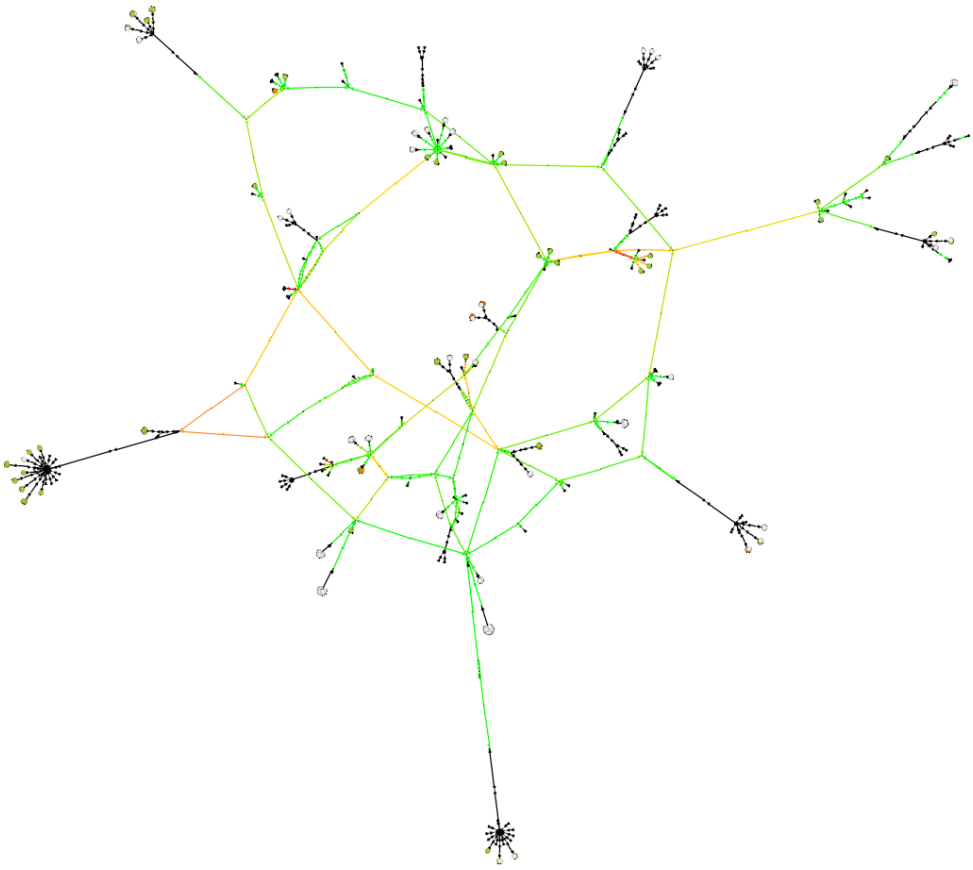

Figure D.9: Network graph with coloured lines w.r.t. their loading $k = 1.2$.

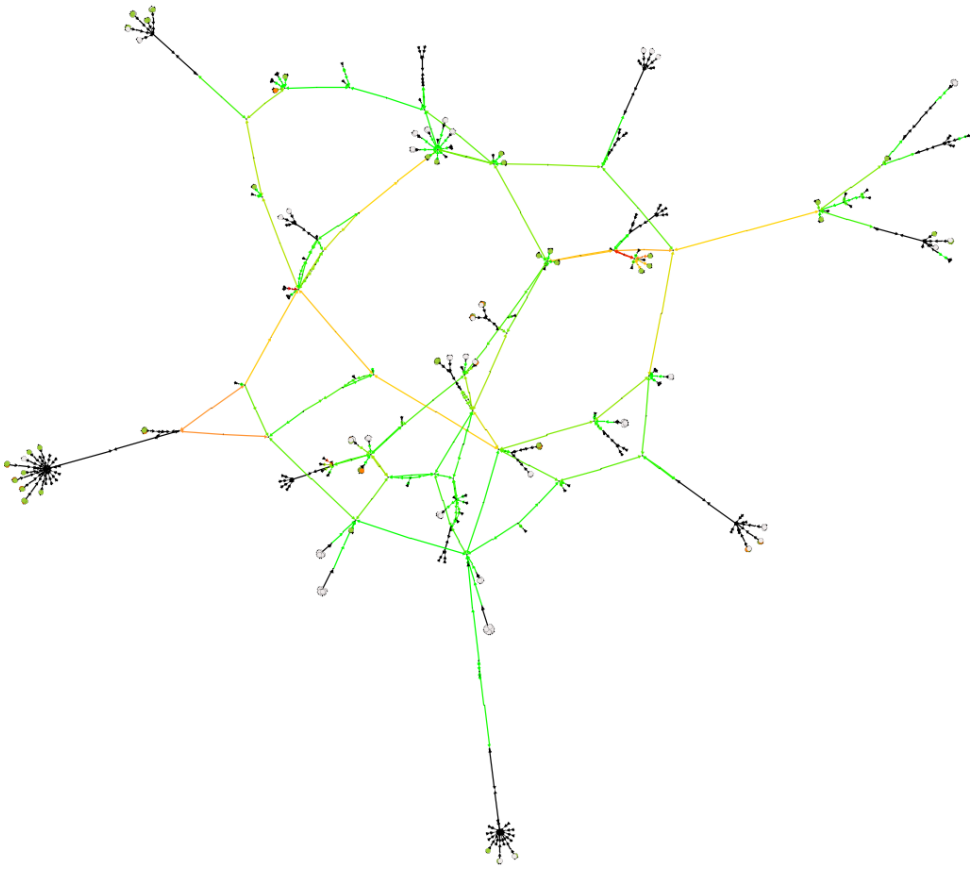

Figure D.10: Network graph with coloured lines w.r.t. their loading $k = 1.4$.

E

EUROPEAN BALANCING MARKETS

This Appendix introduces the current state of balancing markets and the ancillary service (AS) integration initiatives within EU. Balancing markets can be defined as a set of markets in which different types of ancillary services are acquired by system operators to keep power systems secure. Commonly used types of AS and their usage in case of power/voltage deviations are shown in Figure E.1.

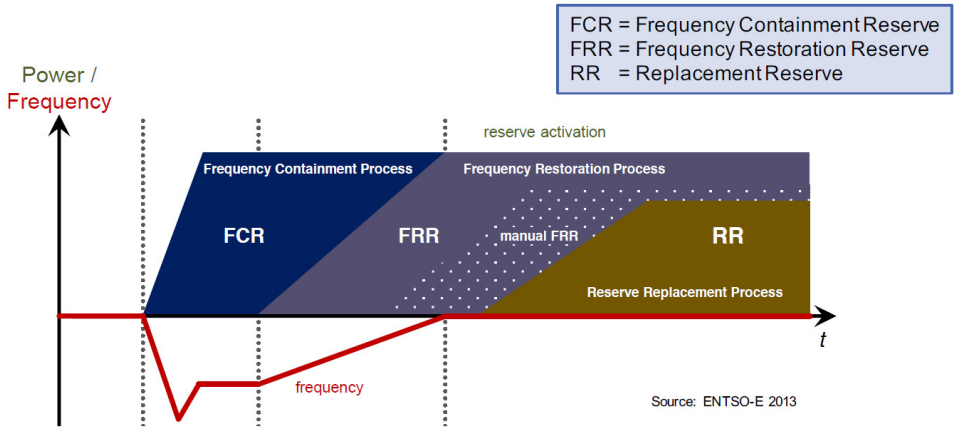

Figure E.1: Types of ancillary services. Frequency containment reserve (FCR) is used for constant containment of frequency deviations from nominal value to maintain the power balance. Frequency restoration reserve (automatic aFRR or manual mFRR) is used to restore frequency to the nominal value and power balance to the scheduled value after sudden system imbalance occurrence. Replacement Reserve (RR) is used to restore the required level of operating reserves to be prepared for a further system imbalance.

E.1. CURRENT STATE OF BALANCING MARKETS IN EU

In this section, the current state of balancing markets in Europe is presented. More information about balancing markets in EU can be found in literature [135] or [136].

As mentioned before, for keeping the power system frequency within secure limits, TSOs shall maintain the balance between load and generation on a short term basis. For this, TSOs initially apply Frequency Containment Reserves (FCR). These reserves are activated fast (typically within 30s), stabilize the power system frequency and make sure that the frequency will not further deviate from the nominal point. Frequency Restoration Reserves (FRR) are intended to replace FCR and restore the frequency to the target frequency, in Europe usually 50.00Hz. Where applied, Replacement Reserves (RR) restore or support the required level of FRR to be prepared for additional system imbalances.

It is important to mention that not all TSOs use all three types of ancillary services. Figure E.2 illustrates the implementation of aFRR in ENTSO-E member states.

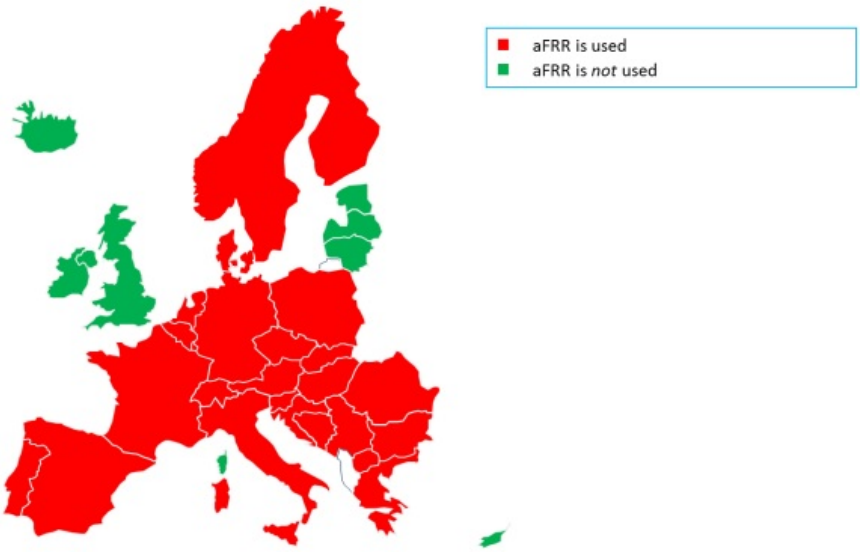

Figure E.2: Capacity models used in EU. Source: https://www.entsoe.eu/Documents/MC%20documents/balancing_ancillary/160229_Report_aFRR_study_merit_order_and_harmonising_FAT_%28vs_1.2%29.pdf

TSOs that apply aFRR, also apply manual FRR (mFRR) and sometimes Replacement Reserves (RR). Figure E.3 shows that the shares of aFRR in the total balancing energy are very different throughout Europe.

There are currently two strategies for the activation of the aFRR:

- Merit order,
- Pro-rata.

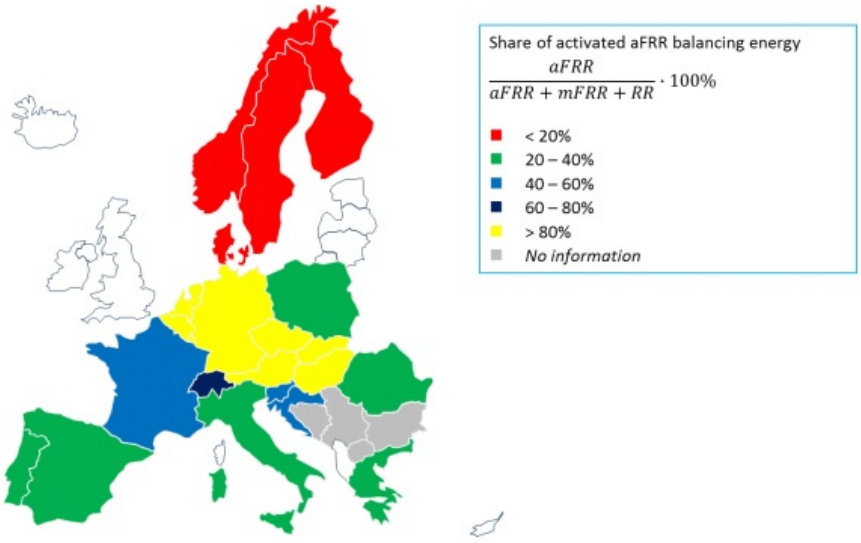

Figure E.3: Share of aFRR energy in total activated FRR/RR balancing energy in EU. Source: https://www.entsoe.eu/Documents/MC%20documents/balancing_ancillary/160229_Report_aFRR_study_merit_order_and_harmonising_FAT_%28vs_1.2%29.pdf

Merit order represents a "select cheapest" strategy. It activates the aFRR with respect to its activation cost, i.e., the cheapest aFRR is activated first. Pro-rata is a strategy in which the demanded amount of aFRR is divided s.t. each provider contributes the same share of aFRR. Both strategies have their advantages and disadvantages. Merit order is considered as a economically effective solution but it ignores possible network congestion. Pro-rata is a more conservative strategy that generally do not contribute to the network congestion but at the price of potentially higher activation cost. Figure E.4 shows the use of these strategies in ENTSO-E member states.

The aFRRs in each individual country have its own specifics. TSOs have specific sets of parameters that the aFRR must meet, e.g., the ramp rate or full activation time. The aFRR providers shall be able to follow the ramp rate in LF Controller's activation signal to maintain a given level of network security. For this, minimum requirements are specified in most LFC Blocks. These minimum requirements are stipulated in different ways: Some TSOs require an aFRR Full Activation Time (FAT), defined as a time period between the instruction by the LF controller and the corresponding activation or deactivation of aFRR. Other TSOs define the maximum time to first response and a minimum ramp rate.

Figure E.5 shows the different response requirements throughout Europe. It can be concluded that the range is large, from 2 minutes in the Nordic LFC Block, 2-3 minutes in Switzerland and 3 minutes in Italy to 15 minutes in many other blocks. In addition, we note that in Germany and Austria, the ramp rate requirements apply to the prequalified volume of the aFRR provider. Inevitably, with aFRR activation bids smaller than the prequalified volume this results in higher ramp rates and faster response.

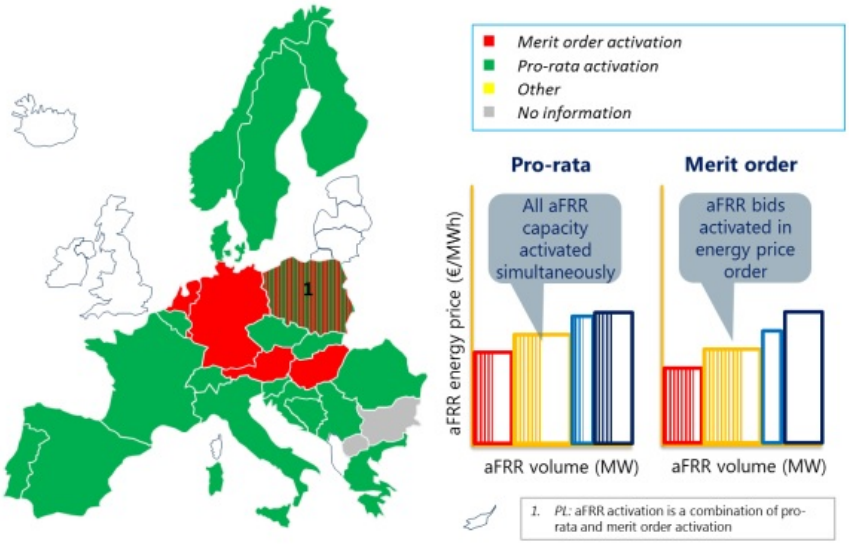

Figure E.4: Merit order versus Pro-rata strategies in ENTSO-E member states. Source: https://www.entsoe.eu/Documents/MC%20documents/balancing_ancillary/160229_Report_aFRR_study_merit_order_and_harmonising_FAT_%28vs_1.2%29.pdf

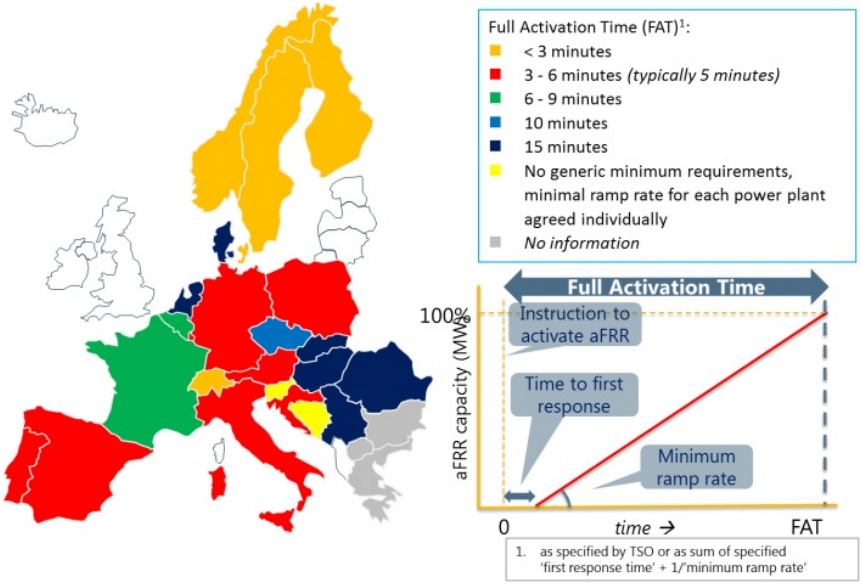

Figure E.5: aFRR response requirements (for some countries the requirements are converted to aFRR Full Activation Times). Source: https://www.entsoe.eu/Documents/MC%20documents/balancing_ancillary/160229_Report_aFRR_study_merit_order_and_harmonising_FAT_%28vs_1.2%29.pdf

This section has shown the current state of balancing markets within EU. Ancillary services within Europe differ in used types, quality and acquisition strategy. This can lead to various types of market inefficiencies due to, e.g., counter-trading, limited amount of supply (monopoly), price and quantity regulations, or bilateral agreements outside the market. To reduce market inefficiencies, several initiatives have been set up. These initiatives are described in the next section.

E.1.1. EUROPEAN INTEGRATION INITIATIVE

The previous sections have described the current state of balancing markets in the individual European countries. In this section, the ENTSO-E initiative to standardize the ancillary service types and integrate the balancing markets in Europe is presented. European electricity markets are currently in the state of a partial integration. There are several initiatives that represent either the form of imbalance netting or aFRR synchronization. The most important initiatives are described next.

REPLACEMENT RESERVES

Currently, TERRE project foreseen as "Western core CoBA" for RR. Project TERRE (Trans European Replacement Reserves Exchange) is one of a number of pilot initiatives set up by ENTSO-E at the request of the Agency for the Cooperation of Energy Regulators (ACER), with the aim of creating a market for Replacement Reserves as requested by the Guideline on Electricity Balancing (EBGL). TERRE is currently the leading early pilot project for the creation of an internal balancing market for Replacement Reserves (RR).

TERRE is about setting up and operating a multi-TSO platform capable of gathering all the offers for Replacement Reserves (RR) and to optimize the allocation of RR across the systems of the different TSOs involved. This platform is called LIBRA[1] and will gather all the RR offers from the participating TSOs' local balancing markets and provide, on a regional level, an optimized allocation of RR in order to meet the TSOs' imbalance needs. Figure E.6 shows full participants and potential candidates in the TERRE project.

Replacement Reserves are traded in a standard product. Standard RR product for TERRE [2]

- Full activation time: 30 min
- Scheduled (00, 15, 30, 45)
- Delivery of 15 min which can be linked together
- Min. duration 15 min
- Max. duration 60 min
- Min. quantity 1 MW

[1] https://goo.gl/YwMKpx
[2] https://goo.gl/ffSjZp

Figure E.6: TERRE project participants and observers in 2017

IMBALANCE NETTING

As part of their responsibility for the transmission system, the Transmission System Operators (TSOs) are obliged to maintain the balance between electricity generation and consumption at all times in their respective LFC Areas. Imbalance netting is the process of two or more Areas that allows for the avoidance of simultaneous aFRR activation in opposite directions by taking into account the respective area control errors as well as the activated aFRR and correcting the input of the involved frequency restoration processes accordingly. Imbalance netting projects are shown in Figure E.7.

IGCC The IGCC (International Grid Control Cooperation) is a cooperation between TSOs which deals exclusively with Imbalance Netting for automatic Frequency Restoration Reserves (i.e. to avoid counter activation of aFRR in different Control Areas) under residual available transfer capacity (ATC) constraints at the borders to provide operational security. Its objectives are to lower the solicitation of aFRR, to strengthen the security of supply for each IGCC Member and to generate social welfare for the whole cooperation. The IGCC is a regional project which currently involves 11 TSOs from 8 countries. These are the TSOs from AT (APG), BE (Elia), CH (Swissgrid), CZ (CEPS), DE (50Hertz, Amprion, TenneT DE, TransnetBW), DK (Energinet.dk), FR (RTE), NL (TenneT NL). The volumes of exchanged energy of each IGCC member are published in real time on the German platform at [3].

[3] https://www.regelleistung.net/ext/data/

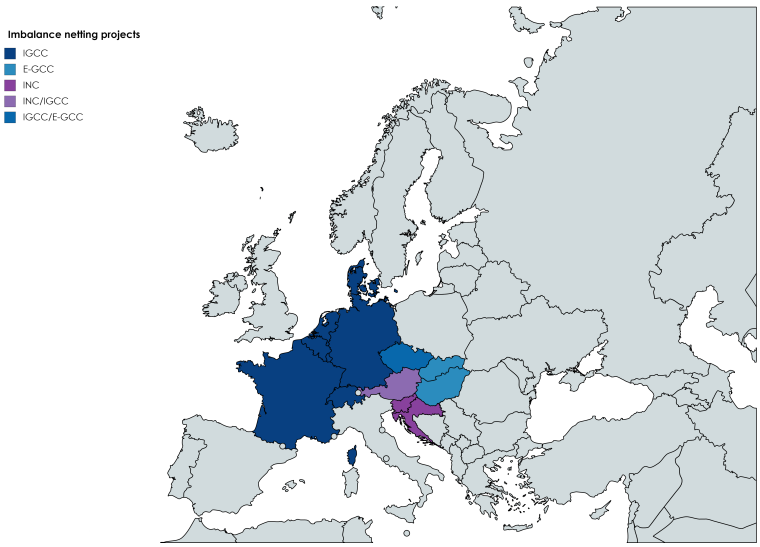

Figure E.7: Current Imbalance netting projects. Note, the Czech Republic is a member of IGCC and E-GCC and Austria is a member of INC and IGCC.

E-GCC E-GCC is a regional project established in 2012 which currently involves three TSOs. These are the TSOs from CZ (CEPS), SK (SEPS), HU (MAVIR). The primary function of the system is to provide the interchange of energy between ČEPS, SEPS, and MAVIR as well as subsequent connection to IGCC. The E-GCC is the passing requests to activate aFRR to the central optimization system in real time. E-GCC builds on this principle and provides processing of data concerning the interchanged balancing energy for subsequent assessment. It performs financial evaluation of the interchanged regulation energy, assessment of payments for the interchanged energy, and provides all data to the transmission system operators using GCC.

INC The INC (Imbalance Netting Cooperation) was founded in mid-May of 2013 by Austria and Slovenia. In 19.4.2016, the Croatian TSO HOPS has joined the INC. Within such Imbalance Netting Cooperation the automatic activation of aFRR is optimized through the netting of the balancing demand from the participating control areas, striving for the best possible avoidance of counter activation. Since APG is cooperating with the IGCC, activation of aFRR within INC is optimized in two steps. First, the netting is performed within the INC (APG, ELES, and HOPS). The residual demand is further optimized within the IGCC, see Figure E.8.

MANUAL FREQUENCY RESTORATION RESERVES (MFRR)

There are currently many regional projects that want to harmonize cross-border exchange of mFRR, e.g., Nordic mFRR market (NOIS), Explore study, DE/AT mFRR market, TERRE mFRR discussions, Amprion/RTE proposal for the design of mFRR market DE/FR. The important mFRR integration projects are presented next.

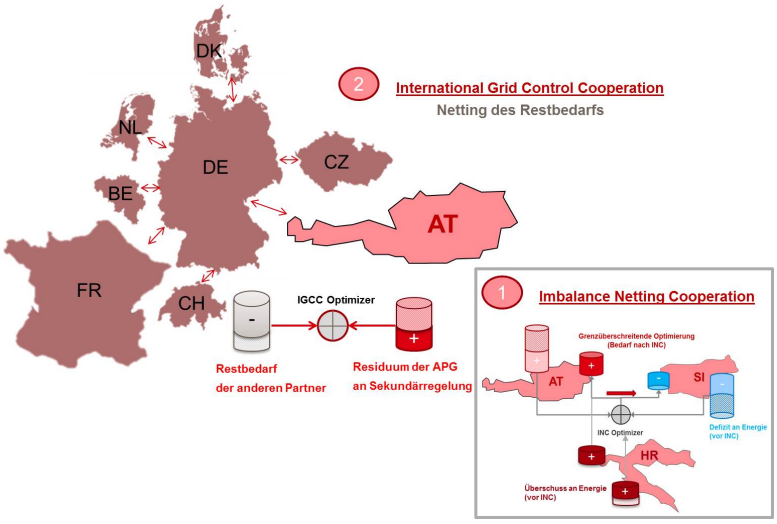

Figure E.8: Cross border aFRR optimization through Imbalance Netting Cooperation (INC)

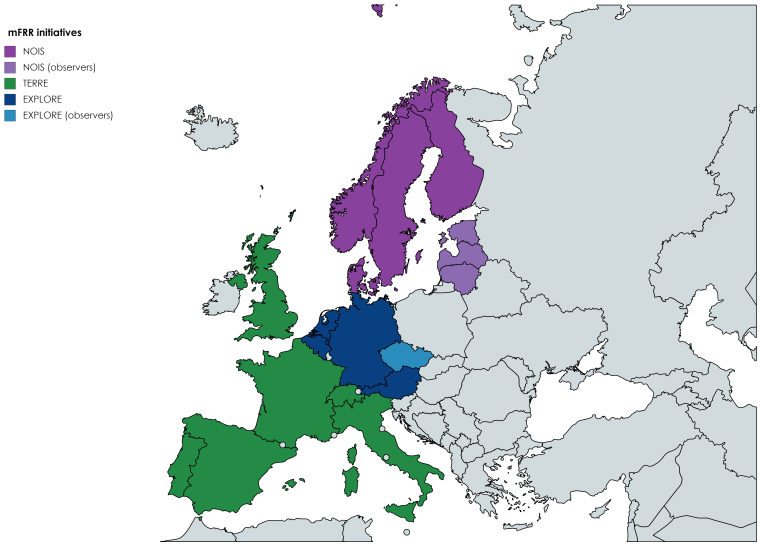

Figure E.9: Manual frequency restoration reserves iniciatives. Various projects to harmonize mFRR. TERRE started discussions about a potential mFRR product.

EXPLORE Since the beginning of 2015, the TSOs of the EXPLORE (European X-border Project for LOng term Real-time balancing Electricity market design) countries – Austria, Belgium, Germany and the Netherlands – have been studying the possibility of integrating their FRR energy markets in the scope of the requirements of the draft guidelines of electricity balancing. The EXPLORE project focuses on the consistency of the complete market model and identifies necessary points of harmonization taking into account the draft guidelines of electricity balancing [137]. Some important findings are related to the complexity in the application of marginal pricing in cross-border balancing markets, due to the close link with TSO operational needs, and to the role of respectively mFRR and aFRR in cross-border markets.

NOIS As one tool to collect the planning data on a Nordic level, the Nordic TSOs use a common platform called NOIS (Nordic Operational Information System). The NOIS system was introduced in 2002 and has since then been developed to match upcoming needs and new operational functions used for Nordic coordination have been implemented. The information compiled in NOIS is meant to give the operators a basis on which they can plan and estimate the need of balancing in the upcoming hours. As the information in NOIS is provided by each TSO it is of great importance that the submitted data is comparable when it comes to resolution and quality to be able to perform proactive balancing.

AUTOMATIC FREQUENCY RESTORATION RESERVES (AFRR)

Five TSC members, the Austrian transmission system operator (TSO) APG and the four German TSOs 50Hertz, Amprion, TenneT and TransnetBW, have joined forces in order to create an internal market for automatic frequency restoration reserve. Since 14 July 2016, the five TSOs form the first international cooperation for automatic Frequency Restoration Reserve (aFRR) in Europe. This Austro-German collaboration shown in Figure E.10 serves as a model project in view of the European Guideline on Electricity Balancing that is currently being implemented. The TSOs are already associated with the International Grid Control Cooperation whose members avoid the demand for aFRR via netting their requirements in advance. The need for expensive aFRR-measures is caused by mismatches between electricity input into the grid and electricity consumption. Effective cross-border management is beneficial for cost control as well as for grid stability.

Now the five TSOs enhance their collaborative efforts to further minimize control reserve costs. They will deploy a merit order list of balance power bids sorted by bid prices. As a result, in each case the economically most advantageous bid for aFRR will be favoured. Besides the probing of a joint procurement of aFRR in Germany and Austria, the TSC members will also take action in developing aFRR-related market rules and products.

E.2. ENTSO-E AS INTEGRATION AND HARMONIZATION PROJECTS

The European Network of Transmission System Operators for Electricity has set out an ambitious target to create an integrated European balancing market for all types of ancillary services that would reduce:

Figure E.10: Current aFRR harmonization projects in EU. Currently only the German and Austrian TSOs can acquire aFRR on a single market.

- The ancillary services acquisition and activation cost,
- counter-trading,
- inefficient redispatch,
- improper ancillary services activation.

Moreover, this market would allow an efficient market competition and would be closer to the model of perfect market competition or at least monopolistic competition. To achieve the goals the ENTSOE:

- proposes a set of standardized ancillary services that may be potentially used in the internal market, through a series of assessment studies,
- sets out a process of creation of the European Internal Market (EIM) integration through defining Regional Internal Markets (RIMs) and Coordinated Balancing Areas (CoBAs).

The final state is displayed in Figure E.11, i.e., the goal is the complete integration of the current balancing markets in Europe into a single European market.

As the Guideline on Electricity Balancing (EB GL) adopted by the European Commission on 16 March 2017 and expected to enter into force by the end of 2017 provides the introduction of platforms to enable the exchange of balancing energy from freguency restoration reserves and replacement reserves. To make this happen, ambitious international projects were recently launched by ENTSO-E. These projects are called PICASSO and MARI.

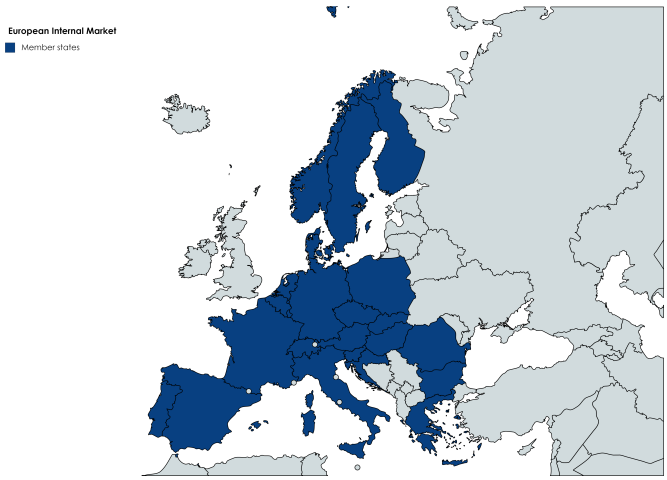

Figure E.11: The internal European ballancing energy market

PICASSO

Currently, the eight TSOs took the voluntary initiative to anticipate the timelines set forth by the EB GL by already starting the work on the design of the aFRR platform to facilitate future European-wide discussions. The Platform for the International Coordination of Automated Frequency Restoration and Stable System Operation (PICASSO) is a regional project initiated by eight TSOs from five countries. The Austrian TSO APG, the Belgian TSO Elia, the Dutch TSO Tennet, the French TSO RTE and the German TSOs – 50Hertz, Amprion, Tennet, TransnetBW – agreed to initiate a project on the design, implementation and operation of a Platform for automatic Frequency Restoration Reserves (aFRR)[4]. Current observers are Czech TSO CEPS, Polish TSO PSE, Hungarian TSO Mavir, Slovenian TSO ELES, Bulgarian TSO ESO, Norwegian TSO Stattnet, Swedish TSO Svenska kraftnät, Finnish TSO Fingrid, and Danish TSO Energinet DK.

The project was launched in October 2017. The goal for this project is to design, implement and operate an aFRR platform compliant with the approved versions of GLEB, GLSO, CACM as well as other regulations. Development of this platform should help to integrate the European aFRR markets while respecting the TSO-TSO model.

MARI

The goal of the MARI project is to create an European platform for mFRR[5][6]. TSOs of the cooperation shown in Figure E.13 started working on the principles of an mFRR platform already in 2016 but the project was launched in 2017. MARI platform shall facilitate the exchange of standard mFRR balancing energy products as defined by all TSOs in accor-

[4] https://electricity.network-codes.eu/network_codes/eb/picasso/

[5] https://www.entsoe.eu/news-events/events/Pages/Events/manually-activated-reserves-initiative-stake
aspx?EventWorkshopId=319

[6] https://www.entsoe.eu/Documents/MC%20documents/balancing_ancillary/2017-06-07/
170607_Manual_Activation_Reserve_Initiative.pdf

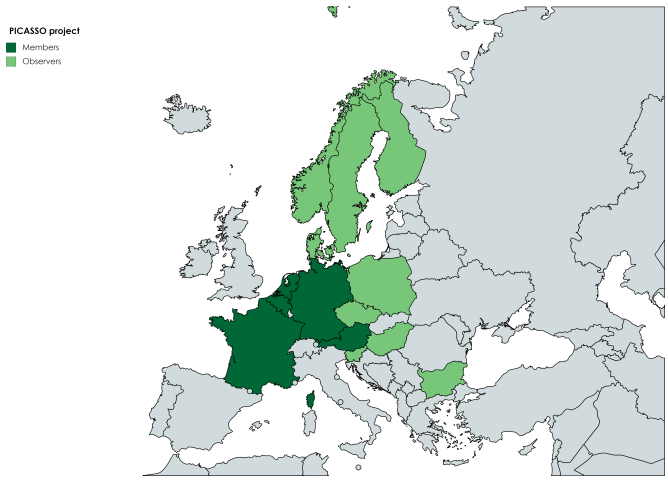

Figure E.12: Members and observers of the PICASSO Project.

dance with EB GL. The final definition of the standard product is to be determined. The EB GL specifies the minimum characteristics of a standard product bid.

E.2.1. ANCILLARY SERVICES STANDARDIZATION

The Guideline on Electricity Balancing (GLEB) foresees that no later than two years after entry into force of this Guideline, all transmission system operators (TSO) shall develop a proposal for a list of standard products for Balancing Capacity and for Balancing Energy for Frequency Restoration Reserves and Replacement Reserves.

The objective of the frequency restoration process (FRP) is to restore frequency to the target frequency, in Europe usually 50.00Hz. For this, the FRP is using manual and automatic Frequency Restoration Reserves (FRR). Automatic FRR (aFRR) is automatically instructed by the central Load Frequency Controller (LF Controller) of the TSO and automatically activated at the aFRR provider. The LF Controller is working continuously, i.e. typically every 4 to 10s the TSO's LF Controller may provide new aFRR activation requests to aFRR providers. aFRR is provided by units that are 'spinning' and therefore aFRR providers can follow the TSO's request from their current setpoint within typically one minute.

Continental European (CE) and Nordic TSOs apply aFRR, however differently. On the continent, LFC Areas are defined and each of the areas has its own LF Controller. Some LFC Areas are aggregated in LFC Blocks in which the aFRR activation of several TSOs is coordinated. For other LFC Areas, the LFC Block consists of one LFC Area only. The objective of the LF Controllers is to restore the Frequency Restoration Control Error (FRCE), which is for LFC Blocks in CE the difference between measured total power value and scheduled control program for the power interchange of the LFC Block, taking into account the effect of the frequency bias for that control area. The objective of all continental European LF Controllers together is to restore and maintain the system fre-

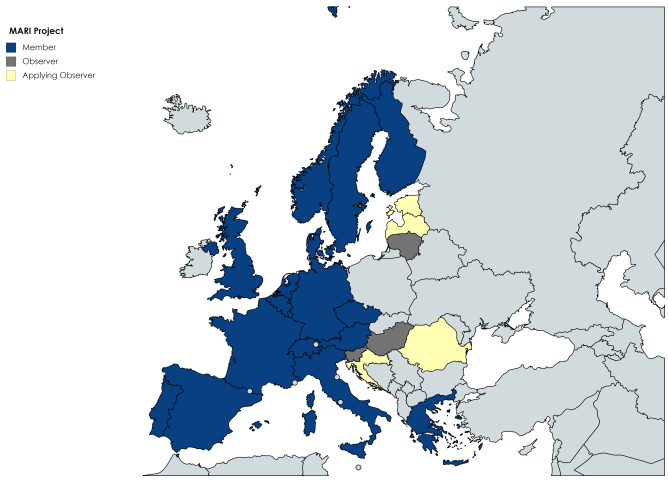

Figure E.13: Members, observers, and applicants of the MARI Project.

quency in the European synchronous system. In the Nordic synchronous area the four TSOs only apply one LF Controller for the entire synchronous area. The objective of this LF Controller is to restore the frequency to the target frequency.

Although the objectives and the high level set-up is very similar, there are major differences in the aFRR requirements and the use of aFRR by the TSOs throughout Europe. Large differences have also been found in applied LF Controllers and parametrisation of these controllers. Furthermore, some TSOs only exceptionally apply manual FRR and balance their system with close to 100% aFRR while other TSOs perform system balancing mainly manually and apply aFRR for less than 10%.

The standardization parameters set by GLEB are the following:

a) preparation period,

b) ramping period,

c) full activation time,

d) minimum and maximum quantity,

e) deactivation period,

f) mode of activation,

g) validity period,

h) minimum and maximum duration of delivery period.

Figure E.14 shows the meaning of all of the parameters mentioned above.
Products are named based on a generic method. For the Direct Activated Product:

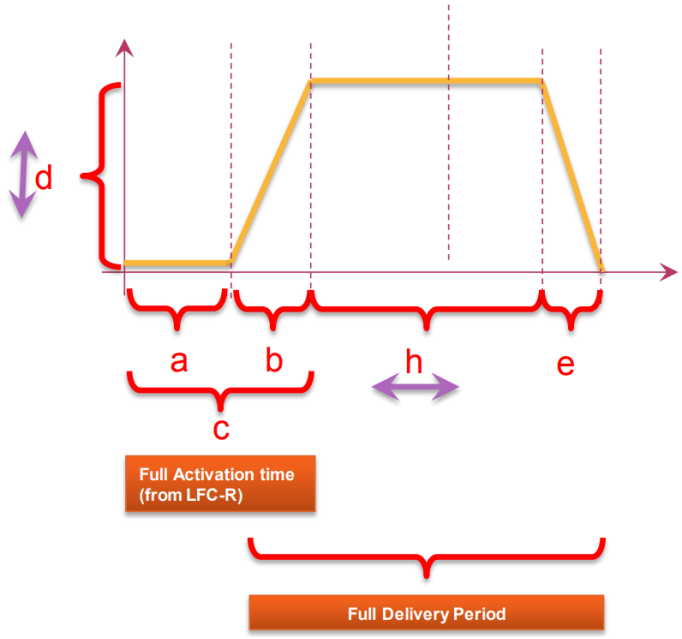

Figure E.14: Parameters description: a) Preparation period, b) Ramping period, c) Full activation time, d) Minimum and maximum quantity, e) Deactivation period, h) Full delivery period

Direct Act. Product	P-[DA]-[FAT]-[MIN DEL. PER.]/[MAX DEL. PER.]
Scheduled Product	P-[SCH]-[FAT]-[MIN DEL. PER.](/[MAX DEL. PER.])

Table E.1: Standardized product naming convention. FAT stands for full activation time. Minimum and Maximum delivery periods are abbreviated as min/max del. per. DA/SCH stand for direct activated or scheduled product

MANUALLY ACTIVATED RESTORATION RESERVES AND REPLACEMENT RESERVES (MFRR/RR)

Latest draft proposal for standard product was made up of 4 products [7]. These are shown in Table E.2.

	P-DA/SCH-15-15/30	P-DA-10-10/25	P-DA-5-5/20	P-SCH-30-15
Type	mFRR	mFRR	mFRR	RR
Activation type	Direct or Scheduled	Direct	Direct	Scheduled
FAT	15	10	5	30
Min. Delivery	15	10	5	15
Max. Delivery	30	25	20	60
Temporal Divisibility	YES	YES	YES	NO
Ramping period	TBD	TBD	TBD	TBD
Bid size	1 to 9999 MW			

Table E.2: List of proposed standard mFRR and RR products.

Direct activated product corresponds to an ancillary service that can be activated directly by the system operation in case of an imbalance. A scheduled ancillary service represents a product that can be only activated at a scheduled time. As shown in Figure E.14, the Full activation time refers to a time period following the AS activation after which it can inject the full contracted output. The FAT in EU varies from 2.5 minutes up to 15 minutes.

Minimum delivery period of the bid is a pre-defined value to request that BSPs should be able to deliver energy at least equal to the Minimum Delivery Period and for the TSO to activate the bid at least for the Minimum Delivery Period. Maximum delivery period of the bid represents a value meaning that BSPs should be able to deliver energy up to the Maximum Delivery Period and for the TSO to activate the bid no more than the Maximum Delivery.

According to the study performed by ENTSOE. The standardized products shown in Table E.2 cover the majority of manually activated ancillary services. Figure E.15 shows the percentage of the ancillary services includes in the standardized product set for ENTSOE member states.

The three DA products are clearly needed and will be used by TSOs. High interest for a P-DA product with 15' Full Activation Time (discussions on minimum and maximum duration ongoing). P-DA-10-10/25 and P-DA-5-5/20 immediately follow. SCH RR (P-SCH-30-15) products are clearly needed and used mainly by those TSO who are member of TERRE project. DA products could be activated in the same way as SCH when the timing allows for it.

[7] https://www.entsoe.eu/Documents/MC%20documents/balancing_ancillary/160630_BSG_TOP2_Products.pdf

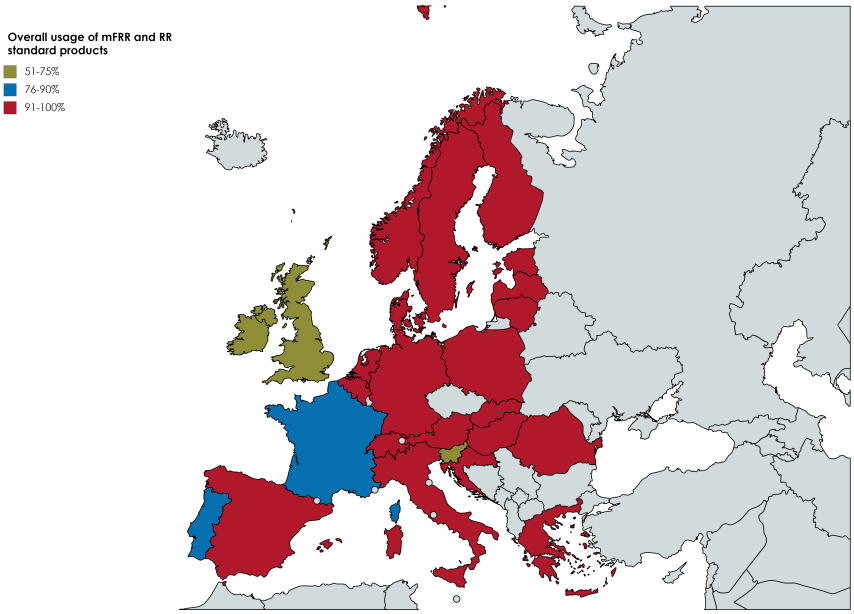

Figure E.15: Percentage of use of standard products given in Table E.2. In can be seen that the list of standard products comprised the majority of manually activated ancillary services throughout ENTSO-E countries. Source ENTSO-E

AUTOMATIC ACTIVATED RESTORATION RESERVES (AFRR)

When trying to find a common type of automatic frequency restoration reserve, there are various criteria functions that can be used. The main criteria are the following:

- Frequency quality,
- Overall cost for the TSO,
- Technical parameters, i.e., FAT, Activation mode, Contracted volumes, Controller settings.

ENTSO-E has picked the frequency quality criteria as the most important. The goal is to introduce a common aFRR product that will not reduce overall frequency quality.

The criteria was set to 15000 minutes outside the standard frequency range per year. The values are derived from probabilistic risk calculation for exhaustion of FCR. It does not introduce a change from the current values.

First debates about harmonization of aFRR are starting about FAT. There is already a limited number of scenarios for the full activation time : 2,5-5-7,5-10-15. The final FAT should be short enough in order to respect frequency criteria. According Figure E.16, full activation times of 5, 7,5 and 10 appear as the most likely scenarios.

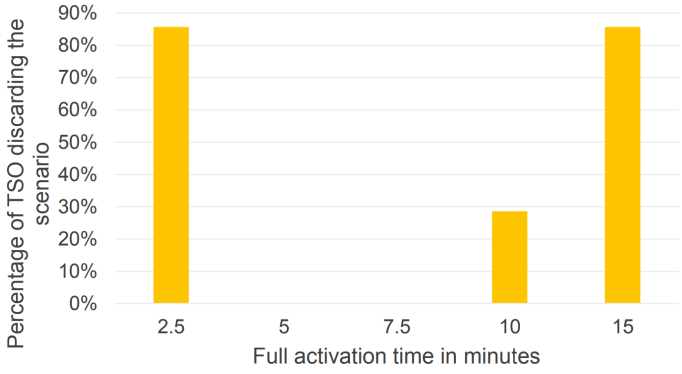

Figure E.16: Percentage of TSO discarding the proposed FAT in minutes

It is highly likely that there will be one standard product per synchronous area. In principle, aFRR products could still be exchanged between synchronous areas. Other aFRR parameters that need to be discussed are shown in Table E.3.

	aFRR standard product
FAT	2,5 – **5 – 7,5 – 10** - 15
Min. Delivery	Not relevant
Max. Delivery	Not relevant
Temporal Divisibility	YES
Activation method	TBD. (CMOL, MO, RATA)
Bid size	1 to x MW (TBD,)

Table E.3: Proposal for aFRR standard products parameters.

REFERENCES

[1] T. P. Hughes, *Networks of Power: Electrification in Western Society, 1880-1930*. The Johns Hopkins University Press, 1983.

[2] T. Steinberg, M.J.;Smith, *Economic Loading of Power Plants and Electric Systems*. McGraw-Hill, 1943.

[3] H. Hale, "Power losses in interconected transmission networks," *AIEE Transactions*, vol. 71, no. 3, pp. 973–998, 1952.

[4] J. Zhu, *Optimization of Power System Operation*. Johm Wiley and Sons, Inc, 2009.

[5] L. Dunstan, "Mashine computation of power network performance," *AIEE Transactions*, vol. 66, no. 1, pp. 610–624, 1947.

[6] H. Clair and G. Stagg, "Experience in compuation of load flow studies using high-speed computers," *AIEE Transactions on Power Aparatus and Systems*, vol. 77, no. 3, pp. 1275–1282, 1959.

[7] J. Cronin and M. Newman, "Digital load flow program for 1000-bus systems," *AIEE Transactions on Power Aparatus and Systems*, vol. 83, no. 7, pp. 718–720, 1963.

[8] G. Glimn, A.F.and Stagg, "Automatic calculation of load flows," *AIEE Transactions on Power Aparatus and Systems*, vol. 76, no. 3, pp. 817–825, 1957.

[9] J. Treece, "Bootstrap gauss-seidel load flow," *Proceedings of the Institution of Electrical Engineers*, vol. 116, no. 5, pp. 866–870, 1969.

[10] W. Tinney and C. Hart, "Power flow solution by newton's method," *AIEE Transactions on Power Aparatus and Systems*, vol. 86, no. 11, pp. 1449–1460, 1967.

[11] B. Scott, "Effective starting process for newton-raphson load flows," *Proceedings of the Institution of Electrical Engineers*, vol. 118, no. 8, pp. 983–987, 1971.

[12] B. Scott, "Review of load-flow calculation methods," *Proceedings of the IEEE*, vol. 62, no. 7, pp. 916–929, 1974.

[13] S. Herraiz, "Review of harmonic load flow formulations," *Proceedings of the IEEE*, vol. 18, no. 3, pp. 1079–1087, 2003.

[14] J. Martinez and J. Mahseredjian, "Load flow calculations in distribution systems with distributed resources. a review," in *Power and Energy Society General Meeting, 2011 IEEE*, 2011, pp. 1–8.

[15] R. Zimmerman, C. Murillo-Sanchez, and R. Thomas, "Matpower: Steady-state operations, planning, and analysis tools for power systems research and education," *Power Systems, IEEE Transactions on*, vol. 26, no. 1, pp. 12–19, Feb 2011.

[16] R. Idema, D. Lahaye, C. Vuik, and L. van der Sluis, "Scalable newton-krylov solver for very large power flow problems," *Power Systems, IEEE Transactions on*, vol. 27, no. 1, pp. 390–396, Feb 2012.

[17] A. Trias, "The holomorphic embedding load flow method," in *Power and Energy Society General Meeting, 2012 IEEE*, July 2012, pp. 1–8.

[18] J. Carpentier, "Contribution to the economic dispatch problem," *Bulletin de la Societe Francaise des Electriciens (in French)*, vol. 8, pp. 431–447, August 1962.

[19] H. Dommel and W. Tinney, "Optimal power flow solutions," *Transactions on Power Apparatus and Systems*, vol. 87, no. 10, pp. 1866–1876, 1968.

[20] G. Maria and J. Findlay, "A newton optimal power flow program for ontario hydro ems," *IEEE Transactions on Power Systems*, vol. 2, no. 3, pp. 576–582, 1987.

[21] J. Momoh, M. El-Hawary, and R. Adapa, "A review of selected optimal power flows literature to 1993 part i: Nonlinear and quadratic programming approaches," *IEEE Transactions of Power Systems*, vol. 14, no. 1, pp. 96–104, 1999.

[22] J. Momoh, M. El-Hawary, and R. Adapa, "A review of selected optimal power flows literature to 1993 part ii: Newton, nonlinear programming and interior point methods," *IEEE Transactions of Power Systems*, vol. 14, no. 1, pp. 105–111, 1999.

[23] M. Huneault and F. Galiana, "A survey of the optimal power flow literature," *IEEE Transactions on Power Systems*, vol. 6, no. 2, pp. 762–770, 1991.

[24] J. Henderson, "Automatic digital compuiter solution of loa flow studies," *AIEE Transactions on Power Aparatus and Systems*, vol. 73, no. 2, 1955.

[25] J. Peschon, D.W.Bree, and L. Hajdu, "Optimal power-flow solutions for power system planning," *Proceedings of the IEEE*, vol. 60, no. 1, pp. 64–70, 1972.

[26] R. Burchett, H. Happ, and K. Wirgau, "Large scale optimal power flow," *IEEE Transactions on Power Apparatus*, vol. PAS-101, no. 10, pp. 3722 – 3732, 1982.

[27] J. Momoh, "Optimal power flow with multiple objective functions," *Power Symposium, 1989., Proceedings of the Twenty-First Annual North-American*, pp. 105– 109, 1989.

[28] G. Angelidis and A. Semlyen, "Optimal power flow using a generalized power balance constraint," *Electrical and Computer Engineering, Canadian Journal of*, vol. 18, no. 4, pp. 191 – 198, 1993.

[29] H. Wei, H. Sasaki, J. Kubokawa, and R. Yokoyama, "An interior point nonlinear programming for optimal power flow problems with a novel data structure," *Power Industry Computer Applications., 1997. 20th International Conference on*, pp. 134 – 141, 1997.

[30] L. Platbrood, H. Crisciu, F. Capitanescu, and L. Wehenkel, "Solving very large-scale security-constrained optimal power flow problems by combining itterative contingency selection and network compression," *Power System Computation Conference, Stockholm, Sweden*, 2011.

[31] J. Twidell, "Changing directions to renewable energy," *British Annual Energy Review*, pp. 63–72, 1991.

[32] C. Nunn, "Ieee colloquium on demand-side management and resource planning in the united kingdom and europe (digest no. 1994/186)„" 1994.

[33] R. Pratt, "Transforming the u.s. electricity system," *Power Systems Conference and Exposition, 2004. IEEE PES*, 2004.

[34] S. Grenard, D. Pudjianto, and G. Strbac, "Benefits of active management of distribution network in the uk," *18th International Conference and Exhibition on Electricity Distribution, 2005. CIRED 2005.*, 2005.

[35] S. Bull, "Renewable energy today and tomorrow," *Proceedings of the IEEE*, vol. 89, no. 8, pp. 1216–1226, 2001.

[36] N. Hatziargyriou, "Energy management and control of island power systems with increased penetration from renewable sources," *Power Engineering Society Winter Meeting, 2002. IEEE*, 2002.

[37] B. Borkovska, "Probabilistic load flow," *Proceedings of IEE*, vol. 121, no. 12, pp. 1551–1556, 1974.

[38] A. Meliopoulos, A. Bakirtzis, and R. Kovacs, "Power system reliability evaluation using stochastic load flows," *IEEE Transactions on Power Apparatus and Systems*, 1984.

[39] F. Boshell and O. Veloza, "Review of developed demand side management programs including different concepts and their results," *Transmission and Distribution Conference and Exposition: Latin America, 2008 IEEE/PES*, 2008.

[40] P. Chen, Z. Chen, and B. Bak-Jensen, "Probabilistic load flow: A review," *Electric Utility Deregulation and Restructuring and Power Technologies, 2008. DRPT 2008. Third International Conference on*, 2008.

[41] E. Janecek and D. Georgiev, "Probabilistic extension of the backward/forward load flow analysis method," *IEEE Transactions on Power Systems*, vol. 27, no. 2, pp. 695–704, 2012.

[42] A. Schellenberg, W. Rosehart, and J. Aguado, "Cumulant-based probabilistic optimal power flow (p-opf) with gaussian and gamma distributions," *IEEE Transactions on Power Systems*, vol. 20, no. 2, pp. 773–781, 2005.

[43] C. Hamon, M. Perninge, and L. Soder, "Applying stochastic optimal power flow to power systems with large amounts of wind power and detailed stability limits," *Bulk Power System Dynamics and Control - IX Optimization, Security and Control of the Emerging Power Grid (IREP), 2013 IREP Symposium*, pp. 1–13, 2013.

[44] G. Li and X. Zhang, "Stochastic optimal power flow approach considering correlated probabilistic load and wind farm generation," *Reliability of Transmission and Distribution Networks (RTDN 2011), IET Conference on*, pp. 1–7, 2011.

[45] B. Scott, O. Alsac, and A. Monticelli, "Security analysis and optimization," *Proceedings of IEEE*, vol. 75, no. 12, pp. 1623–1644, 1987.

[46] K. Karoui, H. Crisciu, A. Szekut, and M. Stubbe, "Large scale security constrained optimal power flow," *16th PSCC, Glasgow, Scotland*, 2008.

[47] F. Capitanescu, J. M. Ramos, P. Panciatici, D. Kirschen, A. M. Marcolini, L. Platbrood, and L. Wehenkel, "State-of-the-art, challenges, and future trends in security constrained optimal power flow," *Electric Power Systems Research*, vol. 81, no. 8, pp. 1731–1741, 2011.

[48] *Principles of Microeconomics, 7th Edition.* South-Western College Pub, 2014.

[49] *Microeconomics, 6th Edition.* Prentice Hall, 2014.

[50] *Intermediate Microeconomics: A Modern Approach (Eighth Edition) 8th Edition.* W. W. Norton and Company, 2009.

[51] M. Hancher L.; Houteclocque, A; Sadowska, *Capacity Mechanisms in EU Energy Markets.* Oxford University Press, 2015.

[52] F. Wu, G. Gross, J. Luini, and P. Look, "A two-stage approach to solving large-scale optimal power flows," *Power Industry Computer Applications Conference, 1979. PICA-79. IEEE Conference Proceedings*, 1979.

[53] A. Yassine, R. Girard, F.-P. Neirac, and G. Thierry, "A criticality criterion to decrease the computational burden in multistage distribution system optimal power flow," *PowerTech (POWERTECH), 2013 IEEE Grenoble*, pp. 1 – 6, 2013.

[54] Y. Hernandez and T. Hiyama, "Minimization of voltage deviations, power losses and control actions in a transmission power system," *Intelligent System Applications to Power Systems, 2009. ISAP '09. 15th International Conference on*, pp. 1 – 5, 2009.

[55] Y. Fu, M. Shahidehpour, and Z. Li, "Long-term security-constrained unit commitment: Hybrid dantzig-wolfe decomposition and subgratident approach," *IEEE Transactions on Power Systems*, vol. 20, no. 4, pp. 2093–2106, 2005.

[56] S.-K. Joo, C. Liu, Y. Shen, Z. B. Zabinsky, and J. Lawarree, "Optimization techniques for available transfer capability (atc) and market calculations," *Journal of Management Mathematics*, pp. 321–337, 2009.

[57] R. Allan and M. Al-Shakarchi, "Probabilistic techniques in a.c. load-flow analysis," *Proceedings of the IEE*, vol. 124, no. 2, pp. 154 – 160, 1977.

[58] A. L. da Silva and V. Arienti, "Probabilistic load flow by a multilinear simulation algorithm," *Generation, Transmission and Distribution, IEE Proceedings C*, vol. 124, no. 2, pp. 154– 160, 1977.

[59] V. Lukic, "Optimal operating policy for energy storage," *IEEE Transactions on Power Apparatus and Systems*, vol. 101, no. 9, pp. 3295–3302, 1982.

[60] D. Boutacoff, "Energy storage - emerging strategies for energy storage," *IEEE Power Engineering Review*, 1989.

[61] J. Sun and L. Tesfatsion, "Dc optimal power flow formulation and solution using quadprogj," Iowa State university, Tech. Rep., 2010.

[62] J. Momoh, R. Koessler, M. Bond, B. Scott, D. Sun, A. Papalexopoulos, and P. Ristanovic, "Challenges to optimal power flow," *IEEE Transactions on Power Systems*, vol. 12, no. 1, pp. 444–447, 1997.

[63] A. Marano-Marcolini, F. Capitanescu, J. Martinez-Ramos, and L. Wehenkel, "Exploiting the use of dc opf approximation to improve iterative ac scopf algorithm," *Transactions on Power Systems*, vol. 27, no. 3, pp. 1459 – 1466, 2012.

[64] F. Capitanescu, M. Glavic, D. Ernst, and L. Wehenkel, "Contingency fintering techniques for preventive security-constrained optimal power flow," *Transactions on Power Systems*, vol. 22, no. 4, pp. 1690–1697, 2007.

[65] R. Chang and C. Lu, "Load profiling and its applications in power market," *Engineering Society General Meeting, 2003, IEEE*, vol. 2, 2003.

[66] R. Chang and C. Lu, "Load profile assignment of low voltage customers for power retail market applications," *Generation, Transmission and Distribution, IEE Proceedings-*, pp. 263 – 267, 2003.

[67] F. Boshell and O. Veloza, "Review of developed demand side management programs including different concepts and their results," *Generation, Transmission and Distribution, IEE Proceedings-*, pp. 1–7, 2008.

[68] P. Malisani, B. Favre, S. Thiers, B. Peuportier, F. Chaplais, and N. Petit, "Investigating the ability of various buildings in handling load shiftings," *Power Engineering and Automation Conference (PEAM), 2011 IEEE*, vol. 2, pp. 393 – 397, 2011.

[69] A. Paetz, T. Kaschub, P. Jochem, and W. Fichtner, "Load-shifting potentials in households including electric mobility - a comparison of user behaviour with modelling results," *European Energy Market (EEM), 2013 10th International Conference on the*, pp. 1–7, 2013.

[70] A. Ipakchi and F. Albuyeh, "Grid of the future," *Power and Energy Magazine, IEEE*, vol. 7, pp. 52 – 62, 2009.

[71] G. Bao, C. Lu, Z. Yuan, and Z. Lu, "Battery energy storage system load shifting control based on real time load forecast and dynamic programming," in *Automation Science and Engineering (CASE), 2012 IEEE International Conference on*, 2012, pp. 815–820.

[72] G. C. Contaxis and A. G. Vlachos, "Constrained optimal power flow in electrical energy grids with large integration of dispatchable wind energy and independent wind power producers," *Proceedings of the 1999 European Union Wind Energy Conference*, 1999.

[73] G. C. Contaxis and A. G. Vlachos, "Optimal power flow considering operation of wind parks and pump storage hydro units under large scale integration of renewable energy sources," *Proceedings of the 1999 European Union Wind Energy Conference*, 1999.

[74] A. Feijoo and J. Cidras, "Modeling of wind farms in the load flow analysis," *IEEE Transactions on Power Systems*, vol. 15, no. 1, pp. 110–115, 2000.

[75] H. Yu, C. Chung, K. Wong, H. Lee, and J. Zhang, "Probabilistic load flow evaluation with hybrid latin hypercube sampling and cholesky decomposition," *IEEE Transactions on Power Systems*, vol. 24, no. 2, pp. 661–667, 2009.

[76] R. Alan and M. Al-Shakarchi, "Probabilistic a.c. load flow," *Proceedings of IEE*, vol. 123, no. 6, pp. 531–536, 1976.

[77] R. Xiaoming, C. Xiaohui, Y. Xiamggen, X. Tieyuan, and L. Huagang, "The algorithm of probabilistic load flow solutions," *Proceedings of the International Conference on Power System Technology*, 2002.

[78] S. Chun-Lien, "Probabilistic load-flow computation using point estimate method," *IEEE Transactions on Power Systems*, vol. 20, no. 4, pp. 1843–1851, 2005.

[79] D. Shirmohammadi, H. Hong, A. Semlyen, and G. Luo, "A compensation-based power flow method for weakly meshed distribution and transmission networks," *IEEE Transactions on Power Systems*, vol. 3, no. 2, pp. 753–762, 1988.

[80] C. Saunders, "Point estimate method addressing correlated wind power for probabilistic optimal power flow," *IEEE Transactions on Power Systems*, 2013.

[81] W. Tian, D. Sutanto, Y. Lee, and H. Outhred, "Cumulant-based probabilistic power system simulation using laguerre polynomials," *IEEE Transactions on Energy Conversion*, vol. 4, no. 4, pp. 567–574, 1989.

[82] P. Zhang and S. Lee, "Probabilistic load flow computation using the method of combined cumulants and gram-charlier expansion," *Power Systems, IEEE Transactions on*, vol. 19, no. 1, pp. 676–682, Feb 2004.

[83] A. Tamtum, A. Schellenberg, and W. Rosehart, "Enhancements to the cumulant method for probabilistic optimal power flow studies," *IEEE Transactions on Power Systems*, 2009.

[84] P. Vorac and D. Georgiev, "Effects of loss models on locational reserve policies in power systems under uncertainty," *52nd Conference on decision and control*, 2013.

[85] E. Guslitser, "Uncertainty immunized solutions in linear programming," Israel Institute of Technology, Tech. Rep., 2002.

[86] A. Olwegard, K. Walve, G. Waglund, H. Frank, and S. Torseng, "Improvement of transmission capacity by thyristor controlled reactive power," *Power Apparatus and Systems, IEEE Transactions on*, vol. PAS-100, no. 8, pp. 3930–3939, Aug 1981.

[87] D. Shirmohammadi, P. R. Gribik, E. T. Law, J. H. Malinowski, and R. O'Donnell, "Evaluation of transmission network capacity use for wheeling transactions," *Power Systems, IEEE Transactions on*, vol. 4, no. 4, pp. 1405–1413, Nov 1989.

[88] K. Kopsidas, S. R. . M. Baharom, and I. Cotton, "Power transfer capacity improvements of existing overhead line systems," *Electrical Insulation (ISEI), Conference Record of the 2010 IEEE International Symposium on*, 2010.

[89] K. Kopsidas, S. Rowland, and B. Boumecid, "A holistic method for conductor ampacity and sag computation on an ohl structure," *Power Delivery, IEEE Transactions on*, vol. 27, no. 3, pp. 1047–1054, July 2012.

[90] P. Hering, P. Janeček, and E. Janeček, "On-line ampacity monitoring from phasor measurements," vol. 19, 2014, pp. 3164–3169. [Online]. Available: http://www.scopus.com/inward/record.url?eid=2-s2.0-84929833430&partnerID=40&md5=f65a5849d7a14b3225cc1079a58c45f8

[91] E. Hnyilicza, S. Lee, and F. Schweppe, "Steady-state security regions: the set-theoretic approach," in *Proc. 1975 PICA Conf.*, pp. pp.347 –355.

[92] R. Fischl and J. DeMaio, "Fast identification of the steady-state security regions for power system security enhancement," in *Proc. 1975 PICA Conf.*, pp. pp.347 –355.

[93] J. Xiao, W. Gu, C. Wang, and F. Li, "Distribution system security region: definition, model and security assessment," *IET Generation, Transmission Distribution*, vol. 6, no. 10, pp. 1029–1035, October 2012.

[94] F. Wu and S. Kumagai, "Steady-state security regions of power systems," *Circuits and Systems, IEEE Transactions on*, vol. 29, no. 11, pp. 703–711, Nov 1982.

[95] C.-C. Liu, "A new method for the construction of maximal steady-state security regions of power systems," *Power Systems, IEEE Transactions on*, vol. 1, no. 4, pp. 19–26, Nov 1986.

[96] Y. Zeng, P. Zhang, M. Wang, H. Jia, Y. Yu, and S. Lee, "Development of a new tool for dynamic security assessment using dynamic security region," in *Power System Technology, 2006. PowerCon 2006. International Conference on*, Oct 2006, pp. 1–5.

[97] Y. Hou, J. Yan, C. Peng, Z. Qin, S. Lei, and H. Ruan, "Risk assessment of critical time to renewable operation with steady-state security region," in *Power Systems Computation Conference (PSCC), 2014*, Aug 2014, pp. 1–6.

[98] Y. Kataoka and Y. Shinoda, "Voltage stability limit of electric power systems with generator reactive power constraints considered," *Power Systems, IEEE Transactions on*, vol. 20, no. 2, pp. 951–962, May 2005.

[99] A. Kumar, S. Srivastva, and S. Singh, "Available transmission capacity determination in a competitive electricity market using ac distribution factors," *Electric Power Components and Systems*, vol. 32, no. 9, pp. 927–939, 2004.

[100] B. Wood, A.; Wollenberg, *Power Generation, Operation, and Control*. John Wiley and Sons, 1996.

[101] V. Ajjarapu and C. Chrisy, "The continuation power flow: A tool for steady state volage stability analysis," *IEEE Transactions on Power Systems*, vol. 7, no. 1, pp. 416–423, 1992.

[102] G. Ejebe, J. Tong, G. Waight, J. Frame, X. Wang, and W. Tinney, "Available power transfer capability calculations," *IEEE Transactions on Power Systems*, vol. 13, no. 4, pp. 1521–1527, 1998.

[103] P. Bresceti, D. Lucarella, P. Marannino, R. Vailati, and F. Zanellini, "An opf based procedure for fast ttc analyses," *Proceedings of Power Engeneering Society General Meeting 2002*, vol. 3, pp. 1504–1509, 2002.

[104] M. Patel and A. Girgis, "New iterative method for available transfer capability calculation," *Power and Energy Society General Meeting, 2011 IEEE*, pp. 1–6, 2011.

[105] S. Greene, I. Dobson, and F. Alvarado, "Sensitivity of transfer capability margins with a fast formula," *IEEE Transactions on Power Systems*, vol. 17, no. 1, pp. 34–40, 2002.

[106] B. Zhang and D. Tse, "Geometry of injection regions of power networks," *Power Systems, IEEE Transactions on*, vol. 28, no. 2, pp. 788–797, May 2013.

[107] J. Lavaei, D. Tse, and B. Zhang, "Geometry of power flows and optimization in distribution networks," *Power Systems, IEEE Transactions on*, vol. 29, no. 2, pp. 572–583, March 2014.

[108] S. Singh, J. Østergaard, and B. Singh, "Reactive power capability of unified dfig for wind power generation," *Power and Energy Society General Meeting, 2010 IEEE*, pp. 1–7, 2010.

[109] O. Senturk, L. Helle, S. Nielsen, P. Rodriguez, and R. Teodorescu, "Power capability investigation based on electrothermal models of press-pack igbt three-level npc and anpc vscs for multimegawatt wind turbines," *IEEE Transactions on Power Systems*, vol. 27, no. 7, pp. 3195–3206, 2012.

[110] C. Wang, F. Luo, H. B. J. Xiao, J. Wang, and Y. L. S. Wang, "An evaluation method for power supply capacity of distribution system," *Electric Utility Deregulation and Restructuring and Power Technologies, 2008. DRPT 2008. Third International Conference on*, 2008.

[111] W. Li, S. Sun, and C. Duan, "Analysis and implementation of power supply capacity based on multi date acquisition," *International Symposium on Information Processing*, 2010.

[112] S. Liu, Y. Cui, and Z. Zhang, "Research on rational capacity-load ration of urban electric network," *China International Conference on Electricity Distribution*, 2010.

[113] R. W. Ferrero, S. M. Shahidehpour, and V. C. Ramesh, "Transaction analysis in deregulated power systems using game theory," *Power Systems, IEEE Transactions on*, vol. 12, no. 3, pp. 1340–1347, 1997.

[114] E. Litvinov, T. Zheng, G. Rosenwald, and P. Shamsollahi, "Marginal loss modeling in lmp calculation," *Power Systems, IEEE Transactions on*, vol. 19, no. 2, pp. 880–888, 2004.

[115] E. Karangelos, P. Panciatici, and L. Wehenkel, "Whither probabilistic security management for real-time operation of power systems?" in *Bulk Power System Dynamics and Control - IX Optimization, Security and Control of the Emerging Power Grid (IREP), 2013 IREP Symposium*, 2013, pp. 1–17.

[116] P. Voráč, D. Georgiev, and E. Janeček, "Modular algorithms for computing intervals of secure power injection," in *2016 IEEE International Energy Conference (ENERGYCON)*, April 2016, pp. 1–6.

[117] D. Georgiev, E. Janecek, and P. Vorac, "Computing intervals of secure injection," in *submitted to IFAC 2014*, 2014.

[118] J. Lavaei and S. H. Low, "Zero duality gap in optimal power flow problem," *IEEE Trans. on Power Systems*, 2012.

[119] B. Rao and K. Kreutz-Delgado, "An affine scaling methodology for best basis selection," *Signal Processing, IEEE Transactions on*, vol. 47, no. 1, pp. 187–200, Jan 1999.

[120] R. Tütüncü, K. Toh, and M. Todd, "Solving semidefinite-quadratic-linear programs using SDPT3."

[121] J. J. Grainger and W. D. J. Stevenson, *Power System Analysis*. McGraw-Hill, Inc.

[122] (1993) Power systems test case archive. University of Washington. www.ee.washington.edu/research/pstca.

[123] A. Birchfield, T. Xu, K. Gegner, K. Shetye, and T. Overbye, "Grid structural characteristics as validation criteria for synthetic networks."

[124] I. Ilic, A. Viskovic, and M. Vrazic, "User p-q diagram as a tool in reactive power trade," in *Energy Market (EEM), 2011 8th International Conference on the European*, May 2011, pp. 580–584.

[125] K. Hedman, R. O'Neill, E. Fisher, and S. Oren, "Optimal transmission switching with contingency analysis," *Power Systems, IEEE Transactions on*, vol. 24, no. 3, pp. 1577–1586, Aug 2009.

[126] M. Khanabadi, H. Ghasemi, and M. Doostizadeh, "Optimal transmission switching considering voltage security and n-1 contingency analysis," *Power Systems, IEEE Transactions on*, vol. 28, no. 1, pp. 542–550, Feb 2013.

[127] P. Vorac and D. Georgiev, "Interval based network operation respecting n-1 security criterion," in *submitted to ISGT Europe 2014*, 2014.

[128] (1993) IEEE power systems test archive. [Online]. Available: http://www.ee.washington.edu/research/pstca/

[129] M. Grant and S. Boyd, *CVX: Matlab software for disciplined convex programming*, 2011.

[130] J. Rajathy, *Data sheets for IEEE 14 bus system*, http://shodhganga.inflibnet.ac.in/bitstream/10603/5247/18/19_appendix.pdf, 2003.

[131] M. Grant and S. Boyd, "CVX: Matlab software for disciplined convex programming, version 2.1," http://cvxr.com/cvx, Mar. 2014.

[132] (2014) dena ancillary services study 2030. German Energy Agency. https://www.dena.de/fileadmin/dena/Dokumente/Themen_und_Projekte/Energiesysteme/dena-Studie_Systemdienstleistungen_2030/dena_Ancillary_Services_Study_2030_-_summary.pdf.

[133] P. Hering, P. Voráč, and P. Janeček, "On secure interface between transmission and distribution power networks," vol. 11, 2016, pp. 334–337. [Online]. Available: http://www.scopus.com/inward/record.url?eid=2-s2.0-84929833430&partnerID=40&md5=f65a5849d7a14b3225cc1079a58c45f8

[134] (2014) Report accompanying the draft rules. German Energy Agency. http://www.rte-france.com/sites/default/files/2014_04_09_french_capacity_market.pdf.

[135] R. A. van der Veen and R. A. Hakvoort, "The electricity balancing market: Exploring the design challenge," *Utilities Policy*, vol. 43, no. Part B, pp. 186 – 194, 2016. [Online]. Available: http://www.sciencedirect.com/science/article/pii/S0957178716303125

[136] E. Rivero, J. Barquín, and L. Rouco, "European balancing markets," in *2011 8th International Conference on the European Energy Market (EEM)*, May 2011, pp. 333–338.

[137] D. Jost, A. Braun, R. Fritz, and S. Otterson, "Dynamic sizing of automatic and manual frequency restoration reserves for different product lengths," in *2016 13th International Conference on the European Energy Market (EEM)*, June 2016, pp. 1–5.